letnik/volume **52** - št./no. **5/06** - str./pp. **267-338**
Ljubljana, maj/May 2006, zvezek/issue **493**

STROJNIŠKI VESTNIK

JOURNAL OF MECHANICAL ENGINEERING

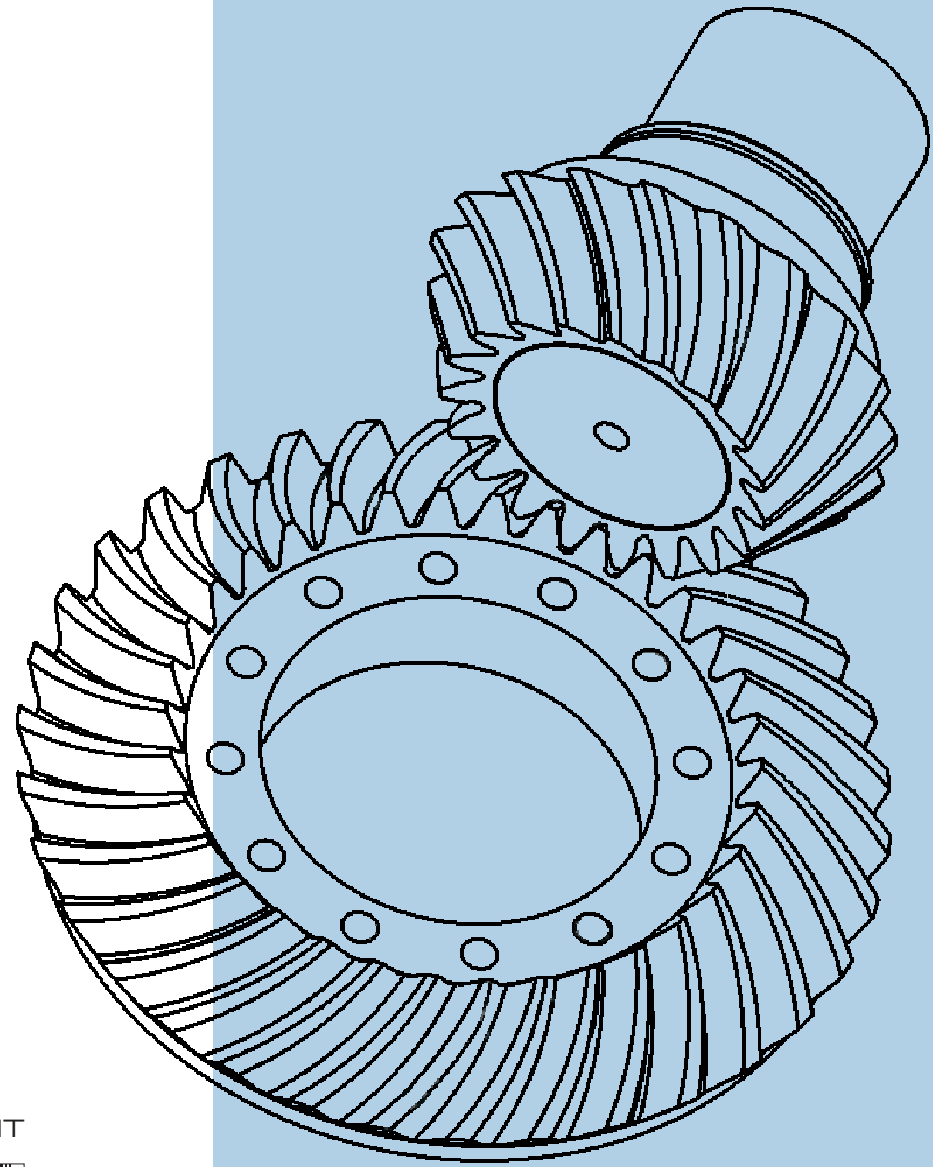

cena 800 SIT

9 770039 248001

ISSN 0039-2480

Vsebina - Contents

Strojniški vestnik - Journal of Mechanical Engineering
letnik - volume 52, (2006), številka - number 5
Ljubljana, maj - May 2006
ISSN 0039-2480

Izhaja mesečno - Published monthly

Strojniški vestnik - Journal of Mechanical Engineering 52(2006)5, 268-291
UDK - UDC 621.86:658.78
Izvirni znanstveni članek - Original scientific paper (1.01)

Načrtovanje in optimiranje avtomatiziranih regalnih skladiščnih sistemov

The Design and Optimization of Automated Storage and Retrieval Systems

Tone Lerher - Iztok Potrč
(Fakulteta za strojništvo, Maribor)

V predloženem prispevku je predstavljen model za načrtovanje in optimiranje avtomatiziranih regalnih skladiščnih sistemov za delo v enem in več hodnikih. Zaradi zahtevanega pogoja o tehnično zelo zmogljivem in stroškovno sprejemljivem skladiščnem sistemu, predstavljajo namensko funkcijo v računskem modelu načrtovanja najmanjši skupni stroški. Namenska funkcija združuje elemente statičnega in dinamičnega dela skladiščnega sistema ter investicijske in obratovalne stroške skladišča. Zaradi nelinearnosti, večparametričnosti in diskretne oblike namenske funkcije smo za optimizacijo projektnih spremenljivk uporabili metodo genetskih algoritmov. Prikazana je analiza izbranega regalnega skladiščnega sistema, pri dveh različnih sistemih regalnega dvigala za delo v enem in več hodnikih. Ugotovili smo, da so stroškovno optimalne rešitve skladišč nahajajo v področju visokih in dolgih skladiščnih regalih, kar vpliva na zmanjšanje števila regalnih hodnikov in števila regalnih dvigal ter skupno na celotne stroške skladišča. Rezultati analize so pokazali, da je izbira posameznega sistema regalnega dvigala, za delo v enem ali več hodnikih, izrazito odvisna od zahtevane pretočne zmogljivosti skladišča. Predloženi model predstavlja uporabno in prilagodljivo orodje za načrtovanje skladiščnih sistemov ter izbiro posameznega sistema regalnega dvigala za delo v enem ali več hodnikih v postopku načrtovanja regalnih skladiščnih sistemov.
© 2006 Strojniški vestnik. Vse pravice pridržane.
(Ključne besede: sistemi skladiščni, skladišča avtomatizirana, načrtovanje, optimiranje)

In this paper a model for the design and optimization of an automated storage-and-retrieval system for single- and multi-aisle systems is presented. Because of the required conditions, i.e., that the warehouse should be technically highly efficient and that it should be designed at reasonable expense, the objective function is represented by minimum total costs. The objective function combines elements of the static and dynamic parts of the warehouse, the investment, and the operational costs of the warehouse. Due to the non-linear, multi-variable and discrete shape of the objective function, the method of genetics algorithms was used for the optimization process of the decision variables. An analysis of the chosen automated warehouse with two types of the single- and multi-aisle automated storage and retrieval systems is presented. It was established that the optimum solutions regarding total costs of the warehouse can be found in the area of high and long storage racks. Consequently, this influences the reduction of the number of picking aisles and the number of storage and retrieval machines. The results of the analysis show that the choice of a type of single- or multi-aisle system depends crucially on the required throughput capacity of the warehouse. The presented model is a very useful and flexible tool for choosing a particular type of single- or multi-aisle system when designing automated warehousing systems.
© 2006 Journal of Mechanical Engineering. All rights reserved.
(Keywords: storage systems, automated warehousing systems, design, optimization)

0 UVOD

Skladišča s svojim osnovnim namenom so nujno potrebna za zvezno in optimalno delovanje tako proizvodnih kakor tudi oskrbnih postopkov. Žal

0 INTRODUCTION

The key feature of a warehouse is the absolute necessity for the continuous and optimum operation of the production and distribution processes.

so bili v preteklosti skladiščni, transportni in pretovorni postopki močno zapostavljeni, kar se še dandanes izkazuje v razmeroma nizki stopnji avtomatizacije v primerjavi s stanjem v proizvodnji. Skladišča so potrebna iz številnih razlogov, ki jih lahko razporedimo v naslednje skupine [1]: (*i*) neusklajen dotok in odtok blaga zaradi neustrezne dinamike v proizvodnji in porabi, (*ii*) prevzemanje blaga številnih izdelovalcev za izdelavo kombiniranih odprem, (*iii*) izvedba dnevne preskrbe blaga v proizvodnji in dostavi, (*iv*) izvedba dodatnih dejavnosti, kakor so pakiranje, končna montaža itn. Skladišča predstavljajo blagovno-tehnični del gospodarjenja z blagom ter glede na zapostavljenost v preteklosti predstavljajo priložnost pri zmanjšanju skupnih stroškov pri načrtovanju in obratovanju skladišča.

V prispevku so predstavljena avtomatizirana skladišča, ki jih imenujejo tudi avtomatizirani regalni skladiščni sistemi (ARSS). V zadnjih desetletjih se izdatno povečuje delež ARSS, ki omogočajo doseganje večjih zmogljivosti v primerjavi z običajnimi skladišči. Razmišljanja o uporabi ARSS segajo že desetletja nazaj, ko je leta 1962 podjetje Demag izdelalo prvi ARSS [2]. Omenjeni ARSS je bilo prvo visoko regalno skladišče višine 20 metrov in je zaznamoval novo obdobje v razvoju transportno-skladiščne tehnike. ARSS so v osnovi sestavljeni iz skladiščnih regalov (SR), regalnega dvigala (RD), zveznih transporterjev, vhodne in izhodne (V/I) lokacije skladišča in računalniškega sistema za vodenje in organizacijo skladiščne dejavnosti. Glavne prednosti v primerjavi z običajnimi sistemi skladišč se izkazujejo z: (*i*) veliko pretočno zmogljivostjo skladišča *Pf*, (*ii*) velikim izkoristkom zalogovnega skladišča *Q*, (*iii*) veliko zanesljivostjo in večjim nadzorom skladiščnega postopka, (*iv*) izboljšanimi varnostnimi razmerami in (*v*) zmanjšanjem poškodb ter izgube blaga. Zaradi njihove tehnološke popolnosti in popolne avtomatizacije sistema, zahtevajo velike investicijske stroške. Prav tako so ARSS, pri katerih RD oskrbuje samo pripadajoč regalni hodnik, neprilagodljivi glede na morebitno spremembo pretočne zmogljivosti skladišča.

Uspešnost izvedbe ARSS je odvisna predvsem od preudarnega in učinkovitega postopka načrtovanja, da bo izpolnjen glavni pogoj o tehnično zelo zmogljivem sistemu, ob predpostavki o optimalnih investicijskih in obratovalnih stroških skladišča. Zmogljivost ARSS je v največji meri odvisna od zmogljivosti transportno-skladiščnega

Unfortunately, in the past, warehousing, transport systems and transferring processes were neglected, and this nowadays shows itself in a relatively low degree of automation in comparison with the production process. Warehouses are needed for the following reasons [1]: (*i*) an imbalance in the flow and outflow of goods due to the inappropriate dynamics of production and consumption, (*ii*) taking goods from numerous producers for the production of combined shipments, (*iii*) the realization of the daily supply of goods in the production and distribution, (*iv*) the realization of additional activities, such as packaging, final assembly, etc. Warehouses represent a technical part of dealing with goods. Since they were neglected in the past, they represent an opportunity to reduce total costs relating to the design and operation processes.

In this study, automated warehouses, also named automated storage and retrieval systems (ASRS), are presented. In the past few decades, the share of ASRS, which in comparison with conventional warehouses provides a higher level of technological efficiency, has increased. The use of the ASRS already received consideration decades ago, when in 1962 the company Demag created the first ASAR [2]. The aforementioned ASRS was the first high-bay warehouse measuring 20 meters in height, which marked the beginning of a new era in the development of material handling equipment in Europe. The ASRS consists of storage racks (SRs), a storage and retrieval machine (SR machine), accumulating conveyors, an input and output location (I/O location) and a computer system for managing and organizing the activities in the warehouse. In comparison with conventional warehousing systems, the key advantages of the ASRS are: (*i*) high throughput capacity *Pf*, (*ii*) high warehouse volume *Q* (rack capacity), (*iii*) high reliability and better control of the warehousing process, (*iv*) improved safety conditions and (*v*) a decrease in the amount of damage and the loss of goods. Due to advanced technology and the complete automation of the system, the ASRS demands extensive investment. Additionally, those ASRSs where the SR machine operates only in the single picking aisle are rather inflexible as far as a possible change of the throughput capacity of the warehouse is concerned.

The success of the ASRS largely depends on a careful and efficient design process, whereby the basic condition that the system is technically highly efficient must be fulfilled, along with the condition of optimum investment and the operational costs of the warehouse. The efficiency of the ASRS mainly depends on the efficiency of the material

sredstva in vrste transportno-skladiščne enote TSE. V tipičnem ARSS samostojno RD oskrbuje samo pripadajoči regalni hodnik, kar imenujemo *sistem* RD *za delo v enem hodniku*. V primeru zahteve po manjši pretočni zmogljivosti in večji prilagodljivosti skladišča, uporabimo *sistem* RD *za delo v več hodnikih* ([4] do [6]). V omenjenem sistemu RD z uporabo pomičnega vozička, ki zagotavlja vožnjo v prečnem hodniku, oskrbuje več regalnih hodnikov. Ker zahteva RD tudi do 40 % [3] vrednosti celotne investicije ARSS, je izbira *sistema* RD *za delo v enem in več hodnikih* eno izmed ključnih vprašanj pri načrtovanju skladišč. Zmogljivost ARSS je odvisna tudi od geometrijske oblike SR in ustrezne skladiščne strategije.

Načrtovanje in optimiranje skladiščnih sistemov (ne nujno ARSS) so v preteklosti obravnavali številni avtorji. Ena izmed prvih objav s področja optimizacije skladišča je delo *Basana in sodelavcev* [7], ki so analizirali optimalne izmere skladišča pri izbrani zalogovni velikosti skladišča v odvisnosti od različnih skladiščnih strategij. *Karasawa in sodelavci* [8] so predstavili model za načrtovanje ARSS. V njihovem delu je namenska funkcija definirana kot nelinearna in večparametrična ter se sestoji iz treh glavnih spremenljivk: (*i*) števila RD, (*ii*) dolžine SR in (*iii*) višine SR; ter nespremenljivih vrednosti: stroškov za nakup zemljišča, stroškov za izdelavo skladiščne zgradbe, stroškov za nakup regalne konstrukcije in stroškov za nakup regalnih dvigal. Pomanjkljivost modela [8] je, da se navezuje samo na *sistem* RD *za delo v enem hodniku* in skladiščno opravilo enojnega delovnega kroga. *Ashayeri in sodelavci* [9] so predstavili model načrtovanja ARSS, ki omogoča določitev glavnih vplivnih parametrov pri načrtovanju skladišč. V nasprotju s *Karasawo in sodelavci* [8], so avtorji upoštevali skladiščno opravilo dvojnega delovnega kroga. *Bafna in sodelavci* [10] ter *Perry in sodelavci* [11] so pri načrtovanju skladišč uporabili kombinacijo analitičnega modela in sistema diskretnih numeričnih simulacij. Pri tem so *Perry in sodelavci* [11] uporabili posebno iskalno metodo za določitev optimalnih rešitev ARSS, ki so jo vključili v simulacijski model ARSS. Za merilo zmogljivosti sistema so uporabili pretočno zmogljivost skladišča, v odvisnosti od števila RD ter števila delovnih mest. Načrtovanje skladišč z upoštevanjem vpliva skladiščno-upravljalne strategije sta predstavila *Rosenblatt in Roll* [12]. Pri opisu skupnih stroškov sta upoštevala, da so le-ti odvisni od: (*i*) stroškov za izgradnjo

handling equipment and the type of transport unit load (TUL). In a typical ASAR, the SR machine independently operates only in the single picking aisle, which is called a *single-aisle* ASRS. In the case of smaller throughput capacities and higher flexibility of the warehouse, the *multi-aisle* ASRS is used ([4] to [6]). In the above-mentioned system, the SR machine serves several picking aisles with the help of the aisle transferring vehicle, which ensures driving in the cross aisle. Since the SR machine takes up to 40% [3] of the entire investment of the ASRS, the choice between a *single*- and *multi-aisle* ASRS is of key importance for the design of the automated warehouse. The efficiency of the ASRS is also dependent on the layout of the SR and the appropriate storage strategy.

The design of warehouses (not necessarily ASRS) has been studied in the past by several authors. One of the first publications on the subject of optimizing warehouses is the work of *Basan et al.* [7], who analyzed the optimum dimensions of the warehouse, considering the chosen volume of the warehouse and the dependence on various storage strategies. *Karasawa et al.* [8] presented a design model of the ASRS. In their work, the objective function is defined as non-linear and multi-variable, consisting of three main variables: (*i*) the number of SR machines, (*ii*) the length of the SR and (*iii*) the height of the SR; and also of constant values: the cost of buying the land, the cost of building the warehouse, the cost of buying the SR construction and the cost of buying the SR machines. The main disadvantage of this model [8] is that it refers only to the *single-aisle* ASRS and the warehousing operation of the single command cycle (SC). *Ashayeri et al.* [9] presented a design model of the ASRS that enables the determination of the main influential parameters when designing warehouses. Unlike *Karasawa et al.* [8], they considered the warehousing operation of the dual command cycle (DC). *Bafna et al.* [10] and *Perry et al.* [11] used a combination of an analytical model and a system of discrete event simulations when designing the warehouse. *Perry et al.* [11] used a special search method to determine the optimum solutions for the ASRS, which they have included in the simulation model of the ASRS. As a measure of the efficiency of the system, they used the throughput capacity of the warehouse, with its dependence on the number of SR machines and the number of workplaces. The design of warehouses with regard to the influence of the storage policy was presented by *Rosenblatt*

skladiščne zgradbe, (*ii*) stroškov za nakup skladiščne opreme, (*iii*) stroškov, ki nastanejo zaradi preobremenitve skladiščnega sistema (trenutno pomanjkanje skladiščnega prostora) ter (*iv*) stroškov, ki so odvisni od posamezne skladiščno-upravljalne strategije. Poglobljen pregled s področja načrtovanja in upravljanja regalnih skladiščnih sistemov je predstavil *Rouwenhorst s sodelavci* [13], in sicer v obliki metodologije za načrtovanje skladiščnih sistemov. Postopek načrtovanja je predstavljen s strukturiranim postopkom, ki pri sprejemanju odločitev upošteva strateško, taktično in opravilno raven odločanja.

Večina opisanih modelov načrtovanja se navezuje na *sistem* RD *za delo v enem hodniku* ([8] do [11]). Razlika med omenjenimi postopki in modeli se zrcali v stroških, ki so vključeni v namensko funkcijo, v izbiri projektnih spremenljivk ter v uporabi optimizacijskih tehnik. Veliko manj je bilo storjeno za druge tipe skladišč, predvsem za sisteme, pri katerih je število RD (S) manjše ali enako od števila regalnih hodnikov (R) (pogoj $S \leq R$) ([3] in [14]). Zaradi tega smo v model načrtovanja vključili izpopolnjene analitične modele za določitev zmogljivosti *sistema* RD *za delo v več hodnikih* ([2] in [15]).

Zahteva po zelo zmogljivih skladiščih in najmanjših investicijskih in obratovalnih stroških skladišča je bila vodilo pri razvoju in izdelavi namenske funkcije *najmanjši skupni stroški* (*NSS - Min. TC*). Zaradi nelinearnosti, diskretne oblike in večparametričnosti namenske funkcije *NSS* [3] smo za optimizacijo projektnih spremenljivk uporabili *postopek genetskih algoritmov* ([16] in [17]). Rezultat modela načrtovanja regalnih skladiščnih sistemov je določitev tehnično zelo zmogljivega ARSS, ob pogoju o najmanjših investicijskih in obratovalnih stroških skladišča.

1 NAČRTOVANJE AVTOMATIZIRANIH REGALNIH SKLADIŠČNIH SISTEMOV

Model načrtovanja ARSS temelji na strukturiranem postopku [13], pri čemer moramo upoštevati vse parametre, ki vplivajo na zalogovno velikost skladišča Q, pretočno zmogljivost skladišča Pf ter investicijske in obratovalne stroške skladišča. Pri razvoju in izdelavi modela načrtovanja smo upoštevali predloge in priporočila preostalih avtorjev ([3], [8], [12] in [18] do [22]). Na sliki 1 je predstavljen algoritem poteka modela načrtovanja ARSS z

and Roll [12]. When describing total costs, the authors took into account: (*i*) the cost of building the warehouse, (*ii*) the cost of buying the storage equipment, (*iii*) the costs arising from overloading the warehousing system (a temporary shortage of storage space) and (*iv*) the costs that depend on a particular storage policy. An in-depth overview of the area of designing and controlling warehouses was presented by *Rouwenhorst et al.* [13] in the form of the methodology of designing warehousing systems. The design process is presented with a structured approach, which takes into account the strategic, tactical and operational level of decision making.

The majority of described models refer only to the *single-aisle* ASAR ([8] to [11]). The difference between the discussed approaches and models lies in the costs included in the objective function, the decision on considered project variables and the use of optimization techniques. Less has been done for other types of warehouses, especially for systems where the number of SR machines (S) is less than or equal to the number of picking aisles (R) (the condition $S \leq R$) ([3] and [14]). Therefore, our newly proposed analytical travel-time models for the efficiency determination of *multi-aisle* ASRS have been included in our design model ([2] and [15]).

The requirement for a highly efficient warehouse and minimum investment and operational costs of the warehouse was the guidance for how to develop and create the objective function *minimum total costs* (*Min. TC*). Due to the non-linear, discrete and multi-variable objective function *Min. TC* [3], *the method of genetics algorithms* ([16] and [17]) to optimize the project variables have been applied. The result of the model for designing warehouses is the determination of the technologically highly efficient ASRS under the condition that investment and operational costs of the warehouse are minimized.

1 DESIGNING AUTOMATED STORAGE AND RETRIEVAL SYSTEMS

The model for designing the ASRS is based on the structured approach [13], where all the parameters influencing the warehouse volume Q (rack capacity), the throughput capacity Pf, the investment, and the maintenance costs have to be taken into account. When developing and creating the design model, propositions and references from other authors were considered ([3], [8], [12] and [18] to [22]). Figure 1 shows the algorithm of the design model of the

naslednjimi glavnimi moduli:

- ***Načrtovanje skladiščne cone***, ki obsega izbiro palete in določitev osnovne transportno-skladiščne enote (TSE). Na podlagi izbrane TSE lahko določimo regalno okno (RO), ki je temelj za postavitev SR. V okviru določitve SR izberemo regalne stranice in regalne veznike, ki skupno sestavljajo regalno konstrukcijo. Vrsto regalne konstrukcije izberemo v odvisnosti od teže TSE ter njihove razporeditve v vodoravni smeri x in v navpični smeri y. Na podlagi zahtevane Q skladišča, geometrijske oblike skladiščnega objekta ter oblike SR, določimo obliko skladiščne cone.
- ***Načrtovanje transportne cone in določitev zmogljivosti skladišča***, ki obsega izbiro osnovnega transportno-skladiščnega sredstva. Izbira se izvede glede na geometrijsko obliko SR in zahtevano *Pf* skladišča. V odvisnosti od zahtevane *Pf* skladišča izbiramo med sistemom: (*i*) RD *za delo v enem hodniku* ter (*ii*) RD *za delo v več hodnikih*. Za premik TSE do skladiščne cone imamo na voljo transportne viličarje ali zvezne transporterje. V odvisnosti od kombinacije transportno-skladiščnih sredstev določimo zmogljivost skladišča in izmere transportne cone.
- ***Določitev skupnih stroškov***, ki se deli na: (*i*) stroške za statični del skladišča, (*ii*) stroške za dinamični del skladišča in (*iii*) stroške za obratovanje skladiščnega sistema v izbranem časovnem obdobju.
- ***Oblikovanje namenske funkcije in optimizacija parametrov namenske funkcije Min. TC***, ki predstavlja kombinacijo projektnih spremenljivk, opravilnih parametrov in skupnih stroškov ARSS ter temelji na optimizacijski *metodi z genetskimi algoritmi* [16] in [17]. Cilj optimizacije *NSS (Min. TC)* je določiti takšno različico ARSS, da bo izpolnjen pogoj o tehnično zelo zmogljivem in stroškovno optimalnem ARSS.

Novost v modelu načrtovanja je uporaba pogoja, da je število RD lahko manjše od števila regalnih hodnikov ($S \leq R$). *Karasawa in sodelavci* [8], *Ashayeri in sodelavci* [9], *Azadivar* [23] so v svojih modelih uporabili pogoj ($S = R$). Glede na dejstvo, da je RD najdražji element v ARSS (približno 40 % celotne investicije [3]), smo v model načrtovanja vključili uporabo RD *s pomičnim voziČkom* [2], ki se navezuje na pogoj, $S \leq R$. Bistvo omenjenega sistema se kaže v veliki prilagodljivosti glede na morebitno povečanje Q in *Pf* skladišča ter v izrazito manjših

ASRS, including the following main modules:

- ***Design of the storage zone***, which includes the choice of the palette and the determination of the basic transport unit load (TUL). On the basis of the chosen TUL, the storage compartment, which forms the basis for setting up the SR, can be determined. When determining the SR, upright frames and rack beams, which together form a storage rack structure, have been chosen. The type of storage-rack structure is selected in accordance with the weight of the TUL and their arrangement in the horizontal x and vertical y directions. On the basis of the required Q of the warehouse, the geometry of the warehouse and the form of SR, and the form of the storage zone, have been determined.
- ***Design of the transport zone and the determination of the efficiency of the warehouse***, which covers the choice of basic material handling equipment. The choice is made according to the geometrical form of the SR and the required *Pf* of the warehouse. Due to the throughput capacity *Pf*, two systems of handling equipment are possible: (*i*) the *single-aisle* system; (*ii*) the *multi-aisle* system. Lift trucks and conveyors are used for manipulating the TUL to the storage-rack zone. Depending on the combination of the material handling equipment and the warehouse volume Q, the dimensions of the transport zone can be determined.
- ***Determination of the total costs***, which is divided into: *(i)* costs of the static part of the warehouse, *(ii)* costs of the dynamic part of the warehouse and *(iii)* costs of operating the warehousing system in a selected time period.
- ***Design of the objective function and optimization of the parameters of the objective function min TC.***, which presents a combination of project variables, operational variables and overall costs of the ASRS, and are based on the optimization *method of genetics algorithms* [16], [17]. The aim of the optimization of the decision variables in *Min. TC* is to define the cost-optimal solution for the ASRS, considering the conditions of technically high and economically optimal solution for the ASRS.

An innovation in the design model is the application of the condition that the number of SR machines is lower than or equal to the number of picking aisles ($S \leq R$). *Karasawa et al.* [8], *Ashayeri et al.* [9], *Azadivar* [23] have applied the condition ($S = R$) to their models. Given that the SR machine is the most expensive element in the ASRS (taking up approximately 40% of the entire investment [3]), the utilization of aisle transferring storage and retrieval machine, which refers to the condition $S \leq R$, has been included in the design model [2]. The essential element of the above-mentioned

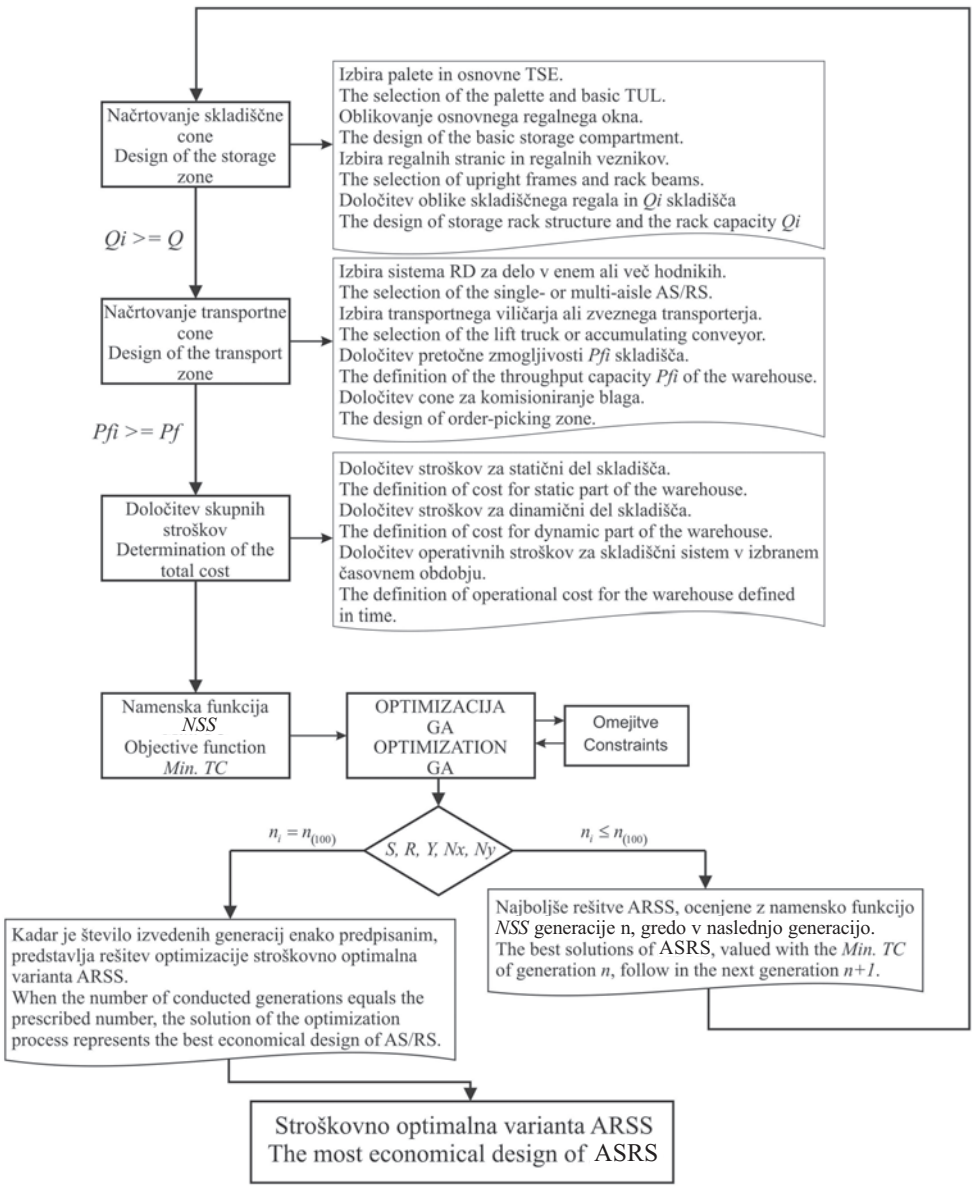

Sl. 1. *Algoritem poteka modela načrtovanja ARSS*
Fig. 1. *The algorithm of the design model of the ASRS*

investicijskih stroških v primerjavi s *sistemom* RD *za delo v enem hodniku*. Enak pogoj, $S \le R$, sta v svojem modelu načrtovanja predstavila *Rosenblatt in Roll* [3] v okviru kombiniranega analitičnega in simulacijskega postopka za načrtovanje ARSS. V njunem modelu je *Pf* skladišča za pogoj, $S \le R$, določena s simulacijo modela ARSS, ki nato zagotavlja vnos glavnih podatkov v analitično-optimizacijski model načrtovanja. Model načrtovanja [3] tako temelji na interakciji med simulacijami ARSS (diskretni sistem) in analitičnim

system reflects in a high degree of flexibility regarding a possible increase of *Q* and *Pf* of the warehouse and in smaller investment costs in comparison with the *single-aisle* ASRS. The same $S \le R$ condition was set out by *Rosenblatt and Roll* [3] in their combined analytical and simulation approach to designing the ASRS. In their model, the *Pf* of the warehouse is determined under the $S \le R$ condition with a simulation of the ASRS, which then ensures the input of the basic relevant information into the analytical optimization design model. The design model [3] is based on the interaction between simulations

modelom (uporaba zvezne optimizacije). Bistvena razlika med modelom načrtovanja [3] in v prispevku predstavljenim modelom načrtovanja, je v vpeljavi izpopolnjenih analitičnih modelov pri pogoju, $S \leq R$. V primerjavi z modelom [3] omogoča predstavljen model načrtovanja izdelavo hitrejšega, v celoti dokumentiranega, tehnično zelo zmogljivega in stroškovno optimalnega predloga ARSS. Poleg naštetih prednosti je bistveni del v modelu načrtovanja vpeljava namenske funkcije *NSS* in optimizacija projektnih spremenljivk znotraj namenske funkcije *NSS*. V nadaljevanju bo zato podrobneje predstavljeno oblikovanje namenske funkcije *NSS*.

1.1 Oblikovanje namenske funkcije najmanjši skupni stroški

Namenska funkcija *NSS* je sestavljena iz *projektnih spremenljivk*, opravilnih parametrov in stroškov pri gradnji in obratovanju skladišča. V modelu načrtovanja ARSS smo pri oblikovanju namenske funkcije uporabili naslednje predpostavke in omejitve:

- Regalno skladišče je ponazorjeno s SR, ki so ločeni z regalnimi hodniki, v katerih obratuje RD. Vsakemu regalnemu hodniku pripadata po dva SR, in sicer

of the ASRS (discrete system) and the analytical model (the utilization of the continuous optimization). The essential difference between the design model [3] and the design model presented in this paper is the introduction of newly improved analytical travel-time models under the condition that $S \leq R$. In comparison with the design model [3], the presented model enables the creation of a faster, entirely documented, technical highly efficient and also the most economical design of the ASRS. Along with the enumerated advantages, the essential element in the design model is represented by the introduction of the objective function *Min. TC* and the optimization of decision variables within the *Min. TC*. Consequently, in the following section the design of the objective function *Min. TC* will be discussed in detail.

1.1 Design of the objective function minimum total costs

The objective function *Min. TC* consists of *decision variables*, operational parameters and the costs of building and operating the warehouse. When designing the objective function, the following assumptions, notations and constraints have been applied to the design model of the ASRS:

- The warehouse is divided into SRs, which are separated by picking aisles, in which the SR

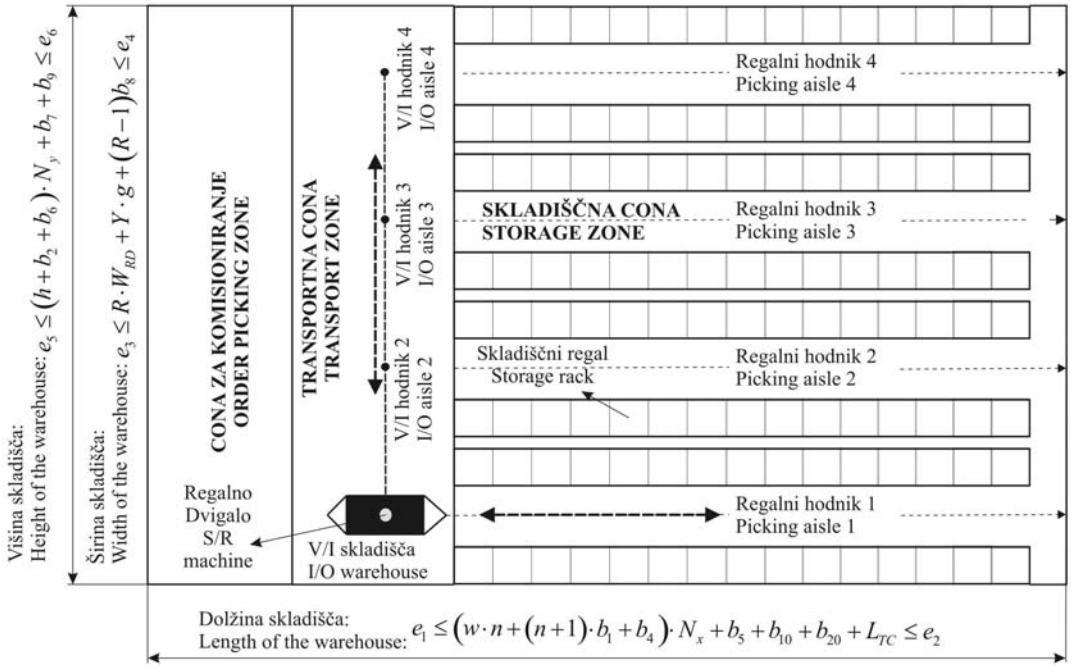

Sl. 2. *Tloris avtomatiziranega regalnega skladiščnega sistema*
Fig. 2. *The layout of the automated warehouse*

na vsaki strani regalnega hodnika po eden SR. V/I lokacija skladišča je nameščena na spodnjem, skrajno levem robu regalnega skladišča (sl. 2).

- Število RD S je lahko manjše ali enako R ($S \leq R$). RD *za delo v več hodnikih* potuje v prečnem hodniku na pomičnem vozičku, ki mu omogoča dostop do poljubnega regalnega hodnika i (sl. 2).
- SR je ponazorjen s pravokotno obliko, pri čemer je V/I lokacija skladiščnega regala i definirana v spodnjem levem robu regala (sl. 2).
- RD omogoča opravilo enojnega in dvojnega delovnega kroga, kateremu moramo prišteti še spremenljivi delež časa za vožnjo v prečnem hodniku ($S \leq R$).
- Pri izvedbi skladiščnega opravila dvojnega delovnega kroga ($S \leq R$) smo obravnavali: (i) sistem uskladiščenja in odpreme v istem regalnem hodniku i in (ii) sistem uskladiščenja in odpreme v dveh naključno izbranih regalnih hodnikih i in j.
- Znane so tehnične značilnosti RD in pomičnega vozička (hitrost v, pospešek in pojemek a) ter dolžina L in višina H skladiščnega regala.
- RD potuje v regalnem hodniku sočasno v vodoravni smeri x in v navpični smeri y.
- Dolžina L in višina H SR sta dovolj veliki, da RD doseže svojo največjo hitrost $v_{max.}$ v vodoravni smeri x in v navpični smeri y.
- Dolžina prečnega hodnika W je dovolj velika, da sklop RD s pomičnim vozičkom doseže največjo hitrost v prečni smeri.
- Uporabili smo strategijo naključnega skladiščenja, kar pomeni, da ima vsaka skladiščna lokacija enako verjetnost, da bo izbrana za opravilo uskladiščenja ali odpreme transportno-skladiščne enote.

S spreminjanjem projektnih spremenljivk: število transportno-skladiščnih sredstev S, število regalnih hodnikov R, število skladiščnih regalov Y, število RO v vodoravni smeri N_x, in število RO v navpični smeri N_y se spreminja vrednost namenske funkcije *NSS* za vsako posamezno različico ARSS. Opravilni parametri se v modelu načrtovanja ARSS navezujejo na oblikovanje skladišča, oblikovanje in določitev zmogljivost ARSS, medtem ko se stroški delijo na stroške za postavitev skladiščne zgradbe, nakupa transportno-skladiščnih sredstev in stroške, ki nastanejo zaradi obratovanja ARSS v izbranem časovnem obdobju. Namenska funkcija *NSS* je

machine operates. To each picking aisle belong two SRs: on each side of the picking aisle there is one SR. The I/O location of the warehouse is set on the low, extreme left-hand side of the warehouse (Fig. 2).

- The number of SR machines S can be lower than or equal to R ($S \leq R$). *The multi-aisle* ASRS travels in the transverse aisle on the aisle transferring vehicle, which enables access to any picking aisle i (Fig. 2).
- The SR is marked by a rectangular shape, whereby the I/O location of the SR i is defined on the low left-hand side of the rack (Fig. 2).
- The SR machine enables the operation of single and dual command cycles, to which a variable time period for traveling in the transverse aisle ($S \leq R$) must be added.
- When performing the warehousing operation of the dual command cycle ($S \leq R$), we have discussed: (i) the storage and retrieval in the same picking aisle i and (ii) the storage and retrieval in two randomly chosen picking aisles i and j.
- The technical characteristics of the SR machine and the traverse vehicle (velocity v, acceleration and deceleration a) as well as the length L and height H of the SR are known.
- The SR machine travels in the picking aisle simultaneously in the horizontal direction x and the vertical direction y.
- The length L and height H of the SR are long enough so that the SR machine can reach its maximum velocity v_{max} in the horizontal direction x and vertical direction y.
- The length of the transverse aisle W is long enough so that the SR machine with the traverse vehicle reaches its maximum velocity v_{max} in the transverse direction.
- A random strategy was applied, so each warehousing location has an equal chance to be chosen for the storage or retrieval of the TUL.

Changing the project variables (the number of SR machines S, the number of picking aisles R, the number of storage racks Y, the number of storage compartments in the horizontal direction N_x and the number of storage compartments in the vertical direction N_y) causes a change in the value of the objective function *Min. TC* for each model of the ASRS. The operational parameters in the design model of the ASRS refer to the design of the warehouse, the design, and the determination of the efficiency of the ASRS. Moreover, the costs comprise the costs of building the warehouse, the costs of buying storage and material handling equipment and the costs arising from operating the ASRS in a selected time period. The objective function

tako kombinacija projektnih spremenljivk, opravilnih parametrov (sl. 2, 3) in skupnih stroškov ter sestoji iz naslednjih modulov:

1) Skladiščni objekt

• *Investicija za nakup zemljišča I_1:*

$$I_1 = \left(P_z \cdot \frac{100}{D_z} \right) \cdot C_1 \quad (1),$$

P_z [m²] pomeni površino zemljišča za skladišče; D_z je delež zazidanosti skladišča in C_1 [€/m²] se navezuje na strošek za nakup zemljišča.

• *Investicija za izdelavo temeljne plošče I_2:*

$$I_2 = \left[\left(\left(w \cdot n + (n+1) \cdot b_1 + b_4 \right) \cdot N_x + b_5 + b_{10} + b_{20} \right) + L_{TZ} \cdot \left(R \cdot W_{RD} + Y \cdot g + (R-1) b_8 \right) \right] \cdot C_2 \quad (2),$$

R, Y in N_x so projektne spremenljivke; n se navezuje na število TSE v RO; w, g in h [mm] predstavljajo širino, dolžino in višino palete/TSE; W_{RD} [mm] je širina RD; L_{TZ} [mm] je dolžina transportne cone; b_1, b_4, b_5, b_8, b_{10}, b_{20} [mm] predstavljajo varnostni dodatek za širino RO, širino stebra, debelino stebra, varnostni razmik med soležnimi regali, dodatek za širino palete na prevzemnem mestu, dodatek na koncu skladišča; C_2 [€/m²] je strošek za postavitev temeljne plošče (sl. 2 in 3).

• **Investicija za postavitev sten skladiščnega objekta I_3:**

$$I_3 = \left[\left(\begin{array}{l} \left(\left(w \cdot n + (n+1) \cdot b_1 + b_4 \right) \cdot N_x + b_5 + b_{10} + b_{20} \right) + L_{TZ} + \\ \left(R \cdot W_{RD} + Y \cdot g + (R-1) b_8 \right) \end{array} \right) \cdot \left((h + b_2 + b_6) \cdot N_y + b_7 + b_9 \right) \right] \cdot 2C_3 \quad (3),$$

Min. TC je torej kombinacija projektnih spremenljivk, opravilnih parametrov (Figs. 2 and 3) in skupnih stroškov. It composes the following modules:

1) The warehouse building

• *The investment in buying the land I_1:*

P_z [m²] indicates the surface of the land for the warehouse; D_z stands for the share of the built warehouse, and C_1 [€/m²] refers to the cost of buying the land.

• *The investment in laying the foundations I_2:*

R, Y and N_x are decision variables; n refers to the number of TUL in the storage compartment; w, g and h [mm] indicate the width, length and height of the palette/TUL; W_{RD} [mm] indicates the width of the SR machine; L_{TZ} [mm] indicates the length of the transport zone; b_1, b_4, b_5, b_8, b_{10}, b_{20} [mm] stand for a safety addition to the width of the storage compartment, the width of the upright frame, the thickness of the upright frame, the safety spacing between racks that are placed close to each other, the addition to the width of the palette at the input buffer, the addition to the end of the warehouse; C_2 [€/m²] stands for the cost of laying the foundations (Figs. 2 and 3).

• **The investment in building the walls of the warehouse I_3:**

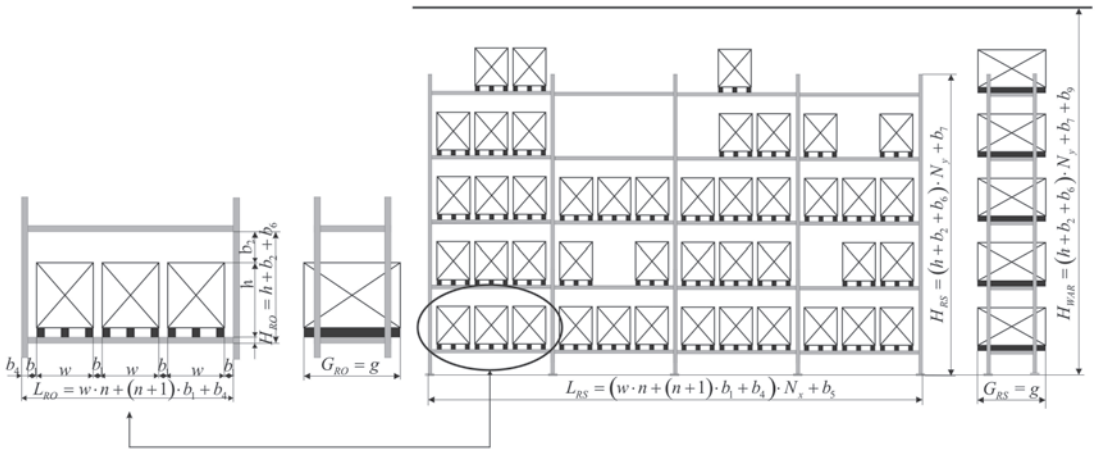

Sl. 3. *Oblika regalnega okna in skladiščnega regala*
Fig. 3. The layout of the storage compartment and storage rack

N_y je projektna spremenljivka; b_2, b_6, b_7, b_9 [mm] predstavljajo varnostni dodatek za višino RO, višino regalnega nosilca, odmik regalnega okna od tal in varnostni dodatek za višino skladišča; C_3 [€/m²] je strošek postavitve sten skladiščnega objekta (sl. 2 in 3).

- *Investicija za postavitev strehe skladiščne zgradbe I_4:*

N_y is the decision variable; b_2, b_6, b_7, b_9 [mm] indicate the safety addition to the height of the storage compartment, the height of rack beams, the deviation of the storage compartment from the floor and a safety addition to the height of the warehouse; C_3 [€/m²] is the cost of building the walls of the warehouse (Figs. 2 and 3).

- *The investment in building the roof of the warehouse I_4:*

$$I_4 = \left[\left(\left(w \cdot n + (n+1)\cdot b_1 + b_4\right)\cdot N_x + b_5 + b_{10} + b_{20}\right) + L_{TZ}\cdot\left(R\cdot W_{RD} + Y\cdot g + (R-1)b_8\right)\right]\cdot C_4 \quad (4),$$

C_4 [€/m²] pomeni strošek za postavitev strehe skladiščne zgradbe (sl. 2 in 3).

C_4 [€/m²] indicates the cost of building the roof of the warehouse (Figures 2 and 3).

2) Transportna in skladiščna sredstva

- *Investicija za nakup regalnih stranic I_5:*

2) Storage and material-handling equipment

- *The investment in buying upright frames I_5:*

$$I_5 = \left((N_x + 1)\cdot 2Y\right)\cdot C_5 \quad (5),$$

C_5 [€/m] pomeni strošek za nakup regalnih stranic.

- *Investicija za nakup regalnih veznikov in dodatek za ojačitev regalne konstrukcije I_6:*

C_5 [€/m] indicates the cost of buying upright frames.

- *The investment in buying rack beams and an addition to the reinforcement of the storage-rack structure I_6:*

$$I_6 = \left(\left(\left((N_x + 1)\cdot 2Y\right)\cdot C_5\right) + \left(N_x \cdot N_y \cdot 2Y \cdot L_v\right)\cdot C_6\right)\cdot\left(1 + \frac{PD}{100}\right) \quad (6),$$

L_v [mm] je dolžina regalnega veznika (nosila); *PD* pomeni dodatek za ojačitev skladiščnih regalov; C_6 [€/m] pomeni strošek za nakup regalnih veznikov.

- *Investicija za nakup prevzemnih miz I_7 in montažo regalne konstrukcije I_8:*

L_v [mm] is the length of the rack beam; *PD* indicates an addition to the reinforcement of storage racks, C_6 [€/m] indicates the cost of buying rack beams.

- *The investment in buying buffers I_7 and the assembly of the storage-rack structure I_8:*

$$\begin{aligned} I_7 &= 2R\cdot C_7 \\ I_8 &= Q\cdot C_8 \end{aligned} \quad (7),$$

C_7 [€] pomeni strošek za nakup prevzemnih miz, C_8 [€] pomeni strošek montaže.

C_7 [€] indicates the cost of buying buffers and C_8 [€] the cost of assembly.

- *Investicija za požarno varnost I_9 in klimatske zahteve I_{10}:*

- *The investment in fire-safety I_8 and air conditioning I_9 equipment:*

$$\begin{aligned} I_9 &= \left(\left(N_x \cdot N_y\right)\cdot 3\cdot 2\right)\cdot C_9 \\ I_{10} &= \left(L_{WAR}\cdot H_{WAR}\cdot W_{WAR}\right)\cdot C_{10} \end{aligned} \quad (8),$$

C_9 [€/PM] pomeni strošek požarne varnosti, C_{10} [€/m³] pa strošek prezračevanja.

C_9 [€/PM] indicates the cost of fire safety and C_{10} [€/m³] the cost of air ventilation.

- *Investicija za transportni I_{11} in regalni viličar I_{12}:*

- *The investment in lift truck I_{11} and reach trucks I_{12}:*

$$\begin{aligned} I_{11} &= S_{TV}\cdot C_{11} \\ I_{12} &= S_{RV}\cdot C_{12} \end{aligned} \quad (9),$$

S_{TV} pomeni število transportnih viličarjev (spremenljivka);
S_{RV} pomeni število regalnih viličarjev (spremenljivka);
C_{11} [€] pomeni strošek za nakup transportnega viličarja;
C_{12} [€] strošek za nakup regalnega viličarja.

S_{TV} indicates the number of lift trucks (variable),
S_{RV} indicates the number of reach trucks (variable);
C_{11} [€] indicates the cost of buying a lift truck;
C_{12} [€] indicates the cost of buying a reach truck.

• *Investicija za RD za delo v enem hodniku I_{13}:*

$$I_{13} = S_{RD} \cdot C_{13} + L_{TZ} \cdot C_{14} \quad (10),$$

• *Investicija za RD za delo v več hodnikih I_{14}:*

$$I_{14} = C_{13} \cdot S_{RD} + \left(L_{TZ} \cdot C_{14}\right) \cdot R - \left(W_{WAR} - \left(\frac{2g + S_{RD}}{2}\right)\right) \cdot C_{15} \quad (11),$$

S_{RD} pomeni število RD (spremenljivka); L_{TZ} [mm] je dolžina skladiščne cone; W_{WAR} [mm] je širina skladišča; C_{13} [€] pomeni strošek za nakup RD; C_{14} [€] pa strošek regalnega hodnika; C_{15} [€] pomeni strošek prečnega hodnika.

Za uskladiščenje in odpremo TSE v regalnem skladišču (vožnja v regalnih hodnikih) so namenjena samo regalna dvigala in regalni viličarji. Transportni viličarji se uporabljajo v izbirnemu in distribucijskemu delu skladišča.

• *Investicija za zvezni transporter I_{15}:*

$$I_{15} = C_{16} + 2 \cdot R \cdot C_{17} \quad (12),$$

C_{16} [€] pomeni strošek zveznega transporterja (krmilni sistemi, krmilni program); C_{17} [€] pa strošek preusmeritvenega elementa.

3) Obratovanje ARSS

• *Stroški vzdrževanja regalnega skladiščnega sistema C_{VZD}:*

$$C_{VZD} = P(\%) \cdot C_{13} \cdot S \quad (13),$$

• *Metoda neto sedanje vrednosti NPV* – diskontni stroški obratovanja, ki predvidevajo določeno dobo trajanja ARSS *i* in diskontno stopnjo *r*:

$$NPV = \sum_{i=1}^{T} \frac{\left(\left(P(\%) \cdot C_{13} \cdot S\right) + C_{OD}\right)}{\left(1 + r\right)^{i}} \quad (14),$$

P(%) pomeni delež vrednosti RD za vzdrževanje; *S* pomeni število transportno-skladiščnih sredstev; C_{OD} je strošek osebnega dohodka za viličariste, ki delajo s transportnimi in regalnimi viličarji; *r* je diskontna stopnja; T_i je predvidena doba trajanja obratovanja ARSS.

Namenska funkcija *NSS* je vsota stroškov za postavitev skladiščnega objekta, nabavo vseh transportnih in skladiščnih sredstev ter stroškov obratovanja za načrtovano dobo trajanja skladišča. V namenski funkciji pomenijo stroški nespremenljivo vrednost in se v odvisnosti od geometrijske oblike skladišča ne spreminjajo. Namenska funkcija *NSS* ima naslednjo obliko:

• *The investment in the single-aisle ASRS I_{13}:*

• *The investment in the multi-aisle ASRS I_{14}:*

S_{RD} indicates the number of SR machines (decision variable); L_{TZ} [mm] is the length of the transport zone; W_{WAR} [mm] is the width of the warehouse; C_{13} [€] indicates the cost of buying the SR machine; C_{14} [€] indicates the cost of the picking aisle; C_{15} [€] indicates the cost of the cross aisle.

For the storage and retrieval operation of the TUL in the high-bay warehouse (routing in the picking aisles), only the SR machines and reach trucks are used. Lift trucks are used in the order picking and distribution area.

• *The investment in the accumulating conveyor I_{15}:*

C_{16} [€] indicates the cost of the accumulating conveyor (the controls, the control system); C_{17} [€] indicates the cost of the diverted element.

3) Operating the ASRS

• *Costs of maintaining the automated storage and retrieval system C_{VZD}:*

• *The method of net present value NPV* – discount operational costs that assume a certain life expectancy of the ASRS *i* and the discount rate *r*

P (%) indicates the share of the value of the SR machine for maintenance; *S* indicates the number of pieces of material-handling equipment; C_{OD} is the cost of personal income for operators working with lift trucks and reach trucks; *r* is the discount rate; T_i is the anticipated life expectancy of the operation of the ASRS.

The objective function *Min. TC* refers to all the costs of building the warehouse, purchasing the material-handling equipment and the costs of operating the warehouse within the expected operational time period. In the objective function, the costs indicate the constant value and do not change depending on the geometry of the warehouse. The objective function *Min. TC* has the following form:

• *Namenska funkcija NSS*

• *The objective function Min. TC*

$$Min.\ TC = I_1 + I_2 + I_3 + I_4 + I_5 + I_6 + I_7 + I_8 + I_9 + I_{10} \\ I_{11} + I_{12} + I_{13} + I_{14} + I_{15} + NPV \quad (15).$$

Pri optimizaciji projektnih spremenljivk *S, R, Y,* N_x, N_y v namenski funkciji *NSS* moramo upoštevati določene omejitve, ki se nanašajo na (1) geometrijske omejitve skladišča, (2) najmanjšo zahtevano *Q* skladišča in (3) število RD je lahko manjše ali enako številu regalnih hodnikov ($S \le R$).

1) Izračunana prostornina skladišča V_i ne sme presegati dovoljene prostornine skladiščne zgradbe *V* (sl. 2).

When optimizing the decision variables *S, R, Y,* N_x, N_y in the objective function *Min. TC,* one must take into account certain constraints referring to (1) the geometrical constraints of the warehouse, (2) the minimum required *Q* of the warehouse, and (3) the fact that the number of SR machines has to be lower than or equal to the number of picking aisles ($S \le R$).

1) The calculated volume of the warehouse V_i cannot exceed the allowed volume of the warehouse *V* (Fig. 2).

• Dolžina skladišča L_{WAR}:

• The length of the warehouse L_{WAR}:

$$e_1 \le \left(w \cdot n + (n+1) \cdot b_1 + b_4\right) \cdot N_x + b_5 + b_{10} + b_{20} + L_{TZ} \le e_2 \quad (16).$$

• Širina skladišča W_{WAR}:

• The width of the warehouse W_{WAR}:

$$e_3 \le R \cdot W_{RD} + Y \cdot g + (R-1) b_8 \le e_4 \quad (17).$$

• Višina skladišča H_{WAR}:

• The height of the warehouse H_{WAR}:

$$e_5 \le \left(h + b_2 + b_6\right) \cdot N_y + b_7 + b_9 \le e_6 \quad (18).$$

2) Izračunana Q_i skladišča mora biti enaka ali večja zahtevani *Q* skladišča:

2) The calculated Q_i of the warehouse must be equal to or higher than the required *Q* of the warehouse:

$$2 \cdot 3 \cdot N_x \cdot N_y \cdot R \ge Q \quad (19).$$

3) Število RD je lahko manjše ali enako številu regalnih hodnikov ($S \le R$)

Osnovo za določitev števila RD pomeni povprečni čas enojnega in dvojnega delovnega kroga. Le-tega določimo na podlagi analitičnih modelov, ki so vključeni v model načrtovanja. V primeru *sistema* RD *za delo v enem hodniku* ($S = R$) smo za določitev števila RD uporabili analitične modele *Vössnerja* [24], *Hwanga in Leeja* [25]. Za določitev števila RD v primeru *sistema* RD *za delo v več hodnikih* ($S \le R$) smo uporabili izpopolnjene analitične modele *Lerher in sodelavci* ([2] in [15]). Na temelju geometrijske oblike SR, števila zahtevanih enojnih in dvojnih delovnih krogov, povprečnega časa enojnega in dvojnega delovnega kroga, določimo potrebno število transportno-skladiščnih sredstev S_{pot}:

3) The number of SR machines can be lower than or equal to the number of picking aisles ($S \le R$).

The determination of the number of SR machines is based on the average time of the single and dual command cycles. It is determined on the basis of analytical models, which are included in the design model. In the case of the *single-aisle* ASRS ($S = R$), the analytical travel- time models from *Vössner* [24] and *Hwang and Lee* [25] have been applied to the design model. To determine the number of SR machines in the case of the *multi-aisle* ASRS ($S \le R$), the newly improved analytical travel-time models by *Lerher et al.* ([2] and [15]) have been applied. With regard to the layout of the SR, the number of the required SC and DC and the average travel time of SC and DC, the necessary number of pieces of material handling equipment S_{pot} can be determined:

$$S_{pot} = \frac{n_{SC} \cdot T(SC) + n_{DC} \cdot T(DC)}{T \cdot \eta} \quad (20),$$

T [h] pomeni čas delovne izmene.

V primeru uporabe *sistema* RD *za delo v enem hodniku* algoritem v modelu načrtovanja pri pogoju, $S = R$, vsakemu regalnemu hodniku predpiše samostojno RD. Algoritem tudi hkrati preveri, ali je predpisano RD, ki ustreza pogoju, $S = R$, zmožno dosegati zahtevano *Pf* skladišča. Če je izračunana Pf_i manjša od predpisane *Pf*, algoritem izvede izbiro novega tipa RD. Kadar je izbran *sistem* RD *za delo v več hodnikih*, ki omogoča vožnjo v prečnem hodniku, ne potrebujemo samostojnega transportno-skladiščnega sredstva v vsakem regalnem hodniku. V tem primeru je izpolnjen pogoj ($S \leq R$), pri čemer algoritem določi potrebno število RD, vendar ne več kot je število regalnih hodnikov R. Če izračunana Pf_i skladišča ne doseže predpisane *Pf*, se izvede izbira novega tipa RD.

Na podlagi diskretne oblike namenske funkcije *NSS*, nelinearnosti in upoštevanja večjega števila projektnih spremenljivk smo za optimizacijo projektnih spremenljivk v namenski funkciji *NSS* uporabili *postopek genetskih algoritmov*. Genetski algoritmi (GA) so hevristični iskalni algoritmi, ki jih uporabljamo za reševanje zahtevnih analiz in optimizacijskih problemov. Metoda z GA simulira razvojne postopke oz. "preživetje najprilagojenejšega organizma" [17].

V modelu načrtovanja GA naključno ustvari zahtevano število *osebkov v generaciji – organizmu*. Osebek predstavlja ARSS, medtem ko so *geni* v *organizmu* ponazorjeni s spremenljivkami N_x, N_y in S. Spremenljivki Y in R v organizmu nista upoštevani neposredno, saj sta neposredno odvisni od spremenljivk N_x, N_y in S. Na podlagi predpisane namenske funkcije *NSS* in projektnih omejitev GA ovrednoti vsak posamezen *osebek* v *generaciji* in jih razvrsti glede na njihovo oceno – najmanjše celotne stroške. Preostali del *generacij* v GA (npr. 95 %) nastaja s *križanjem*, *reprodukcijo* in *mutacijo*. Postopek optimizacije z GA in pomen posameznih genetskih in razvojnih operatorjev so podrobneje predstavljeni v delih [2] in [17].

2 ANALIZA: PRIMER NAČRTOVANJA ARSS

Z optimizacijo projektnih spremenljivk *S, R, Y,* N_x in N_y v namenski funkciji *Min. TC* smo iskali optimalne različice. Optimalni model ARSS mora ustrezati naslednjim projektnim omejitvam: dolžina skladišča L_{WAR} ($e_1 = 0 - e_2 = 100$) m, širina skladišča

T [h] indicates the time for a working shift.

In the case of the application of the *single-aisle* ASRS, the algorithm in the design model assigns the SR machine to each picking aisle, under the condition $S = R$. At the same time the algorithm examines whether the assigned SR machine, which meets the condition $S = R$, is able to reach the required *Pf* of the warehouse. If the calculated Pf_i is lower than the required *Pf*, the algorithm chooses a new type of SR machine. When the *multi-aisle* ASRS, which enables transferring in the cross aisle, is chosen, then a single SR machine serves multiple picking aisles. In this case the condition ($S \leq R$) is fulfilled, whereby the algorithm determines the necessary number of SR machines, which is not higher than the number of picking aisles R. If the calculated Pf_i does not reach the required *Pf*, a new type of SR machine is chosen.

Considering the discrete form of the objective function *Min. TC*, non-linearity and the proposed decision variables, *the method of genetics algorithms* to optimize the decision variables in the *Min TC* has been applied. Genetics algorithms (GA) are heuristic search algorithms that are used to perform demanding analyses and to solve problems of optimization. The method of GA simulates evolutionary processes "the survival of the most flexible organism" [17].

In the design model, the GA randomly creates the required number of *subjects in a generation – organism.* The subject refers to the ASRS, whereas *genes in the organism* are demonstrated by the decision variables N_x, N_y and S. The variables Y and R are not directly considered in the organism, since they are directly dependent on the variables N_x, N_y and S. Based on the *Min. TC* and project constraints, the GA evaluates each *subject in the generation* and arranges them with regard to their evaluation – the minimum total costs. The rest of the *generations* in the GA (e.g. 95%) are created by *crossover, reproduction* and *mutation*. The optimization process of GA and the meaning of individual genetic and evolutionary operators are presented in detail in [2] and [17].

2 ANALYSIS: AN EXAMPLE OF DESIGNING ASRS

With the optimization of the decision variables *S, R, Y,* N_x and N_y in the *Min. TC*, the optimum design of the ASRS was searched for. The optimum design of the ASRS should suit the following project constraints: the length of the warehouse L_{WAR} ($e_1 = 0 - e_2 = 100$) m,

W_{WAR} ($e_3 = 0 - e_4 = 200$) m in višina skladišča H_{WAR} ($e_5 = 0 - e_6 = 20$) m. Vhodni podatki za analizirani primer temeljijo na podatkih iz prakse. Rezultati analize se nanašajo na izbran ARSS [2], ki je določen z naslednjimi parametri; **(*i*) *vhodni parametri:*** zalogovna velikost skladišča Q = 15000 TSE, pretočna zmogljivost skladišča Pf = 140 TSE/h, **(*ii*) *opravilni parametri skladišča:*** w = 800 mm, g = 1200 mm, h = 800 mm, m = 1000 kg, b_1 = 100 mm, b_2 = 200 mm, n = 3, b_3 = 1100 mm, b_4 = 120 mm, b_5 = 65 mm, b_6 = 162 mm, b_7 = 300 mm, b_8 = 200 mm, b_9 = 1000 mm, b_{10} = 0 mm, T_{01} = 3 s, T_{02} = 3 s, $n_{(SC)}$ = 40, $n_{(DC)}$ = 70, W_{TV} = 800 mm, L_{TV} = 2000 mm, b_{11} = 300 mm, b_{14} = 500 mm, b_{16} = 1800 mm, W_{RD} = 1400 mm, L_{RD} = 2000 mm, b_{22} = 70 %, ***(iii) transportno-skladiščna sredstva:*** RD *za delo v več hodnikih* – Stöklin AT RBG 0-Q: G_{RD} = 1250 kg, H_{RD} = 22000 mm, W_{RD} = 1400 mm, v_x = 3 m/s, v_y = 0,8 m/s, v_i = 0,6 m/s, a_x = 0,5 m/s^2, a_y = 0,8 m/s^2, a_i = 0,4 m/s^2, RD *za delo v enem hodniku* – Single MAN: G_{RD} = 1200 kg, H_{RD} = 21900 mm, W_{RD} = 1400 mm, v_x = 3 m/s, v_y = 1 m/s, a_x = 0,5 m/s^2, a_y = 0,5 m/s^2, *Transportni viličar* – Jungheinrich ERC 214: G_{TV} = 1400 kg, W_{RD} = 800 mm, v_x = 3 m/s, a_x = 0,5 m/s^2, ***(iv) stroški:*** C_1 = 50 €/m^2, C_2 = 168 €/m^2, C_3 = 23 €/m^2, C_4 = 25 €/m^2, C_5 = 30 €/m^2, C_6 = 23 €/m^2, C_7 = 200 €/kos, C_8 = 10 €/RO, C_9 = 5 €/PM, C_{10} = 10 €/m^3, C_{11} = 17000 €/kos, C_{13} = 240000 €/kos, C_{14} = 50 €/m, C_{15} = 40 €/m, C_{16} = 150000 €/m, C_{17} = 50 €/m, b_{23} = 5 %, C_{18} = 12000 €/leto, T = 10, i = 8 (%).

Na temelju opravljene analize optimizacije projektnih spremenljivk v namenski funkciji *NSS* s postopkom *genetskih algoritmov* [17] lahko podamo bistvene sklepe, ki so predstavljeni v diagramih na sliki 4*i,* 4*ii,* 4*iii,* 4*iv*. V nadaljevanju so prikazani diagrami optimizacije projektnih spremenljivk *S, R, Y,* N_x in N_y v namenski funkciji *NSS* pri številu generacij n = 1 in n = 100 v GA.

- **Optimizacija projektnih spremenljivk v namenski funkciji NSS**

V diagramih na sliki 4*i,* 4*ii,* 4*iii,* 4*iv* so predstavljeni rezultati optimizacije projektnih spremenljivk pri številu generacij v GA – n = 1 in n = 100. Odziv optimizacije projektnih spremenljivk *S, R, Y,* N_x in N_y v namenski funkciji *NSS* predstavlja celotne stroške (€) v odvisnosti od števila RO v vodoravni smeri x in v navpični smeri y, pri izbranem *sistemu* RD *za delo v enem ali več hodnikih*. Optimizacija projektnih spremenljivk je bila izvedena glede na naslednje predpisane razvojne in genetske operatorje: *stopnja križanja* – 0,8; *stopnja mutacije*

the width of the warehouse W_{WAR} ($e_3 = 0 - e_4 = 200$) m and the height of the warehouse H_{WAR} ($e_5 = 0 - e_6 = 20$) m. The input data for this example is based on information from practice. The analysis refers to the chosen model of the ASRS [2], which is determined by the following parameters: ***(i) entry-level parameters:*** the storage volume of the warehouse Q = 15000 TUL, throughput capacity of the warehouse Pf = 140 TUL/h, ***(ii) operational parameters of the warehouse:*** w = 800 mm, g = 1200 mm, h = 800 mm, m = 1000 kg, b_1 = 100 mm, b_2 = 200 mm, n = 3, b_3 = 1100 mm, b_4 = 120 mm, b_5 = 65 mm, b_6 = 162 mm, b_7 = 300 mm, b_8 = 200 mm, b_9 = 1000 mm, b_{10} = 0 mm, T_{01} = 3 sec., T_{02} = 3 sec., $n_{(SC)}$ = 40, $n_{(DC)}$ = 70, W_{TV} = 800 mm, L_{TV} = 2000 mm, b_{11} = 300 mm, b_{14} = 500 mm, b_{16} = 1800 mm, W_{RD} = 1400 mm, L_{RD} = 2000 mm, b_{22} = 70 %, ***(iii) material handling equipment:*** the multi-aisle ASRS – Stöklin AT RBG 0-Q: G_{RD} = 1250 kg, H_{RD} = 22000 mm, W_{RD} = 1400 mm, v_x = 3 m/s, v_y = 0,8 m/s, v_i = 0,6 m/s, a_x = 0,5 m/s^2, a_y = 0,8 m/s^2, a_i = 0,4 m/s^2, *the single-aisle ASRS* – Single MAN: G_{RD} = 1200 kg, H_{RD} = 21900 mm, W_{RD} = 1400 mm, v_x = 3 m/s, v_y = 1 m/s, a_x = 0,5 m/s^2, a_y = 0,5 m/s^2, *lift truck* – Jungheinrich ERC 214: G_{TV} = 1400 kg, W_{RD} = 800 mm, v_x = 3 m/s, a_x = 0,5 m/s^2, ***(iv) costs:*** C_1 = 50 €/m^2, C_2 = 168 €/m^2, C_3 = 23 €/m^2, C_4 = 25 €/m^2, C_5 = 30 €/m^2, C_6 = 23 €/m^2, C_7 = 200 €/piece, C_8 = 10 €/RO, C_9 = 5 €/PM, C_{10} = 10 €/m^3, C_{11} = 17000 €/piece, C_{13} = 240000 €/piece, C_{14} = 50 €/m, C_{15} = 40 €/m, C_{16} = 150000 €/m, C_{17} = 50 €/m, b_{23} = 5 %, C_{18} = 12000 €/year, T = 10, i = 8 (%).

Based on the performed analysis of the optimization of the decision variables in the *Min. TC* with the method of GA [17], the main conclusions, which are shown in the diagrams in Figures 4*i*, 4*ii*, 4*iii*, 4*iv*, can be presented. The following section shows the diagrams of the optimization of the decision variables *S, R, Y,* N_x, N_y in the *Min. TC* with the number of generations n =1 and n =100 in the GA.

- **The optimization of decision variables in the objective function minimum total costs**

The diagrams in Figures 4*i*, 4*ii*, 4*iii*, 4*iv* show the results of the optimization of decision variables with the number of generations in the GA n = 1 and n = 100. The response to the optimization of the decision variables *S, R, Y,* N_x, N_y in the *Min. TC* indicates the total costs (€), depending on the number of storage compartments in the horizontal direction x and the vertical direction y for the chosen *single-* or *multi-aisle* ASRS. The optimization of the project variables was carried out according to the following evolutionary and genetics operators: *the degree of crossover* – 0.8; *the*

– 0,05; *stopnja elitizma* – 0,05; *velikost populacije* – 100; *število generacij* – 100. Vrednosti stopnje *križanja*, *mutacije* in *elitizma* so izbrane glede na izkušnje raziskovalcev [17], ki so se ukvarjali z razvojem in uporabo metode GA. Vrednosti so izbrane tako, da rešitev ne zaide v lokalni optimum, temveč je rešitev v globalnem optimumu. Velikost populacije je odvisna predvsem od števila spremenljivk v namenski funkciji *NSS*, kar posredno vpliva tudi na potrebno število generacij. Zaradi sorazmerno majhnega števila projektnih spremenljivk *S, R, Y,* N_x in N_y v namenski funkciji *NSS,* se je pri obsežnem analiziranju izkazalo, da GA v večini primerov najde stroškovno optimalno rešitev že pri stotih generacijah. V primeru večjega števila predpisanih generacij bi

degree of mutation – 0.05; *the degree of elitism* – 0.05; *the size of the population* – 100; *the number of generations* – 100. The values of the *crossover, mutation* and *elitism degrees* are chosen based on the experiences of researchers [17] who have been engaged in the development and application of the GA method. The values are chosen so that the solution does not get into a local optimum, but it lies in the global optimum. The size of the population depends a great deal on the number of decision variables in the *Min. TC*, which indirectly influences the necessary number of generations. Due to the relatively small number of project variables *S, R, Y,* N_x, N_y in the *Min. TC*, the comprehensive analyses has indicated that in most cases the GA finds the most economical solution with just 100 generations. In the case of a larger number of generations, the GA would

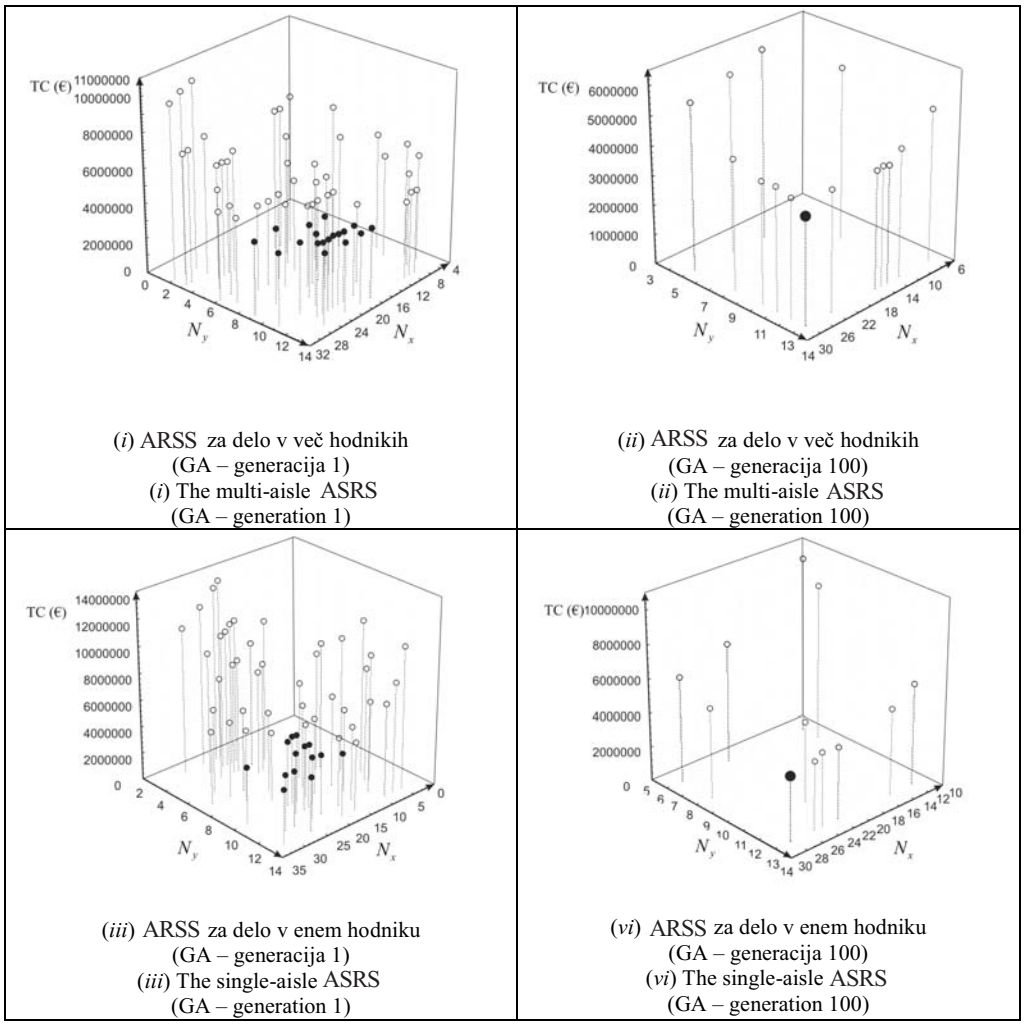

(*i*) ARSS za delo v več hodnikih
(GA – generacija 1)
(*i*) The multi-aisle ASRS
(GA – generation 1)

(*ii*) ARSS za delo v več hodnikih
(GA – generacija 100)
(*ii*) The multi-aisle ASRS
(GA – generation 100)

(*iii*) ARSS za delo v enem hodniku
(GA – generacija 1)
(*iii*) The single-aisle ASRS
(GA – generation 1)

(*vi*) ARSS za delo v enem hodniku
(GA – generacija 100)
(*vi*) The single-aisle ASRS
(GA – generation 100)

Sl. 4. *Diagrami celotnih stroškov sistemov RD za delo v enem in več hodnikih*
Fig. 4. *The total costs of the single- and multi-aisle ASRS*

GA prav tako prišel do rešitve, vendar bi za rešitev porabil več časa.

V diagramih na slikah 4*i* in 4*iii* lahko vidimo, da tvori GA za obe različici transportno-skladiščnega sredstva (RD *za delo v enem hodniku* in RD *za delo v več hodnikih*) izbrano število naključnih različic ARSS. Skladiščne različice, ki ne ustrezajo predpisanim omejitvam, definiranim pri optimizaciji projektnih spremenljivk *S, R, Y,* N_x in N_y v namenski funkciji *NSS*, so izbrisane in na diagramih niso prikazane. Število naključno izbranih različic ARSS je tako enako velikosti populacije *n* ali v večini primerov manjše od *n*. Zaradi naključnega izbire množice ARSS, ki pomenijo nadaljnjo osnovo za optimizacijo, so vrednosti skupnih stroškov v namenski funkciji *NSS* največje prav v generaciji *n* = 1, kar velja za obe različici transportno-skladiščnega sredstva. V diagramih (slika 4*i* in 4*iii*) lahko vidimo, da skladiščne različice, označene s potemnjenimi simboli, pomenijo stroškovno najugodnejše rešitve ARSS. Večina najugodnejših rešitev je v področju večjega števila RO v vodoravni smeri *x* in v navpični smeri *y*, kar pomeni, da imajo omenjene rešitve ARSS na podlagi metode *izbire z razvrščanjem* veliko verjetnost, da bodo vključene v naslednjo generacijo.

Na podlagi predpisanih *razvojnih* in *genetskih* operatorjev se izvedejo naslednje *generacije n* = (1 – 100), pri čemer je vsaka *generacija* boljša ali pa vsaj njej enaka. V diagramih na sliki 4*ii* in 4*iv* so prikazani rezultati optimizacije projektnih spremenljivk pri generaciji *n* = 100. Opazimo lahko, da je število različic ARSS v generaciji *n* = 100 manjše kakor v primerjavi z generacijo *n* = 1, kar nakazuje na pravilno delovanje GA. Stroškovno optimalna rešitev ARSS se navezuje na ARSS z N_x = 28 RO v vodoravni *x* in N_y = 13 RO v navpični smeri *y*, za obe različici transportno-skladiščnega sredstva (v diagramu 4*ii* in 4*iv* označena s potemnjenim simbolom). Vidimo lahko, da so skupni stroški najmanjši (optimalni) pri sorazmerno visokem N_y = 13 in dolgem N_x = 28 SR (glede na podane geometrijske omejitve e_i skladišča) za obe izvedbi transportno-skladiščnih sredstev. Predstavljeno odvisnost lahko komentiramo z dejstvom, da imamo v primeru velikega SR ($>> N_x$ in $>> N_y$), veliko zalogovno velikost *Q*, pri manjšem številu SR ter zato majhno širino skladišča < *W*. Slednje ima za posledico manjše potrebno število transportno-skladiščnih sredstev *S* (še posebej očitno pri *sistemu* RD *za delo v enem hodniku*), kar ima velik vpliv na celotno investicijo skladišča.

also arrive at a solution, but it would take more time to do so.

The diagrams in Figures 4*i* and 4*iii* show that the GA forms a chosen number of random designs of the ASRS for both types of the *single*- and *multi-aisle* ASRS. Warehouses that do not follow the required constraints, defined at the optimization of the decision variables *S, R, Y,* N_x, N_y in the *Min. TC*, are deleted and not considered in the next generations. The number of randomly chosen designs of the ASRS is the same as the size of the population *n* or in most cases smaller than *n*. Because of the random selection of the number of ASRS, which present a further basis for the optimization, the values of the total costs in the *Min. TC* are the highest in the generation *n* = 1, which holds true for both types of the *single*- and *multi-aisle* ASRS. The diagrams ion Figures 4*i* and 4*iii* illustrate that warehouse designs, marked with darkened symbols, present the most economical designs of the ASRS. The majority of the most economical designs lies in the area of a large number of storage compartments in the horizontal direction *x* and the vertical direction *y*. Accordingly, the above-mentioned designs of the ASRS have a strong likelihood of being included in the next generation on the basis of *the selection method with ranging*.

Based on the specified *evolutionary* and *genetics* operators, the next generations *n* = (1 – 100) are carried out, whereby each generation is better or at least equally good. The diagrams in Figures 4*ii* and 4*iv* show the results of the optimization of the decision variables with the generation *n* =100. It can be seen that the number of designs of the ASRS in the generation *n* = 100 is smaller than in the generation *n* = 1, which indicates the correct operation of the GA. The most economical design of the ASRS refers to the ASRS with N_x = 28 storage compartments in the horizontal *x* and N_y = 13 storage compartments in the vertical direction *y*, for both types of storage systems (in diagrams 4*ii* and 4*iv,* marked with a darkened symbol). It can be seen that the total costs are minimum (optimum) at a relatively high N_y = 13 and long N_x = 28 storage racks (with regard to the given geometrical constraints e_i of the warehouse) for both variants of the *single*- and *multi-aisle* ASRS. One can comment on the presented dependence that in the case of a large SR ($>> N_x$ and $>> N_y$) we have a large storage volume *Q*, a small number of SR and consequently a small width of the warehouse < *W*. The latter takes the consequence of a lower number of necessary numbers of SR machines *S* (apparently obvious with the *single-aisle* ASRS), which has a significant influence on the entire investment in the warehouse.

V odvisnosti od *S* lahko vidimo, da pri uporabi *sistema* RD *za delo v enem hodniku* potrebujemo 7 RD, medtem ko pri uporabi *sistema* RD *za delo v več hodnikih* potrebujemo le 4 RD. Čeprav omogoča ARSS s *sistemom* RD *za delo v več hodnikih* samo uporabo 4 RD, je znesek investicije za določen primer ARSS [2] (Q = 15 000 TSE in Pf = 140 TSE/h), približno enak za oba ARSS (3,626 • 10^3 € – slika 4*ii* in 3,800 • 10^3 € – slika 4*iv*). Vrednost RD *za delo v več hodnikih* je za približno 60 % večja od vrednosti RD *za delo v enem hodniku* prav zaradi dodatnih elementov (pomični voziček za vožnjo v prečnem hodniku, dodatna vodila, stikala, obsežnejše krmiljenje itn), ki omogočajo izvedbo skladiščnega opravila. Odločitev o uporabi posameznega *sistema* RD je v največji meri odvisna od zahtevane *Pf* skladišča. V nadaljevanju bo zato prikazana primerjava učinkovitosti (v odvisnosti od *NSS*) *sistema* RD *za delo v enem in več hodnikih* pri različnih *Pf* skladišča.

2.1 Učinkovitost sistemov regalnega dvigala za delo v enem in več hodnikih

V primeru zahteve naročnikov skladišč po izdelavi ARSS se lahko odločamo med *sistemoma* RD *za delo v enem ali več hodnikih*. Kateri od *sistemov* RD se v določenem položaju najbolje obnese, je odvisno predvsem od zahtevane *Pf* skladišča. V analizi smo uporabili ARSS z zalogovno velikostjo Q = 15000 TSE, pri katerem smo spreminjali zahtevano pretočno zmogljivost skladišča v mejah od Pf = 60 do 160 TSE/h, glede na naslednje projektne omejitve: L_{WAR} ($e_1 = 0 - e_2 = 100$) m, širina skladišča W_{WAR} ($e_3 = 0 - e_4 = 200$) m in višina skladišča H_{WAR} ($e_5 = 0 - e_6 = 20$) m. Opravilni parametri, transportno-skladiščna sredstva in stroški se navezujejo na ARSS [2] in so podrobneje predstavljeni v poglavju 3. Rezultati analize v preglednici 1 in na sliki 5, predstavljajo stroškovno optimalne različic ARSS, dobljene z optimizacijo projektnih spremenljivk *S, R, Y,* N_x in N_y v namenski funkciji *NSS* pri generaciji n = 100.

- **Primerjava učinkovitosti sistemov RD za delo v enem in več hodnikih**

V preglednici 1 so prikazane različne izvedbe ARSS v odvisnosti od zahtevane *Pf* skladišča. Osnova za primerjavo *sistemov* RD predstavlja ARSS s *sistemom* RD *za delo v enem hodniku* z naslednjimi osnovnimi podatki: zalogovna velikost

In dependence on the *S,* when applying the *single-aisle* ASRS we need 7 SR machines, whereas when applying the *multi-aisle* ASRS we need only 4 SR machines. Even though the *multi-aisle* ASRS requires the application of only 4 SR machines, the investment in the analysed ASRS [2] (Q = 15000 TUL and Pf = 140 TUL/h) is approximately the same for both types of the *single-* and *multi-aisle* ASRS ($3.626 \cdot 10^3$ € – diagram 4*ii* and $3.800 \cdot 10^3$ € – diagram 4*iv*). The cost of the SR machine for the *multi-aisle* system is approximately 60% higher than the cost of the SR machine for the *single-aisle* system due to additional elements (aisle transferring vehicle for traveling in the cross aisle, additional controls and switches, extensive control system, etc.) which make it possible to operate the warehouse. The decision on the application of a particular *single-* or *multi-aisle* system depends mainly on the required *Pf* of the warehouse. Consequently, in the following section a comparison between the *single-* and *multi-aisle* systems, with regard to various *Pf* of the warehouse, is presented.

2.1 The efficiency of the single- and multi-aisle ASRS

When an order for the creation of the ASRS is placed, we can decide between *the single-aisle* and *multi-aisle* ASRS. Which of both systems is most suitable for a particular case depends largely on the required *Pf* of the warehouse. In the analysis the ASRS with the storage volume Q = 15000 TUL has been used. The required throughput capacity has been changed from Pf = 60 to 160 TUL/h, with regard to the following project constraints: the length of the warehouse L_{WAR} ($e_1 = 0 - e_2 = 100$) m, the width of the warehouse W_{WAR} ($e_3 = 0 - e_4 = 200$) m and the height of the warehouse H_{WAR} ($e_5 = 0 - e_6 = 20$) m. Operational parameters, material handling equipment and costs refer to the ASRS [2] and are presented in detail in Section 3. The analysis results in Table 1 and Figure 5 present the most economical design of the ASRS, obtained from optimizing the decision variables *S, R, Y,* N_x, N_y in the *Min. TC* within the generation n = 100.

- **Efficiency comparison between *the single-* and *multi-aisle* ASRS**

Table 1 shows different types of the ASRS depending on the required *Pf* of the warehouse. The basis for making the comparison between both systems is the *single-aisle* ASRS with the following data: storage volume of the warehouse Q = 15000 TUL, throughput

Preglednica 1: *Primerjava sistema RD za delo v več hodnikih v odvisnosti od sistema RD za delo v enem hodniku*
Table 1. *The comparison of the multi-aisle ASRS in dependence on the single-aisle ASRS*

	PRIMERJAVA ZMOGLJIVOSTI SKLADIŠČA COMPARISON OF THE WAREHOUSE EFFICIENCY					
	$Pf_2 = 60$ [TSE/h] [TUL/h]	$Pf_2 = 80$ [TSE/h] [TUL/h]	$Pf_3 = 100$ [TSE/h] [TUL/h]	$Pf_4 = 120$ [TSE/h] [TUL/h]	$Pf_5 = 140$ [TSE/h] [TUL/h]	$Pf_6 = 160$ [TSE/h] [TUL/h]
Q	15000	15000	15000	15000	15000	15000
R	7	7	7	7	7	7
S	2	3	3	4	4	5
N_x	28	28	28	28	28	28
N_y	13	13	13	13	13	13
η (%)	82	72,2	89	80	94	74
NSS [€] *Min. TC* [€]	$2,960 \cdot 10^3$	$3,284 \cdot 10^3$	$3,284 \cdot 10^3$	$3,609 \cdot 10^3$	$3,626 \cdot 10^3$	$3,951 \cdot 10^3$
Razlika v stroških [€] Differences in costs [€]	$-840 \cdot 10^3$	$-516 \cdot 10^3$	$-516 \cdot 10^3$	$-191 \cdot 10^3$	$-174 \cdot 10^3$	$+151 \cdot 10^3$

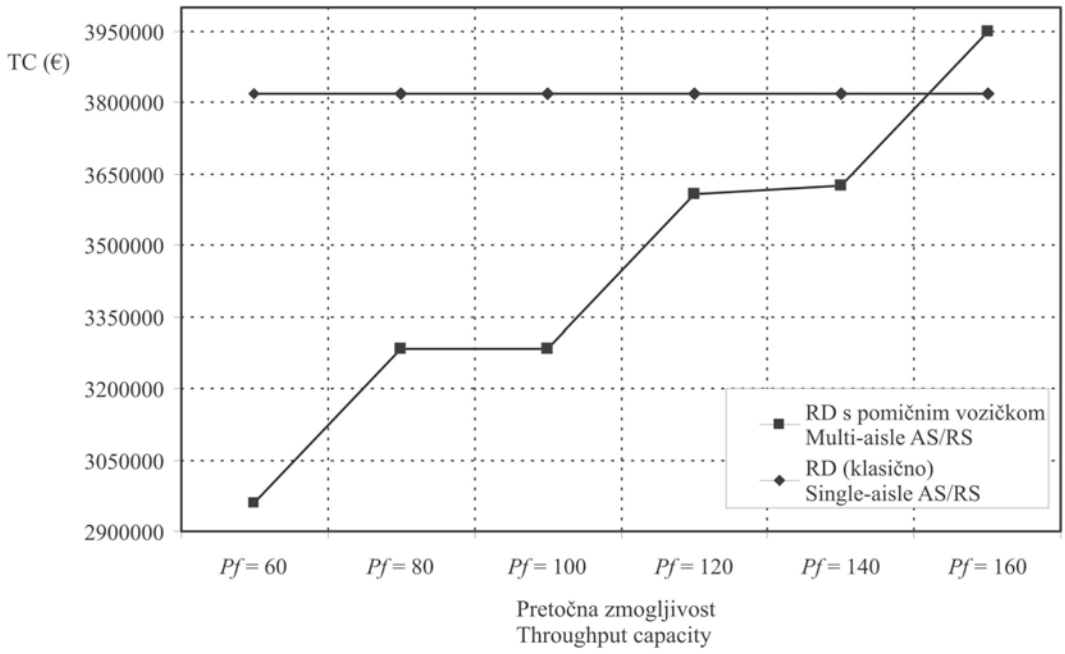

Sl. 5. P*orazdelitev najmanjših skupnih stroškov v odvisnosti od Pf skladišča*
Fig. 5. *Distribution of minimum total costs depending on the Pf of the warehouse*

skladišča Q = 15000 TSE, pretočna zmogljivost skladišča Pf = 160 TSE/h, število regalnih hodnikov R = 7, število RD S = 7, število SR Y = 14, število RO v vodoravni x smeri N_x = 28, število RO v navpični smeri y N_y = 13, najmanjši skupni stroški *NSS* = $3,800 \bullet 10^3$ €.

Na sliki 5 je prikazana odvisnost zahtevane *Pf* skladišča glede na stroškovno optimalno izvedbo ARSS za oba *sistema* RD. Vidimo lahko, da je *sistem*

capacity Pf = 160 TUL/h, the number of picking aisles R = 7, the number of SR machines S = 7, the number of SR Y = 14, the number of storage compartments in the horizontal direction N_x = 28, the number of storage compartments in the vertical direction N_y = 13, and the minimum overall costs *Min. CS* = $3.800 \cdot 10^3$ €.

The diagram in Figure 5 shows the dependence of the required *Pf* of the warehouse, with regard to the most economical design of the ASRS for

RD *za delo v več hodnikih* smiselno uporabiti pri nižjih zmogljivostih skladišča << *Pf*, saj je investicija skladišča neprimerno manjša kakor pri *sistemu* RD *za delo v enem hodniku*. V tem primeru je prispevek pri stroških v primerjavi s *sistemom* RD *za delo v enem hodniku* močno izrazit in znaša 840•10³ € (*Pf* = 60 TSE/h). Z naraščanjem *Pf* skladišča se zmanjšuje tudi prispevek pri stroških in primernost uporabe *sistema* RD *za delo v več hodnikih se zmanjšuje*. V primeru zahtevane pretočne zmogljivosti nad vrednostjo *Pf* = 140 TSE/h je upravičenost omenjenega *sistema* RD že vprašljiva, saj je RD že močno obremenjeno (η = 94 %), prispevek pri stroških pa neizrazit. Opazimo lahko, da je investicija pri vrednosti *Pf* = 160 TSE/h za vrednost 151•10³ € večja v primerjavi s *sistemom* RD *za delo v enem hodniku*, saj je v ARSS treba zagotoviti že 5 RD. Prav tako pa so pri omenjeni pretočni zmogljivosti vprašljivi primernost uporabe in problem vodenja ter nadzora 5 RD pri 7 regalnih hodnikih. Analiza je bila izvedena za primer skladiščne strategije (*i*) naključnega uskladiščenja in (*ii*) naključne odpreme TSE, brez vpeljave skladiščnih con. Z uporabo izpopolnjenih strategij bi bila zmogljivost *sistema* RD *za delo v več hodnikih* neprimerno večja. Sklenemo lahko, da na splošno za (zahtevane) >> *Pf*, pri uporabi klasične naključne skladiščne strategije, uporabimo *sistem* RD *za delo v enem hodniku*. Prav nasprotno velja v primeru sorazmerno << *Pf*, pri katerih pride v poštev predvsem *sistem* RD *za delo v več hodnikih*. Večjo zmogljivost *sistema* RD *za delo v več hodnikih* lahko v največji meri dosežemo prav z uporabo učinkovitejše skladiščne strategije in vpeljave skladiščnih con ABC.

3 SKLEPI

V tem prispevku je predstavljen izpopolnjen model načrtovanja ARSS. Zaradi vedno večje zahtevnosti skladišč in optimiranja skladiščnih virov, prehaja klasični postopek načrtovanja na višje in zahtevnejše stopnje, v obliki računalniško podprtega načrtovanja in optimiranja skladiščnih sistemov [13]. Model načrtovanja je tako zasnovan na sestavljenem postopku [13] in se navezuje na področje enoglobinskega regalnega skladiščnega sistema. Bistveni del v modelu načrtovanja je vpeljava in uporaba dveh različnih *sistemov* RD, in sicer (*i*) *sistem* RD *za delo v enem* ter (*ii*) *sistem* RD *za delo v več hodnikih*. V nasprotju s *sistemom* RD *za delo v enem hodniku* ([24] in [25]) so *sistemi* RD *za delo v*

both systems. It can be seen that at low throughput capacities of the warehouse (<< *Pf*) it is reasonable to apply the *multi-aisle* ASRS, since the investment in the warehouse is much smaller than in the case of the *single-aisle* ASRS. In this case the difference in costs (840·10³ € - *Pf* = 60 TUL/h) is more significant in comparison with the *single-aisle* ASRS. With the rising of the *Pf* of the warehouse, the costs increase and also the appropriateness of applying the *multi-aisle* ASRS decreases. If the required throughput capacity is above *Pf* = 140 TUL/h, the application of the *multi-aisle* ASRS becomes rather questionable, since the SR machines are already overloaded (η = 94%) and the differences in costs are quite small. It can be seen that the investment within *Pf* = 160 TUL/h is larger for the value of 151·10³ € in comparison with the single-aisle ASRS, since 5 SR machines must be used in the ASRS. Additionally, in the above-mentioned *Pf* the application and the problem of the management and control of 5 SR machines at 7 picking aisles is rather questionable. The analysis has been carried out for the case of (*i*) random storage strategy and (*ii*) random retrieval strategy, without the introduction of the class-based storage. With the application of improved strategies, the efficiency of the *multi-aisle* ASRS would be much higher. It can be concluded that for the required >> *Pf*, with the application of the classical random strategy, we should generally apply the *single-aisle* ASRS. The opposite holds true for relatively << *Pf*, where especially the *multi-aisle* ASRS should be applied. A higher efficiency of the *multi-aisle* ASRS can be achieved by applying the most effective storage strategies and introducing a class-based ABC storage system.

3 CONCLUSIONS

In this paper an improved design model of the ASRS is presented. Due to the great complexity and the difficult optimization of the warehouse, the conventional design process rises to higher and more demanding levels, in the form of the computer-aided design and optimization of warehousing systems [13]. The presented design model is based on the structured approach [13] and refers to the single deep-storage system with several picking aisles. The essential part of the design model is the application of two different systems: (*i*) the *single-aisle* ASRS and (*ii*) the *multi-aisle* ASRS. Unlike the *single-aisle* ASRS ([24] and [25]) the *multi-aisle* ASRS has not been investigated much in the literature

več hodnikih v literaturi veliko manj raziskani [22]. Zato smo v model načrtovanja vključili izpopolnjen analitični model za določitev zmogljivosti omenjenih sistemov [2]. Zaradi zahtev po stroškovno optimalni in hkrati tehnično zelo zmogljivi izvedbi skladišča, smo oblikovali namensko funkcijo *Min. TC*. Namenska funkcija je predstavljena z matematičnim modelom, ki vključuje projektne spremenljivke (S, R, Y, N_x, N_y), vse pomembne obratovalne in fizične parametre ter investicijske in obratovalne stroške [2]. Zaradi nelinearnosti namenske funkcije, njene diskretne oblike in predlaganih projektnih spremenljivk smo za optimizacijo projektnih spremenljivk v namenski funkciji *NSS* uporabili *postopek genetskih algoritmov* ([16] in [17]). Na temelju rezultatov optimizacije projektnih spremenljivk v namenski funkciji *Min. TC* in glede na določen *sistem* RD, lahko podamo naslednje glavne sklepe opravljene analize:

Glede na vrednost skupnih stroškov (diagrami na slikah 4*i*, 4*ii*, 4*iii* in 4*iv*) v odvisnosti od števila RO v vodoravni smeri x in v navpični smeri y, lahko povzamemo, da je stroškovno optimalna različica ARSS (za oba *sistema* RD) dosežena pri visokem N_y = 13 RO in dolgem N_x = 28 RO skladiščnem regalu. Omenjena odvisnost se navezuje na določen ARSS in predpisane projektne omejitve skladišča e_i [2]. Ugotovitev lahko pojasnimo z dejstvom, da veliki SR omogočajo doseganje visoke Q skladišča, kar vpliva na manjše število hodnikov R in zato na manjšo površino skladišča. To ima za posledico manjše število RD < S (še posebej očitno pri *sistemu* RD *za delo v enem hodniku)*, kar se izkazuje skozi celotne stroške investicije.

V odvisnosti primerjave *sistema* RD *za delo v enem in več hodnikih* (sl. 5) opazimo izrazit vpliv *Pf* skladišča na znesek celotne investicije. Analiza je bila izvedena za določen ARSS z zalogovno velikostjo Q = 15000 TSE in pretočno zmogljivostjo, ki smo jo spreminjali v mejah od *Pf* = (60 do 160) TSE/h [2]. Splošna ugotovitev glede naraščanja zahtevane *Pf* skladišča je, da je za obravnavani ARSS, pri << *Pf* skladišča, primerno uporabiti *sistem* RD *za delo v več hodnikih*. V primeru uporabe *sistema* RD *za delo v več hodnikih* pri zahtevani *Pf* = 60 TSE/h, znaša odstopanje med *sistemoma* RD 840•10^3 €, kar narekuje nujno potrebo po vrednotenju obeh izvedb RD v postopku načrtovanja skladišč. Na sliki 5 lahko vidimo, da se znesek investicije v odvisnosti od zahtevane *Pf* skladišča povečuje diskretno in ustreza izbiri vse do vrednosti *Pf* = 140 TSE/h. Nad omenjeno

[22]. Therefore, newly improved analytical travel-time models for the *single*- and *multi-aisle* systems have been included in the design model [2]. Due to requirements for the most economical design and at the same time technically highly efficient warehouse, the objective function *Min. TC*. has been formed. The objective function is represented by a mathematical model, which includes the decision variables (S, R, Y, N_x, N_y), all the relevant operational and physical parameters, the investment and the operating costs [2]. Due to the non-linearity of the *Min. TC*, its discrete shape and proposed decision variables, *the method of genetics algorithms* has been applied ([16] and [17]) in order to optimize the decision variables. On the basis of the results of the optimization of the decision variables in the *Min. TC* and with regard to the *single*- and *multi-aisle* system, the following conclusions can be drawn.

With regard to the total costs (the diagrams in Figures 4*i*, 4*ii*, 4*iii*, 4*iv*) in accordance with the number of storage compartments in the horizontal direction x and the vertical direction y, it can be concluded that the most economical design (for both types of the ASRS) is achieved with a high, (N_y = 13 storage compartments), and long (N_x = 28 storage compartments) storage rack. The above-mentioned dependence refers to the analysed ASRS and the prescribed project constraints e_i [2]. This finding can be explained with the fact that large SRs enable the achievement of a high warehouse volume of the warehouse, which influences a small number of picking aisles R and consequently a smaller width of the warehouse. Therefore, the number of SR machines is lower < S (particularly evident with the *single-aisle* ASRS), which shows in the overall costs of the investment.

Depending on the comparison of the *single*- and *multi-aisle* ASRS (Figure 5), a significant influence of the *Pf* of the warehouse on the total costs of the investment can be seen. The analysis was carried out for the ASRS with the storage volume Q = 15000 TUL and throughput capacity that was changed within the limits of *Pf* = (60 to 160) TUL/h [2]. The general ascertainment regarding the increase of the required *Pf* of the warehouse is that for the particular ASRS, at << *Pf* of the warehouse, it is reasonable to apply the *multi-aisle* ASRS. If the *multi-aisle* ASRS is applied at the required *Pf* = 60 TUL/h, there is a deviation (of 840·10^3 €) between the two systems, which calls for of the need to evaluate both *single*- and *multi-aisle* systems in the design process. Figure 5 indicates that the investment according to the required *Pf* of the warehouse increases

vrednostjo je smiselno izbrati *sistem* RD *za delo v enem hodniku*, saj je *sistem* RD *za delo v več hodnikih* že močno obremenjen in obsega že štiri RD pri sedmih regalnih hodnikih (S = 4, R = 7). Predstavljena odvisnost na sliki 5 ima zelo velik pomen pri načrtovanju skladišč in omogoča ustrezno izbiro *sistema* RD v odvisnosti od zalogovne velikosti Q in zahtevane pretočne zmogljivosti Pf skladišča.

steadily and suits the choice up to the value Pf = 140 TUL/h. Above this value it is reasonable to choose the *single-aisle* ASRS, since the *multi-aisle* ASRS is already overloaded and encompasses four SR machines with seven picking aisles (S = 4, R = 7). The dependence shown in Figure 5 is extremely important when designing warehouses, since it enables the appropriate choice of the ASRS depending on the warehouse volume Q and the required throughput capacity Pf of the warehouse.

Zahvala

Projekt razvoja orodja za načrtovanje in optimiranje avtomatiziranih regalnih skladiščnih sistemov je med drugimi v okviru projekta "*Združitev kapacitet in razvoj znanja za realizacijo projektov visoko regalnih skladišč*" podprlo in sofinanciralo podjetje Metalprim d.o.o. iz Maribora.

Avtorja prispevka, bi se na tem mestu še posebej rada zahvalila vodstvu podjetja za vsestransko podporo in vzpodbudo pri nastanku znanstveno-raziskovalnega dela ter vsem sodelavcem na Fakulteti za strojništvo v Mariboru, ki so kakorkoli pripomogli k nastanku omenjenega dela.

Acknowledgments

The project of the development of a tool for designing and optimizing ASRS has been among others supported and financed by the Metalprim d.o.o. company from Maribor.

The authors of this paper would like to express special thanks to the management of this company for their complete support and encouragement for setting up this scientific and research project. Also, we would like to extend this thanks to all collaborators at the Faculty of Mechanical Engineering and others colleagues who have in any way contributed to this project.

4 OZNAKE
4 NOMENCLATURE

Projektne spremenljivke			**Decision variables**
število regalnih hodnikov	R		the number of picking aisles
število skladiščnih regalov	Y		the number of SR
število regalnih dvigal	S		the number of S/R machines
število regalnih oken v vodoravni smeri	N_x		the number of storage compartments in the horizontal direction
število regalnih oken v navpični smeri	N_y		the number of storage compartments in the vertical direction
Operacijski parametri			**Operational parameters**
zalogovna velikost skladišča	Q	TSE/TUL	warehouse volume (rack capacity)
pretočna zmogljivost	Pf	TSE/h / TUL/h	throughput capacity
število TSE v regalnem oknu	n		the number of TUL in storage compartment
širina palete	w	mm	the width of the pallet
dolžina palete	g	mm	the length of the pallet
višina TSE	h	mm	the height of the TUL
število enojnih delovnih krogov	n_{SC}		the number of single command cycles
število dvojnih delovnih krogov	n_{DC}		the number of dual command cycles
povprečni čas enojnega delovnega kroga	T(SC)	s	the average single command cycle time
povprečni čas dvojnega delovnega kroga	T(DC)	s	the average dual command cycle time

čas za delovno izmeno	T	h	time for one shift
zmogljivost regalnega dvigala	η		the efficiency of the S/R machine
dolžina regalnega veznika (nosila)	L_v	mm	the length of the rack beam
dodatek za ojačitev skladiščnih regalov	PD	%	the addition to the reinforcement of storage racks,
dolžina regalnega okna	L_{RO}	mm	the length of the storage compartment
višina regalnega okna	H_{RO}	mm	the height of the storage compartment
globina regalnega okna	G_{RO}	mm	the width of the storage compartment
dolžina skladiščnega regala	L_{RS}	mm	the length of the SR
višina skladiščnega regala	H_{RS}	mm	the height of the SR
dolžina transportne cone	L_{TZ}	mm	the length of the transport zone
dolžina skladišča	L_{WAR}	mm	the length of the warehouse
višina skladišča	H_{WAR}	mm	the height of the warehouse
širina skladišča	W_{WAR}	mm	the width of the warehouse
površina zemljišča za skladišče	P_Z		the surface of the land for the warehouse
delež zazidanosti skladišča	D_Z		the share of the built warehouse
varnostni dodatek za širino regalnega okna	b_1	mm	the safety addition to the width of the storage compartment
varnostni dodatek za višino regalnega okna	b_2	mm	the safety addition to the height of the storage compartment
širina stebra	b_4	mm	the width of the upright frame,
debelina stebra	b_5	mm	the thickness of the upright frame
višina regalnega nosila	b_6	mm	the height of rack beams
odmik regalnega okna od tal	b_7	mm	the deviation of the storage compartment from the floor
varnostni razmik med soležnimi regali	b_8	mm	the safety spacing between racks that are placed close to each other
varnostni dodatek za višino skladišča	b_9	mm	the safety addition to the height of the warehouse
dodatek za širino palete na prevzemnem mestu	b_{10}	mm	the addition to the width of the palette at input buffer
dodatek na koncu skladišča	b_{20}	mm	the addition to the end of the warehouse
Investicijski parametri			**Investment cost parameters**
strošek za nakup zemljišča	C_1	€/m^2	cost of buying the land
strošek za postavitev temeljne plošče	C_2	€/m^2	cost of laying the foundations
strošek za postavitev sten skladišča	C_3	€/m^2	warehouse cost of building the walls of the
strošek za postavitev strehe skladišča	C_4	€/m^2	cost of building the roof of the warehouse
strošek za nakup regalnih stranic	C_5	€/m^2	cost of buying upright frames
strošek za nakup regalnih veznikov	C_6	€/m^2	cost of buying rack beams
strošek za nakup prevzemnih miz	C_7	€	cost of buying buffers
strošek montaže	C_8	€	cost of the assembly
strošek požarne varnosti	C_9	€	cost of fire safety
strošek prezračevanja	C_{10}	€	cost of air ventilation
strošek za nakup transportnega viličarja	C_{11}	€	cost of buying a lift truck
strošek za nakup regalnega viličarja	C_{12}	€	cost of buying a reach truck
strošek za nakup regalnega dvigala	C_{13}	€	cost of buying S/R machine
strošek regalnega hodnika	C_{14}	€	cost of the picking aisle
strošek prečnega hodnika	C_{15}	€	cost of the cross aisle
strošek zveznega transporterja	C_{16}	€	cost of the accumulating conveyor
strošek preusmeritvenega elementa	C_{17}	€	cost of the diverted element

Parametri stroškov obratovanja			**Operational cost parameters**
delež vrednosti regalnega dvigala za vzdrževanje	P	%	the share of the value of the S/R machine for maintenance
strošek osebnega dohodka za viličariste, ki delajo z transportnimi in regalnimi viličarji	C_{OD}	€	the cost of personal income for operators working with lift trucks and reach trucks
neto sedanja vrednost	NPV	–	net present value
predvidena življenska doba obratovanja ARSS	T_i	let/years	the anticipated life expectancy of the operation of the AS/RS
diskontna stopnja	r	%	the discount rate

5 LITERATURA
5 REFERENCES

[1] Bartholdi, J. J. (2002) Warehouse and distribution science. School of Industrial and System Engineering, *Georgia Institute of Technology*, Atlanta.

[2] Lerher, T. (2005) Model for designing automated storage and retrieval systems, Ph.D. dissertation. *Faculty of Mechanical engineering, University of Maribor*.

[3] Rosenblatt, M. J., Roll, J. (1993) A combined optimization and simulation approach for designing automated storage and retrieval systems, *IIE Transactions*, vol. 25, no. 1, str. 40–50.

[4] Siemens Dematic, http://siemens.de/logistics-assembly

[5] Stöcklin Logistik, http://www.sld.ch

[6] Dambach, http://www.dambach.de

[7] Bassan, Y., Roll, Y., Rosenblatt, M. J. (1980) Internal layout design of a warehouse, *AIIE Transactions*, vol. 12, št. 4, str. 317–322.

[8] Karasawa, Y., Nakayama, H., Dohi, S. (1980) Trade-off analysis for optimal design of automated warehouses, *International Journal of System Science,* vol. 11, št. 5.

[9] Ashayeri, J., Gelders, L. F. (1985) A microcomputer-based optimization model for the design of automated warehouses, *International Journal of Production Research*, vol. 23, št. 4, str. 825–839.

[10] Bafna, K. M., Reed, R. (1972) An analytical approach to design of high-rise stacker crane warehouse Systems. *Journal of Industrial Engineering,* vol. 4, št. 10, str. 8–14.

[11] Perry, R. F., Hoover, S. F., Freeman, D. R. (1983) Design of automated storage and retrieval systems using simulation modeling, Institute of Industrial Engineers, Atlanta, Georgia, *ICAW Proceedings*, str. 57–63.

[12] Rosenblatt, M. J., Roll, J. (1984) Warehouse design with storage policy considerations, *International Journal of Production Research*, vol. 22, št. 5, str. 809–821.

[13] Rouwenhorst, B., Reuter, B. (2000) Warehouse design and control: Framework and literature review, *European Journal of Operational Research*, vol. 122, št. 3, str. 515–533.

[14] Drobir, T.J. (2004) Spielzeitberechnung kurvengängiger Hochregallagersysteme: Dissertation. Ph.D. dissertation. *Techniche Universität Graz*.

[15] Lerher, T., Sraml, M., Kramberger, J., Borovinsek, M., Zmazek, B., Potrc, I. (2005) Analytical travel time models for multi aisle automated storage and retrieval systems. *Int. j. adv. manuf. technol.* Electronic publication: http://dx.doi.org/10.1007/s00170-005-0061-6

[16] Genetics algorithm, http://www.lapthorn.net/article/3/a-simple-c-genetic-algorithm.

[17] Holland, J.H. (1975) Adaption in natural and artificial systems, *MIT Press*.

[18] Potrč, I., Lerher, T., Kramberger, J., Šraml, M. (2003). Analytical and simulation approach for design of automated storage and retrieval systems. *Int. j. simul. model*, Vol. 2, No. 3, 70-77.

[19] Buchmeister, B., Kremljak, Z., Pandza, K., Polajnar, A. (2004). Simulation study on the performance analysis of various sequencing rules, *Int. J. Simul. Model*, Vol. 3, No. 2-3, 80-89.

[20] Lerher, T. (2005). Design and evaluation of the class-based multi-aisle automated storage and retrieval systems. *Int. J. Simul. Model*, Vol. 5, No. 1.

[21] Fahnert, V., Kunz, D. (1976) Rechnergestützte Entwicklung eines Warenverteilungssystems für Betriebe mit gemischter Lager und Kundenfertigung - Schlussbericht, Aachen.
[22] Hwang, H., Ko Chang, S. (1988) A study on multi-aisle system served by a single storage/retrieval machine, *International Journal of Production Research*, vol. 26, no. 11, str. 1727–1737.
[23] Azadivar, F. (1986) Maximization of the throughput of a computerized automated warehousing systems under systems constraint. *International Journal of Production Research*, vol. 24, št. 3, str. 551–566.
[24] Vössner, S. (1994) Spielzeitberechnung von Regalförderzeugen, Ph.D. Dissertation, *Techniche Universität Graz*.
[25] Hwang, H., Lee, S. B. (1990) Travel time models considering the operating characteristics of the storage and retrieval machine, *International Journal of Production Research*, vol. 28, št. 10, str. 1779–1789.

Naslov avtorjev: dr. Tone Lerher
prof.dr. Iztok Potrč
Univerza v Mariboru
Fakulteta za strojništvo
Smetanova 17
2000 Maribor
tone.lerher@uni-mb.si
iztok.potrc@uni-mb.si

Authors' address: Dr. Tone Lerhet
Prof.Dr. Iztok Potrč
University of Maribor
Faculty of Mechanical Eng.
Smetanova 17
2000 Maribor, Slovenia
tone.lerher@uni-mb.si
iztok.potrc@uni-mb.si

Prejeto: 30.11.2005
Received:
Sprejeto: 23.2.2006
Accepted:
Odprto za diskusijo: 1 leto
Open for discussion: 1 year

Strojniški vestnik - Journal of Mechanical Engineering 52(2006)5, 292-308
UDK - UDC 004.94:621.039.519:532.5
Izvirni znanstveni članek - Original scientific paper (1.01)

Simuliranje eksplozije pare v reaktorski votlini s splošnim programom za računsko dinamiko tekočin

Simulation of a Reactor Cavity Steam Explosion with a General Purpose Computational Fluid Dynamics Code

Matjaž Leskovar - Boštjan Končar - Leon Cizelj
(Institut "Jožef Stefan", Ljubljana)

Do eksplozije pare v reaktorski votlini lahko pride, če med hipotetično resno nezgodo v jedrski elektrarni popusti reaktorska posoda in se staljena sredica izlije v vodo, ki je v reaktorski votlini. Eksplozija pare je pojav medsebojnega delovanja goriva in hladiva pri katerem je časovna lestvica prenosa toplote s staljene sredice na vodo manjša od časovne lestvice za tlačno razbremenitev. To lahko povzroči tlačne udarne valove in kasneje, med raztezanjem pare, ki je pod visokim tlakom, nastanek izstrelkov, ki lahko poškodujejo okoliške objekte. Namen prispevka je predstaviti, kako je eksplozije pare mogoče obravnavati s splošnim programom za računsko dinamiko tekočin (RDT), podati vpogled v dogajanja med eksplozijo pare v reaktorski votlini tipičnega tlačnovodnega jedrskega reaktorja, in podati grobo oceno ogroženosti sten reaktorske votline in reaktorske posode ob eksploziji pare. Za dosego teh ciljev smo najprej razvili ustrezen namenski model eksplozije pare in nato opravili obsežno, primerno konzervativno parametrično analizo eksplozije pare v poplavljeni reaktorski votlini. Večfazni tok v reaktorski votlini med raztezanjem visokotlačne mešanice razpršene taline, kapljevite vode in vodne pare smo simulirali s programom CFX-5.7.1 za RDT, napetosti v stenah reaktorske votline pa s programom za simulacijo mehanike trdnin ABAQUS/Explicit.
© 2006 Strojniški vestnik. Vse pravice pridržane.
(Ključne besede: reaktorji jedrski, nezgode reaktorjev, eksplozija pare, votlina reaktorska, računska dinamika tekočin)

A reactor cavity steam explosion might occur when, during a hypothetical severe reactor accident, the reactor vessel fails and the molten core pours into the water in the reactor cavity. A steam explosion is a fuel-coolant interaction process where the heat transfer from the melt to the water is so intense and rapid that the timescale for the heat transfer is shorter than the timescale for the pressure relief. This could lead to the formation of shock waves and the production of missiles at later times, during the expansion of the highly pressurized water vapour, which might endanger surrounding structures. The purpose of the paper is to demonstrate how steam explosions can be treated with a general purpose Computational Fluid Dynamics (CFD) code, to give an insight into the steam-explosion phenomenon in a typical Pressurized Water Reactor (PWR) cavity, and to provide a rough assessment of the vulnerabilities of cavity structures to steam explosions. To achieve this, a fit-for-purpose steam-explosion model was developed, followed by a comprehensive and reasonably conservative parametric steam-explosion study. The multiphase flow in the reactor cavity during the high-pressure pre-mixture expansion was simulated with the CFD code CFX-5.7.1 and the stresses in the reactor cavity walls were determined with the stress-analysis code ABAQUS/Explicit.
© 2006 Journal of Mechanical Engineering. All rights reserved.
(Keywords: nuclear reactor accident, steam explosion, reactor cavity, computational fluid dynamics)

0 UVOD

Eno od najpomembnejših nerešenih vprašanj na področju taljenja sredice med hipotetično resno

0 INTRODUCTION

One of the most important remaining issues in core-melt progression during a hypothetical severe

nezgodo v jedrski elektrarni je, kakšna je verjetnost nastanka eksplozije pare in kakšne so lahko njene posledice. Eksplozija pare se lahko razvije, ko pride staljena sredica v stik s hladilno vodo v reaktorski votlini. Eksplozija pare je pojav interakcije goriva in hladiva, pri katerem je časovna lestvica prenosa toplote s staljene sredice na vodo manjša od časovne lestvice tlačne razbremenitve ([1] do [3]). To lahko povzroči tlačne udarne valove in kasneje med raztezanjem pare, ki je pod visokim tlakom, nastanek izstrelkov, ki lahko poškodujejo okoliške objekte. Eksplozija pare je zapleten, močno nelinearen, večsestavinski in večfazen pojav, ki poteka na različnih krajevnih in časovnih lestvicah. Posledično je modeliranje eksplozij pare zelo zahtevno, negotovosti simuliranj resnih nezgod opravljenih z računalniškimi programi, ki temeljijo na modeliranju osnovnih pojavov eksplozije pare, pa so še vedno zelo velike. Zato je za oceno ogroženosti sten reaktorske votline in reaktorske posode med eksplozijo pare potreben parametričen postopek, ki zajame negotovosti razumevanja in modeliranja eksplozije pare. V ta namen smo razvili parametričen model eksplozije pare, ki ga je mogoče preprosto uporabiti in neposredno vključiti v splošne programe za računsko dinamiko tekočin (RDT).

Glavni namen opravljene študije je predstaviti, kako je eksplozije pare mogoče obravnavati s splošnim programom za RDT, podati fizikalno sliko dogajanj med eksplozijo pare v reaktorski votlini tipičnega tlačnovodnega jedrskega reaktorja in podati grobo oceno ogroženosti sten reaktorske votline in reaktorske posode ob eksploziji pare. Eksplozijo pare smo modelirali kot raztezajočo se visokotlačno mešanico staljene sredice, kapljevite vode in vodne pare, ki je v delno poplavljeni reaktorski votlini. Podoben, vendar manj zahteven postopek so uporabili tudi v študiji eksplozije pare, ki je predstavljena v [4]. Večfazni tok med raztezanjem visokotlačne mešanice smo simulirali s programom CFX-5.7.1 za RDT [12], napetosti v stenah reaktorske votline pa s programom za simulacijo mehanike trdnin ABAQUS/Explicit [13].

1 OPIS MODELA

1.1 Model eksplozije pare

Pri mešanju dveh kapljevin, pri katerih je temperatura ene kapljevine višja od temperature vrelišča druge, lahko pride do eksplozije pare. Potek

accident in a nuclear power plant is the likelihood and the consequences of a steam explosion, which might occur when the hot core melt comes into contact with the coolant water. A steam explosion is a fuel-coolant interaction process where the heat transfer from the melt to the water is so intense and rapid that the timescale for the heat transfer is shorter than the timescale for the pressure relief ([1] to [3]). This could lead to the formation of shock waves and the production of missiles at later times, during the expansion of the highly pressurized water vapour, which might endanger surrounding structures. A steam explosion is a complex, highly non-linear, coupled multi-component, multi-phase, multi-space-scale and multi-time-scale phenomenon. Consequently, the modelling of steam explosions is a difficult task and the uncertainties of reactor simulations performed with steam-explosion codes based on modelling fundamental steam explosion processes are still large. Therefore, for assessing the vulnerability of reactor-cavity structures to an ex-vessel steam explosion a parametric approach capturing the uncertainties in steam-explosion understanding and modelling is needed. For this purpose a comprehensive parametric steam-explosion model that can also be straightforwardly implemented in general purpose Computational Fluid Dynamics (CFD) codes was developed.

The main purpose of the performed study was to present how steam explosions can be treated with a general purpose CFD code, to give an insight into the steam-explosion phenomenon in a typical Pressurized Water Reactor (PWR) cavity, and to provide a rough assessment of the vulnerabilities of cavity structures to steam explosions. The steam explosion was modelled as an expanding high-pressure pre-mixture of dispersed molten fuel, liquid water and vapour in the partially flooded reactor cavity. A similar, but less sophisticated, approach was also used in the steam-explosion study presented in [4]. The multiphase flow during the high-pressure pre-mixture expansion was simulated with the CFD code CFX-5.7.1 [12] and the stresses in the cavity walls were determined with the stress analysis code ABAQUS/Explicit [13].

1 MODEL DESCRIPTION

1.1 Steam Explosion Model

Steam explosions are a subclass of what is called fuel-coolant interactions (FCI) in the safety studies of nuclear reactors. Based on the phenomena

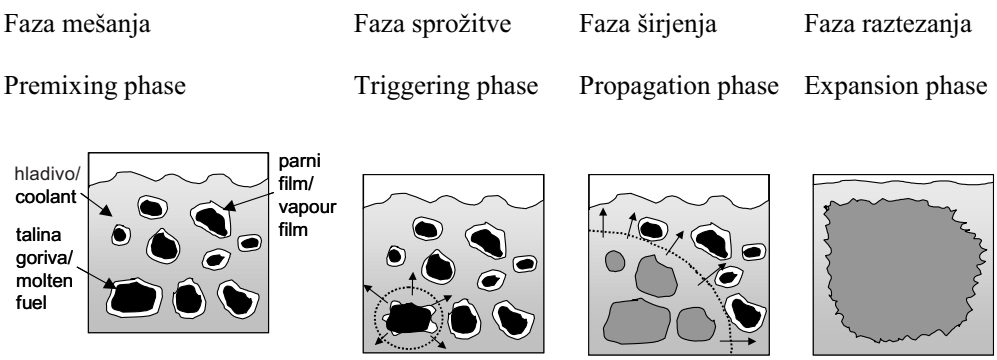

Sl. 1. *Shema štirih zaporednih faz eksplozije pare*
Fig. 1. *Schematic presentation of the four consecutive phases of the steam explosion*

eksplozije pare lahko glede na dogajanja razdelimo v štiri zaporedne faze: faza mešanja, faza sprožitve, faza širjenja in faza raztezanja (sl. 1).

V **fazi mešanja** nastane območje, v katerem je staljena sredica grobo pomešana s hladilno vodo. Ker so delci taline obdani s plastjo pare, je prenos toplote s taline na vodo razmeroma majhen. V **fazi sprožitve** se eksplozija pare sproži. Sprožitveni dogodek je motnja, ki destabilizira plast pare okoli nekega delca taline, tako da pride do neposrednega stika med talino in vodo, ki privede do lokalnega povečanja prenosa toplote in povišanja tlaka ter fine fragmentacije delca. Med **fazo širjenja** pride do stopnjevanja eksplozije pare zaradi sklopitve potujočih tlačnih valov, fine fragmentacije delcev in prenosa toplote po sprožitvenem dogodku. Med **fazo raztezanja** se toplotna energija hladiva spreminja v mehansko energijo. Raztezanje visokotlačne mešanice razpršenega staljenega goriva, vode in vodne pare, ki povzroča odmikanje okoliških tekočin in tlačno obremenitev okoliških struktur, določa možen obseg škode, ki jo lahko povzroči eksplozija pare. Bolj izčrpen opis posameznih faz eksplozije pare je podan v [1] do [3].

Da bi lahko obravnavali eksplozijo pare s splošnim programom za RDT, smo razvili ustrezen parametrični model eksplozije pare. Za razliko od specializiranih programov za RDT za simulacijo eksplozij pare, pri katerih eksplozije pare modelirajo na mikroskali z osnovnimi povprečenimi ohranitvenimi enačbami večfaznega toka ([1], [2], [5] do [7]), v predstavljenem postopku eksplozijo pare modeliramo kot raztezajočo se visokotlačno mešanico razpršene taline goriva, kapljevite vode in vodne pare. Podoben postopek so uporabili tudi v študiji eksplozije pare, predstavljeni v [4], kjer so eksplozijo

occurring during a steam explosion it can be divided into four consecutive phases: the premixing phase, the triggering phase, the propagation phase and the expansion phase (Fig. 1).

In the **pre-mixing phase** a coarsely mixed region of molten corium and coolant water is formed. The melt and the water are separated by a vapour film, so the heat transfer between the melt and the water is relatively low. In the **triggering phase** the steam explosion is triggered. The triggering event is a disturbance that destabilizes the vapour film around a melt particle allowing liquid-liquid contact, which leads to locally enhanced heat transfer, pressurization and local fine fragmentation. During the **propagation phase** there is an escalation process resulting from the coupling between the pressure-wave propagation, the fine fragmentation, and the heat transfer after the triggering event. During the **expansion phase** the thermal energy of the coolant is converted into mechanical energy. The expansion of the high-pressure pre-mixture of dispersed molten fuel, water and vapour against the inertial constraints imposed by the surroundings determines the damage potential of the steam explosion. A more comprehensive description of the steam-explosion phases is presented in [1] to [3].

To be able to treat the steam explosion with a general purpose CFD code, an appropriate fit-for-purpose analytical model of the steam explosion was developed. In contrast to specialized steam-explosion CFD codes, where the steam explosion is modelled on a micro-scale using fundamental averaged multiphase flow conservation equations ([1], [2], [5] to [7]), in the presented approach the steam explosion is modelled reasonably simplified as an expanding high-pressure pre-mixture of dispersed molten fuel, liquid water and vapour. A similar approach was also used in the steam-explosion study presented in [4], where the steam

pare obravnavali bolj preprosto kot raztezajoč visokotlačni parni mehur.

V splošnem predlagani model eksplozije pare temelji na Hicks-Menziesovem termodinamičnem postopku [1], vendar poleg tega upošteva tudi zamisel mikrointerakcijskega območja [8]. Zamisel mikrointerakcijskega območja praktično pomeni, da med eksplozijo pri termični interakciji med delci taline in hladivom ne sodeluje celotno hladivo, ampak le tisto, ki se nahaja v okolici delcev taline. Na sliki 2 je shematično prikazan model eksplozije pare. Staljena sredica je označena s črno barvo in nadpisom *cor*, vodna para s svetlo sivo barvo in nadpisom *vap* in kapljevita voda s temno sivo barvo in nadpisom *wat*. Predpostavili smo, da si vse faze delijo isto hitrostno polje in isti tlak, kar je smiselna poenostavitev. V prikazani nadzorni prostornini je vsaka faza opisana s prostorninskim deležem faze α, prostornino V, gostoto ρ in temperaturo T. Mikrointerakcijsko

explosion was treated less sophisticatedly as an expanding high-pressure vapour bubble.

In general, the developed steam-explosion model is based on the Hicks-Menzies thermodynamic approach [1], taking into account the micro-interaction zone concept [8]. According to the micro-interaction zone concept not all the coolant thermally participates in the explosion, but only the coolant that is in the surrounding of the melt particles. In Figure 2 the steam-explosion model is schematically presented. The corium phase is denoted by the black colour and the superscript *cor*, the vapour phase by the light-grey colour and the superscript *vap,* and the liquid water phase with the dark-grey colour and the superscript *wat*. It was assumed that all the phases share the same velocity field and the same pressure, which is a reasonable simplification. In the presented control volume each phase is described with the phase volume fraction α, volume V, density ρ and temperature T.

a) Faza mešanja (indeks 1) / Premixing phase (index 1)

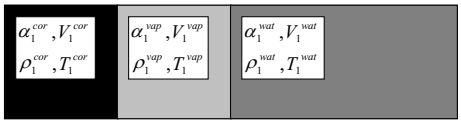

b) Faza sprožitve in širjenja / Triggering and Propagation phase

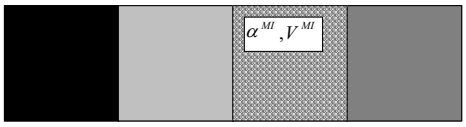

c) Konec faze širjenja in začetek faze raztezanja (indeks 2) / End of Propagation phase and Start of Expansion phase (index 2)

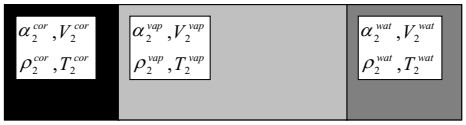

d) Konec faze raztezanja (indeks 3) / End of Expansion phase (index 3)

Sl. 2. *Shema modela eksplozije pare (črna – staljena sredica, svetlo siva – para, temno siva – kapljevita voda, pikčasta siva – kapljevita voda v mikrointerakcijski coni)*

Fig. 2. *Schematic presentation of steam-explosion model (black – molten core, light grey - vapour, dark grey – liquid water, dotted grey – liquid water in micro-interaction zone)*

območje je označeno s pikčasto sivo barvo in indeksom *MI*.

V modelu smo predpostavili, da se ves prenos toplote med staljenim gorivom in hladivom dogodi v prvih treh fazah eksplozije pare in da se v fazi raztezanja proizvedena para, ki je pod visokim tlakom, razteza adiabatno. Opravljeno delo med predpostavljeno adiabatno fazo raztezanja $A_{2,3}$ lahko izračunamo iz enačbe:

The micro-interaction zone is denoted with the dotted grey colour and the index *MI*.

In the model it was assumed that all the heat transfer from the molten fuel to the coolant occurs during the first three steam-explosion phases, and that during the expansion phase the generated vapour, which is at high pressure, adiabatically expands. The work performed during the presumed adiabatic expansion phase $A_{2,3}$ can be calculated as:

$$A_{2\to3} = \int_{V_2^{vap}}^{V_3^{vap}} pdV = -\frac{p_2\left(V_2^{vap}\right)^{\kappa}}{\kappa-1}\frac{1}{V^{\kappa-1}}\Bigg|_{V_2^{vap}}^{V_3^{vap}} = \frac{p_2 V_2^{vap}}{\kappa-1}\left(1-\left(\frac{p_3}{p_2}\right)^{\frac{\kappa-1}{\kappa}}\right) \quad (1),$$

kjer sta p_2 in p_3 tlaka na začetku in na koncu faze raztezanja, κ pa razmerje med specifično toploto pare pri stalnem tlaku in pri stalni prostornini. Pomemben parameter eksplozije pare je energijski izkoristek eksplozije pare, ki ga merijo tudi pri preizkusih eksplozije pare, in pomeni razmerje med opravljenim mehanskim delom med eksplozijo in začetno notranjo energijo staljene sredice [1]. V našem modelu pomeni energijski izkoristek eksplozije pare η osnovo za izračun vseh preostalih parametrov eksplozije pare. Ko izberemo razmere med fazo mešanja, lahko tlak na začetku faze raztezanja p_2 izračunamo iterativno z enačbo:

where p_2 and p_3 are the pressures at the start and the end of the expansion phase, and κ is the ratio of the vapour specific heats at constant pressure and at constant volume. An important parameter of the steam explosion is the steam-explosion energy-conversion ratio, which is also quantified in steam-explosion experiments and reflects how much internal energy of the melt is transformed into the mechanical energy of the explosion [1]. In our model the steam-explosion energy-conversion ratio, η, was used as the basis for the calculation of all the other steam-explosion parameters. After the conditions during the pre-mixing phase are chosen, the pressure at the start of the expansion phase, p_2, can be calculated by iteratively solving the equation:

$$p_2 = \eta\frac{(\kappa-1)\rho_1^{cor}\alpha_1^{cor}c^{cor}\left(T_1^{cor}-T_1^{sat}\right)}{\alpha_2^{vap}\left(1-\left(\frac{p_3}{p_2}\right)^{\frac{\kappa-1}{\kappa}}\right)} \quad (2),$$

kjer so p_3 tlak v zadrževalnem hramu, c^{cor} specifična toplota sredice in T_1^{sat} temperatura nasičenja vode pri tlaku v zadrževalnem hramu. Prostorninski delež mikrointerakcijskega območja α^{MI}, ki določa prostorninski delež pare na začetku faze raztezanja $\alpha_2^{vap} = \alpha^{MI} + \alpha_1^{vap}$, smo izbrali tako, da je bil tlak p_2 na začetku faze raztezanja največji, pri čemer smo upoštevali fizikalno izvedljivost pojava. Zaradi predpostavke o adiabatnem raztezanju pare je mogoče gostoto mešanice med raztezanjem $\rho_{2\to3}^{mix}$ izračunati le kot funkcijo tlaka:

where p_3 is the containment pressure, c^{cor} is the core specific heat and T_1^{sat} is the water-saturation temperature at the containment pressure. The volume fraction of the micro-interaction zone α^{MI}, which determines the vapour volume fraction at the beginning of the expansion phase $\alpha_2^{vap} = \alpha^{MI} + \alpha_1^{vap}$, was chosen in such a manner that the pressure at the start of the expansion phase, p_2, was maximized, considering the physical feasibility of the process. Due to the assumption of the adiabatic vapour expansion, the density of the pre-mixture during the expansion process $\rho_{2\to3}^{mix}$ can be calculated solely as a function of pressure:

$$\rho_{2\to3}^{mix}(p) = \frac{\rho_2^{mix}}{\left(1-\alpha_2^{vap}\right)+\frac{\alpha_2^{vap}\rho_2^{vap}}{\rho_{2\to3}^{vap}(p)}} = \frac{\rho_2^{mix}}{1+\alpha_2^{vap}\left(\left(\frac{p_2}{p}\right)^{\frac{1}{\kappa}}-1\right)} \quad (3),$$

kjer sta ρ_2^{mix} gostota mešanice na začetku faze raztezanja in $\rho_{2\to3}^{vap}$ gostota pare med fazo raztezanja.

where ρ_2^{mix} is the pre-mixture density at the start of the expansion phase and $\rho_{2\to3}^{vap}$ is the vapour density during the expansion phase.

Z razvitim analitičnim modelom eksplozije pare določimo začetne pogoje na začetku faze raztezanja, samo fazo raztezanja pa je treba simulirati s programom za RDT ob upoštevanju enačbe stanja mešanice (en. 3). Pomanjkljivost predlaganega parametričnega modela eksplozije pare je, da je izračunan tlak mešanice p_2 na začetku faze raztezanja odvisen od izbranih razmer med fazo mešanja, saj je mogoče doseči enak energijski izkoristek eksplozije pare η z različnimi kombinacijami prostorninskega deleža pare v mešanici α_2^{vap} in tlaka mešanice p_2 (nižji α_2^{vap} povzroči višji p_2). Ker so razdiralne posledice eksplozije odvisne predvsem od tlačnega sunka (tj. integrala tlaka po času), ta lastnost modela ni resna pomanjkljivost za našo študijo. Namreč, pri nižjem α_2^{vap} je zaradi enačbe stanja mešanice (en. 3) tudi čas trajanja tlačnega impulza krajši, kar nadomesti vpliv povišanega največjega tlaka. Sicer pa je treba zaradi velikih negotovosti razumevanja in modeliranja eksplozij pare pri kateremkoli postopku postopati dovolj konservativno. Natančen opis razvitega modela eksplozije pare je podan v [9].

1.2 Model računske dinamike tekočin

Večfazni tok med četrto fazo eksplozije pare, tj. fazo raztezanja, smo simulirali s programom CFX-5.7.1. Večfazni tok sestavljajo tri faze: faza mešanice (mešanica razpršenega staljenega goriva, kapljevite vode in vodne pare), faza kapljevite vode in faza zraka. Da bi lahko opazovali tudi tlačne valove, smo vse tri tekočine obravnavali kot stisljive in jih modelirali s homogenim Eulerjevim modelom, ki predpostavlja, da si vse faze delijo skupno hitrostno in tlačno polje. Vpliv turbulence smo upoštevali z modelom turbulence k-ε. Energijske enačbe ni bilo treba reševati, saj smo prenos toplote med eksplozijo pare upoštevali že pri začetnih pogojih, ohlajanje pare v mešanici med raztezanjem pa smo upoštevali že z adiabatno enačbo stanja mešanice (en. 3). Enačbo stanja vode smo določili po standardnih preglednicah pare, zrak pa smo obravnavali kot idealen plin. Za preostale snovske lastnosti smo vzeli vrednosti, ki jih podaja program CFX-5.7.1.

Ker se izračuni RDT niso zbliževali na razmeroma redki numerični mreži, ki bi bila s fizikalnega vidika sicer ustrezna, in ker bi bili potrebni računski časi za izračun na trirazsežni (3D) zgoščeni

With the developed analytical steam-explosion model the initial conditions at the start of the expansion phase are determined, whereas the expansion phase itself has to be simulated with the CFD code, taking into account the derived equation of state for the pre-mixture (Eq. 3). The drawback of the proposed parametrical steam-explosion model is that the calculated pre-mixture high-pressure p_2 at the start of the expansion phase depends on the chosen pre-mixing conditions, since an identical steam-explosion energy conversion ratio η can be obtained with different combinations of the pre-mixture vapour fraction α_2^{vap} and pre-mixture pressure p_2 (lower α_2^{vap} results in a higher p_2). As the destructive consequences of an explosion depend mainly on the pressure impulse of the explosion (i.e., the integral of pressure over time), this characteristic of the model does not present a severe weakness for our study. Namely, according to the pre-mixture equation of state (Eq. 3), the duration of the pressure impulse is also shorter at lower α_2^{vap}, which compensates for the effect of the increased pressure peak. In any case, due to the large uncertainties in the understanding and modelling of steam explosions, a sufficient degree of conservatism has to be introduced in whichever approach is taken. A detailed description of the developed steam-explosion model is provided in [9].

1.2 Computational Fluid Dynamics Model

The multiphase flow during the steam-explosion expansion phase, consisting of three phases – the pre-mixture phase (mixture of dispersed molten fuel, liquid water and vapour), the liquid water phase and the air phase – was simulated using the CFX-5.7.1 code. To simulate the pressure waves, all three fluids were treated as compressible and were modelled by the homogeneous Eulerian model, which assumes that all the phases share a common velocity and pressure field. The effect of turbulence was taken into account with the k-ε turbulence model. The energy equation was not solved since the heat transfer during the steam explosion was taken into account already during the initial conditions, and the cooling of the vapour in the pre-mixture during the expansion process was taken into account already within the adiabatic pre-mixture equation of state (Eq. 3). The equation of state for water was determined using the standard water steam tables and air was treated as an ideal gas. For the other material properties the default values as provided by the CFX-5.7.1 code were used.

Since the CFD calculation did not converge on a relatively coarse numerical grid appropriate from the physical point of view, and since the required CPU times

mreži bistveno predolgi, smo izračune opravili z dvorazsežnim (2D) geometrijskim modelom. Da bi zagotovili, da bodo rezultati simuliranj z 2D modelom kakovostno in kolikostno veljavni tudi za pravo 3D geometrijsko obliko reaktorske votline, je bilo treba izbrati ustrezno 2D geometrijsko obliko in ustrezne začetne ter robne pogoje. Zato smo uporabili dva različna 2D modela 3D geometrije reaktorske votline: **osno simetrični model**, ki je omejen na osno simetrične pojave v valjastem delu reaktorske votline neposredno pod reaktorsko posodo in okoli nje, ter **2D model reaktorske votline**, ki sicer obravnava celotno reaktorsko votlino, vendar ne upošteva 3D geometrijske oblike reaktorske votline in 3D narave pojavov. Geometrijska oblika in mreža 2D modela reaktorske votline sta prikazani na sliki 3. Natančen opis razvitega modela RDT je podan v [9].

Težave z zbliževanjem zaradi nezveznih začetnih pogojev smo odpravili tako, da smo vse

for the three-dimensional (3D) calculation on the refined grid would be exceedingly long, the calculations were performed using a two-dimensional (2D) geometry model. To ensure that the simulation results with the 2D model would also be qualitatively and quantitatively valid for the real 3D geometry of the reactor cavity, the 2D geometry and the initial conditions had to be appropriately selected. Therefore, the simulations were performed using two different 2D approximations for the 3D geometry of the reactor cavity: the **axially symmetric model**, which is limited to axially symmetric phenomena in the cylindrical part of the reactor cavity directly below the reactor vessel and around it; and the **2D cavity model**, which treats the whole reactor cavity but does not take into account the 3D geometry of the cavity and the 3D nature of the phenomena. The geometry and mesh of the 2D cavity model are presented in Figure 3. A detailed description of the CFD model is provided in [9].

To avoid convergence problems due to discontinuous initial conditions, all the discontinuous

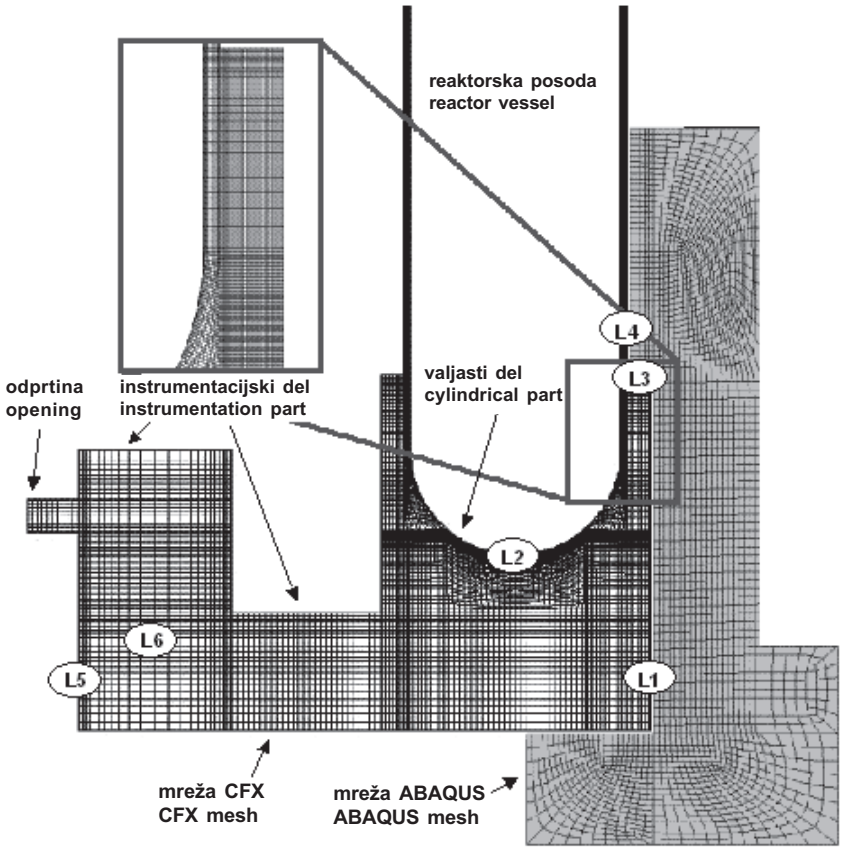

Sl. 3. *Geometrijska oblika in mreža modela CFX računske dinamike tekočin za 2D model reaktorske votline in model mehanike trdnin ABAQUS za osno simetričen model stene reaktorske votline*
Fig. 3. *Geometry and mesh of CFX computational fluid dynamics 2D cavity model of reactor cavity and ABAQUS structural axially symmetric model of cavity wall*

nezvezne začetne pogoje ustrezno zgladili z zvezno odvedljivo posplošeno sigmoidno funkcijo:

$$y(x) = 1 - \frac{1}{1 + e^{-10\frac{(x-x0)}{\Delta x}}} \quad (4),$$

kjer je $x0$ točka, v kateri se funkciji $y(x)$ spremeni vrednost od 1 na 0 prek območja Δx. Na sliki 4 je predstavljen graf funkcije (en. 4) za $x0 = 1$ z $\Delta x/x0 = 0{,}1$ (črna krivulja) in $\Delta x/x0 = 0{,}2$ (siva krivulja) v primerjavi z nezvezno funkcijo (prekinjena črta).

Pri opravljenih izračunih smo vse nezvezne začetne pogoje smiselno zgladili prek območja 10% v navpični smeri in prek območja 20% v vodoravni smeri. Z zvezno odvedljivo funkcijo je bilo treba zgladiti predvsem začetno tlačno polje, saj se je, najverjetneje zaradi uporabljene interpolacijske sheme Rie-Chow v programu za RDT, tudi rešitev zglajenega začetnega problema, pri katerem pa je bila uporabljena nezvezno odvedljiva funkcija, razhajala po nekaj časovnih korakih. Interpolacijska shema Rhie-Chow se v programih za RDT uporablja za izračun tlaka na nepremaknjenih numeričnih mrežah in pri obravnavi velike večine splošnih tokov ne povzroča težav [10].

initial conditions were appropriately smoothed with the continuously differentiable sigmoid-type function:

where $x0$ is the point where the function $y(x)$changes its value from 1 to 0 over the range Δx. In Figure 4 the graph of the function (Eq. 4) is presented for $x0 = 1$ with $\Delta x/x0 = 0{,}1$ (black curve) and with $\Delta x/x0 = 0{,}2$ (grey curve) in comparison with the discontinuous function (dotted line).

In the performed simulations all the discontinuous initial conditions were reasonably smoothed over the range of 10% in the vertical direction and over the range of 20% in the horizontal direction. In particular, the initial pressure field had to be smoothed with a continuously differentiable function, since most probably due to the used Rhie-Chow pressure interpolation scheme in the CFD code, also the solution of a smoothed initial problem, but with a discontinuous differentiable function, diverged after just a few performed time steps. The Rhie-Chow interpolation scheme is used in CFD codes for the pressure calculation on collocated numerical grids and works relatively well for the vast majority of general flows [10].

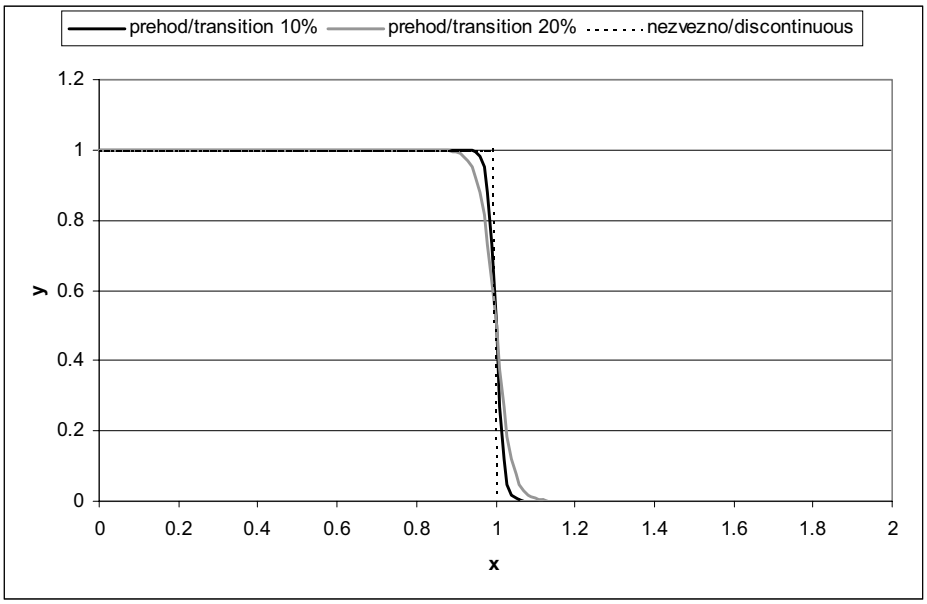

Sl. 4. *Graf posplošene sigmoidne funkcije za 10% in 20% območje prehoda Δx/x0 v primerjavi z nezvezno funkcijo*

Fig. 4. *Graph of sigmoid-type function for 10% and 20% transition range Δx/x0 in comparison with discontinuous function*

1.3 Model mehanike trdnin

Glede na problem smo ocenili, da za ustrezno modeliranje sten reaktorske votline zadoščata dva modela: **osno simetrični model** valjastega dela reaktorske votline in **3D model** instrumentacijskega dela reaktorske votline. Modela ustrezno upoštevata dejstvo, da so stene reaktorske votline do določene višine obdane s temelji zadrževalnega hrama.

Vse stene, ki so v tipičnem tlačnovodnem jedrskem reaktorju izpostavljene mogočim vplivom eksplozije pare, so narejene iz armiranega betona. Predpostavili smo, da je najmanjša potrebna tlačna trdnost betona 30 MPa in da je najmanjša natezna trdnost betonskega jekla 400 MPa. V simulacijah smo gradiva modelirali zelo poenostavljeno, saj naš cilj ni bil natančno napovedovanje poteka deformacij zapletenega nehomogenega železobetona, ampak predvsem zaznavanje pomembnih poškodb. Zato smo predpostavili, da se železobeton tako pri tlačnih kakor nateznih napetostih odziva kot homogen in pretežno elastičen material. Ob predpostavki, da je v železobetonu 10 vol.% železa, smo za dejanske parametre našega homogenega modela izračunali naslednje vrednosti: gostota 2945 kg/m^3, Young-ov modul 45 GPa in Poissonovo razmerje 0,174. Predpostavili smo, da je meja plastičnosti 250 MPa in tako omogočili uporabo modelov poškodb, ki so na voljo v programu ABAQUS/Explicit. Predpostavili smo, da pride do poškodb, če hidrostatični tlak (natezni ali tlačni) preseže vrednost 50 MPa. Obremenitve sten vključujejo lastno težo in potek tlaka, ki smo ga dobili iz rezultatov simuliranj s programom CFX. Časovne in krajevne spremembe tlaka smo vključili v program ABAQUS/Explicit s FORTRAN podprogramom VDLOAD. Vrednosti med razpoložljivimi podatki smo določili z linearno interpolacijo po času in po kraju.

Na sliki 3 je prikazana mreža končnih elementov za osno simetričen model stene reaktorske votline. Natančen opis modela mehanike trdnin je podan v [9].

2 REZULTATI

2.1 Potek eksplozije pare

Da bi dobili fizikalno sliko dogajanja med eksplozijo pare v poplavljeni reaktorski votlini tipičnega tlačnovodnega jedrskega reaktorja in da bi okvirno ocenili tlačne obremenitve sten reaktorske

1.3 Structural Model

Based on the geometry of the problem, it is deemed sufficient to develop two models: an **axially symmetric model** of the cylindrical part of the reactor cavity and a **3D model** of the in-core instrumentation access. These models properly take into account the fact that the cavity walls are to a significant height embedded by the foundation of other containment structures.

All the walls potentially affected by the steam explosion in a typical PWR reactor cavity are made of heavily reinforced concrete. The minimum required compressive strength of the concrete was assumed to be 30 MPa, and the minimum required yield strength of the reinforcement steel was assumed to be 400 MPa. The material model used in the simulations is simplified to a significant extent and is aimed at the detection of significant damage rather than to give an accurate account on the deformation history of the complex and non-homogeneous reinforced concrete. A homogeneous and essentially elastic response was therefore assumed, both in tension and compression. The main "effective" parameters of the homogenous model, assuming about 10 vol.% of reinforcement steel, were as follows: a density of 2945 kg/m^3, a Young's modulus of 45 GPa and a Poisson's ratio of 0.174. The yield stress of 250 MPa was arbitrarily assumed to enable the use of approximate damage models, which are built in the ABAQUS/Explicit code. The damage was assumed to occur with hydrostatic pressure (tensile or compressive) exceeding 50 MPa. The loads include dead weight and pressure histories obtained from the CFX simulation results. The variations of pressures in time and space were included in the ABAQUS/Explicit code using the FORTRAN subroutine VDLOAD. Linear interpolation between the data points was used both in space and in time.

The finite-element model of the cavity walls for the axially symmetric model is presented in Figure 3. A detailed description of the structural model is provided in [9].

2 RESULTS

2.1 Steam-Explosion Scenario

A comprehensive reasonably conservative parametric analysis considering different steam-explosion scenarios was performed to get an insight into the steam-explosion phenomenon in a typical

votline in reaktorske posode med eksplozijo pare, smo opravili obsežno, smiselno konservativno parametrično analizo različnih potekov eksplozije pare [9]. V tem prispevku predstavljamo le dva tipična primera eksplozije pare, ki se razlikujeta po kraju izliva taline (stranski izliv in osrednji izliv). Skupne predpostavke v obeh predstavljenih primerih so naslednje: tlak v zadrževalnem hramu: 1,5 bar; temperatura vode v reaktorski votlini: 343 K; raven vode v reaktorski votlini: 3 m; temperatura staljene sredice: 2800 K; velikost izliva taline: 0,25 m^2; primarni sistem je tlačno razbremenjen, prostorninski deleži v mešanici: staljena sredica 0,1; vodna para 0,1; kapljevita voda 0,8 in energijski izkoristek eksplozije pare 1 odstotek, kar privede do tlaka mešanice 400 bar. Pri preizkusih s prototipičnimi gradivi sredice (UO_2+ZrO_2, itn.) ([1] do [3]) so bili največji izkoristki eksplozij pare približno 0,5 odstotka in največje izmerjene vrednosti tlačnih konic približno 200 bar. Glede na te preizkuse, ki so bili opravljeni na pomanjšanih modelih reaktorskih razmer, so izbrane predpostavke konservativne.

Primer 1 predstavlja stranski izliv taline na koncu reaktorske votline, ki privede do nastanka mešanice debeline 0,5 m, **primer 2** pa predstavlja izliv taline v sredini reaktorske votline, ki privede do nastanka mešanice z radijem 0,8 m.

2.2 Rezultati simuliranj in razprava

Da bi dobili kakovostno in kolikostno sliko večfaznega toka med eksplozijo pare v reaktorski votlini, so na slikah 5 in 6 predstavljeni osnovni rezultati simulacij RDT četrte faze eksplozije pare, tj. faze raztezanja, za stranski izliv taline (primer 1) in za osrednji izliv taline (primer 2). Na slikah je prikazan časovni razvoj tlačnega polja in prostorninskega deleža mešanice ter vode. Za osrednji izliv taline je prikazano tudi hitrostno polje. Vidimo, da se fazne meje med mešanico, vodo in zrakom, ki so na začetku simulacije ostre, s časom razlezejo zaradi numerične difuzije, ki je značilna za diskretne numerične metode ([5] in [7]). Ta razpršitev medfaznih površin zaradi narave našega postopka obravnave eksplozije pare nima večjega vpliva na bistvene rezultate simuliranj in prav tako ne na sklepe opravljene študije.

Za simuliranje primera 1 (stranski izliv taline; slika 5) smo uporabili 2D model reaktorske votline, ki obravnava celotno reaktorsko votlino. Izhodišče eksplozije pare pri začetnem času (t =0 sekund) je

PWR cavity, to provide a rough estimation of the expected pressure loadings on the cavity structures during a steam explosion and to assess the vulnerabilities of cavity structures to steam explosions [9]. In this paper only two typical cases differing in the location of the melt pour (side pour and central pour) are presented in some detail. The common assumptions of the presented cases are as follows: containment pressure, 1.5 bar; cavity water temperature, 343 K; water level in cavity, 3 m; core temperature, 2800 K; melt pour size, 0.25 m^2; and a depressurised primary system. The pre-mixture volume fractions are as follows: core 0.1, vapour 0.1, liquid water 0.8, and steam explosion energy conversion ratio 1%, resulting in the pre-mixture pressure of 400 bar. During experiments with prototypic corium materials (UO_2+ZrO_2, etc.) ([1] to [3]) the maximum obtained steam-explosion energy conversion ratios are about 0.5%, and the maximum measured peak pressures are about 200 bar, so the assumptions are conservative regarding these small-scale experiments.

Case 1 presents a side-melt pour resulting in a pre-mixture of width 0.5 m at the cavity-end side, and **Case 2** presents a central-melt pour resulting in a pre-mixture with radius 0.8 m in the cavity centre.

2.2 Simulation Results and Discussion

To get a qualitative and quantitative picture of the multiphase flow during the steam explosion in the reactor cavity, in Figures 5 and 6 the basic results of the CFD simulation of the steam-explosion expansion phase for the side-melt pour (Case 1) and the central-melt pour (Case 2) are presented. In the figures the time development of the pressure field and the volume fractions of the mixture and water are shown. For the central melt pour the velocity field is also presented. It can be seen that the initially sharp interfaces between the mixture, the water and the air phases spread during the transient due to numerical diffusion, which is characteristic for discrete numerical methods ([5] and [7]). Due to the nature of our modelling approach this interface spreading has no significant influence on the main simulation results and on the conclusions of the performed study.

For the simulation of Case 1 (side-melt pour; Figure 5) the 2D cavity model, treating the entire reactor cavity in 2D, was used. The origin of the steam explosion at the initial time (t = 0 seconds) is indicated by the

označeno s svetlo sivo pobarvanim visokotlačnim območjem in s svetlo sivo pobarvanim območjem mešanice na desni strani pod reaktorsko posodo. Zaradi visokega tlaka v mešanici, ki nastane zaradi burnega uparjanja, se začne mešanica raztezati in odrivati vodo in zrak iz reaktorske votline skozi ozek obročast kanal okoli reaktorske posode in skozi odprtino na levi strani reaktorske votline v instrumentacijskem delu. Med dvigovanjem ravni vode le ta trči v dno reaktorske posode (t = 0,013 s) in na tem območju povzroči lokalni porast tlaka, ki potiska reaktorsko posodo na stran in navzgor. Mešanica se razteza hitreje v navpični smeri proti zraku, saj je gostota zraka precej manjša od gostote vode. Po 0,044 s mešanica trči v zgornji del reaktorske votline (točka L3 na sliki 3), kjer se začne ozek obročast del reaktorske votline, in tam se tlak krajevno zviša. Medtem ko se tlak v reaktorski votlini naglo znižuje, se mešanica razteza še naprej in potiska vodo proti instrumentacijskem delu reaktorske votline. Po približno pol sekunde doseže raven vode odprtino v instrumentacijskem delu in voda začne odtekati v zadrževalni hram. Največje hitrosti tekočin presežejo 300 m/s in so dosežene na izhodu iz obročastega kanala po približno 0,05 s.

Primer 2 (osrednji izliv taline; sl. 6) smo simulirali z osno simetričnim modelom reaktorske votline, ki obravnava le valjasti del reaktorske votline. Področje, kjer pride do eksplozije pare, je označeno s svetlo sivo pobarvanim visokotlačnim območjem in s svetlo sivo pobarvanim območjem mešanice ob simetrijski osi pod reaktorsko posodo. Zaradi visokega tlaka v mešanici se začne mešanica, ki je v sredini reaktorske votline, raztezati in odrivati vodo in zrak skozi obročast kanal okoli reaktorske posode. Po 0,0125 s je mešanica praktično popolnoma obdana z vodo, saj se lahko voda odmika le navzgor (v stranskih stenah valjastega dela reaktorske votline nismo modelirali nobenih odprtin). Kasneje, ko so tlaki že nizki, steče voda nazaj v reaktorsko votlino in ustvari se velik vrtinec. Največje hitrosti tekočin presežejo 300 m/s in so dosežene na izhodu iz obročastega kanala po približno 0,05 s.

Na slikah 7 in 8 je prikazan potek tlaka v izbranih krajih, ki so pomembne z vidika ocene ogroženosti sten reaktorske votline in reaktorske posode. Te lokacije so označene na sliki 3 z L1 do L6. Pri 2D modelu reaktorske votline so tlačne krivulje podane za vse lokacije L1 do L6 (sl. 7), medtem ko lahko pri osno simetričnem modelu, zaradi omejene

light-grey-coloured high-pressure region and by the light-grey coloured pre-mixture region embedded on the right-hand side below the reactor vessel. Due to the high pressure in the mixture, which is caused by the generated vapour, the mixture phase expands and pushes the water and air out of the cavity through the annulus around the reactor vessel and through the opening on the left-hand side in the instrumentation part of the cavity. As the water level rises, the water eventually hits the bottom of the reactor vessel (t = 0.013 s) causing a local pressure increase in this region, pressing the vessel sideways and upwards. The mixture phase expands faster towards the air since the density of air is much lower than the density of water. After 0.044 s the mixture phase hits the upper part of the cavity (point L3 in Figure 3), where the narrow annular part of the cavity begins, and the pressure there locally increases. As the pressure rapidly decreases with time, the mixture phase expands further and pushes the water towards the instrumentation part of the cavity. After about half a second the water level in the instrumentation part reaches the opening and is discharged into the containment. The maximum fluid velocities are above 300 m/s and are reached at the outlet of the annulus at about 0.05 s.

Case 2 (central-melt pour; Figure 6) was simulated using the axially symmetric cavity model, where only the cylindrical part of the reactor cavity is treated. The area indicating the origin of the steam explosion is shown with the light-grey-coloured high-pressure region and with the light-grey-coloured mixture region embedded below the centre of the reactor vessel. The high-pressure in the pre-mixing zone in the central part of the cavity causes an expansion of the mixture, which pushes the water and air through the annulus around the reactor vessel. After 0.0125 s the mixture is practically completely surrounded with water, as the water can be pushed only upwards (no openings in the side walls of the cylindrical part of the cavity are modelled). At later times, when the pressure is already low, the water flows back into the cavity and a big vortex is formed. The maximum fluid velocities are above 300 m/s and are reached at the outlet of the annulus at about 0.05 seconds.

In Figures 7 and 8 the pressure histories at selected locations, which are of importance for the assessment of the vulnerability of cavity structures, are presented. These locations are denoted in Figure 3 with L1 to L6. At the 2D cavity model the pressure curves are given for all the locations L1 to L6 (Figure 7), whereas for the axially symmetric model the

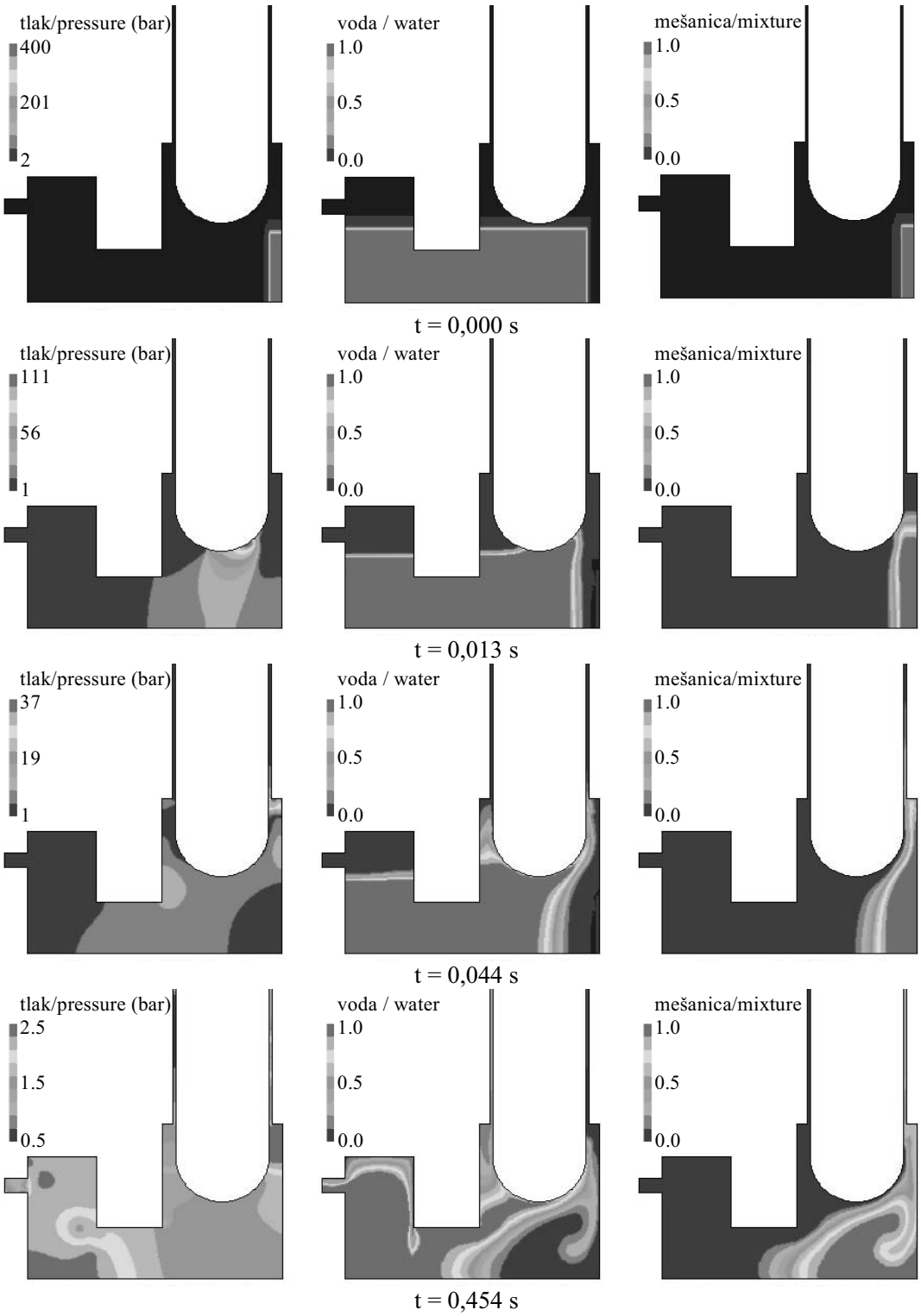

Sl. 5. *Tlak in prostorninski deleži faz v reaktorski votlini za stranski izliv (primer 1) pri različnih časih*
Fig. 5. *Pressure and volume fractions of phases in the reactor cavity for side-melt pour (Case 1) at different times*

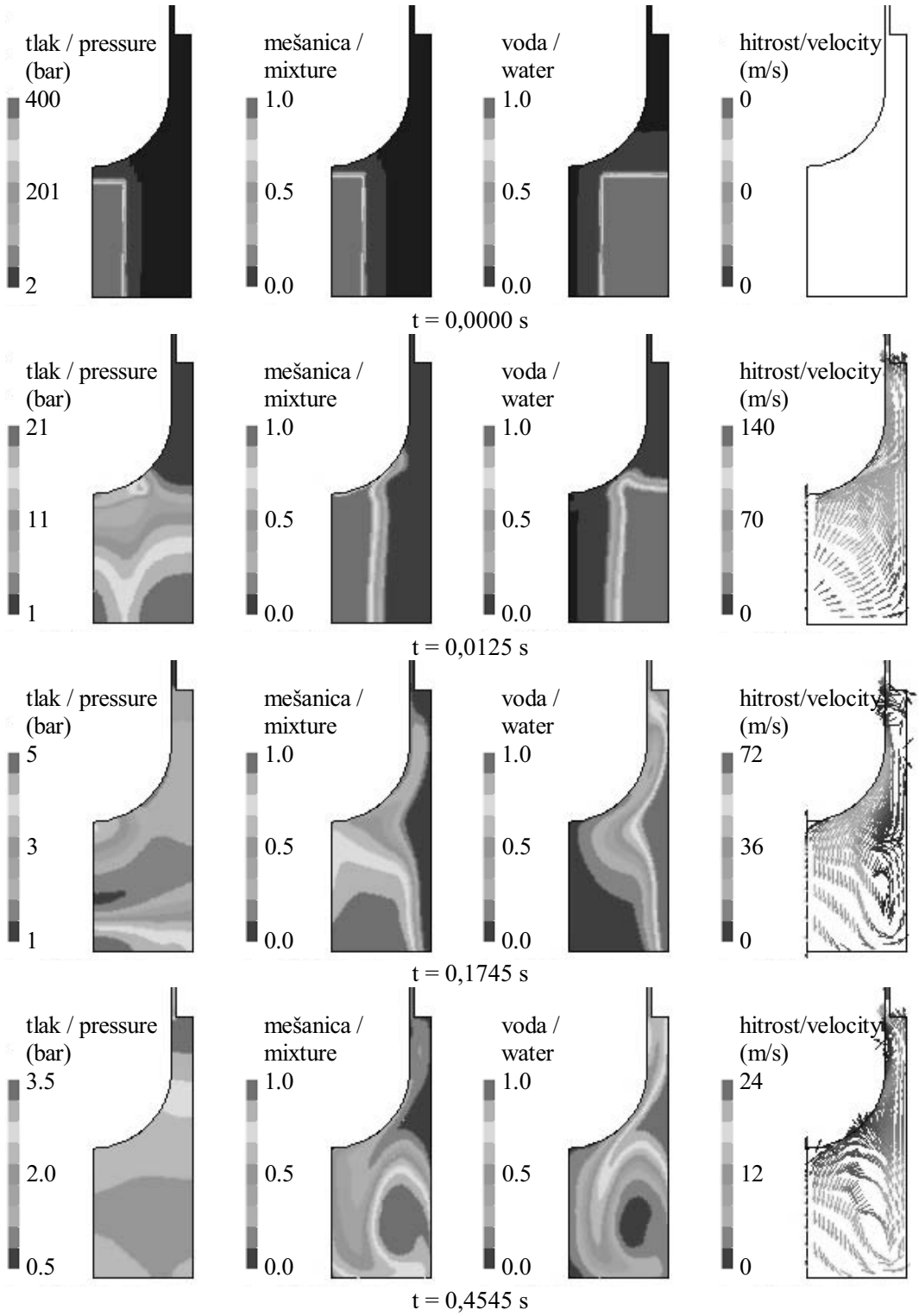

Sl. 6. *Tlak, prostorninski deleži faz in hitrostno polje v valjastem delu reaktorske votline za osrednji izliv (primer 2) pri različnih časih*

Fig. 6. *Pressure, volume fractions of fluid phases and velocity field in cylindrical part of reactor cavity for central-melt pour (Case 2) at different times*

geometrijske oblike, podamo tlačne krivulje le za kraje L1 do L4 (sl. 8). Vidimo, da je tlak najvišji v prvih milisekundah prehodnega pojava med tlačno razbremenitvijo visokotlačne mešanice, ko proti stenam potujejo tudi tlačni udarni valovi. Tlačne obremenitve sten reaktorske votline pri kasnejših časih, ki jih povzročijo trki tekočin z veliko hitrostjo, so mnogo manjše.

Analiza mehanike trdnin ABAQUS je pokazala, da se stene reaktorske votline ne bi poškodovale, če bi bila tlačna obremenitev sten manjša od 400 barov v valjastem delu reaktorske votline in manjša od 150 barov v instrumentacijskem delu reaktorske votline. S slike 7 in 8 je razvidno, da ti kriteriji poškodbe sten niso preseženi, tako da lahko sklepamo, da se stene reaktorske votline pri obravnavanih eksplozijah pare (primer 1 in primer 2) ne bi poškodovale. To ugotovitev smo potrdili tudi z dinamično analizo mehanike trdnin ABAQUS, pri

pressure curves can be given only for locations L1 to L4, due to the limited geometry (Figure 8). It can be seen that the pressure is the highest in the first milliseconds of the transient during the pre-mixture high-pressure relief, when the pressure shocks also propagate to the walls. The pressure loads on the cavity walls at later times, which are caused by the impact of the fluids with high velocity, are much lower.

The ABAQUS structural analysis showed that the cavity walls would not be damaged if the pressure loads on the walls in the cylindrical part of the cavity are lower than 400 bar, and in the in-core instrument part of the cavity, lower than 150 bar. From Figures 7 and 8 it can be established that these damage criteria are not exceeded, so one may conclude that the cavity walls during the considered steam-explosion scenarios (Case 1 and Case 2) would not be damaged. This conclusion was also confirmed with dynamic ABAQUS structural mechanical

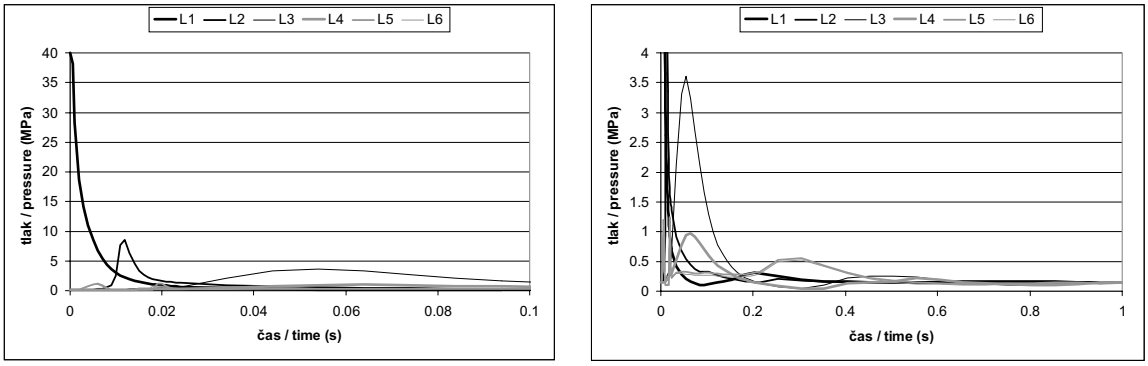

Sl. 7. *Tlak v izbranih krajih kot funkcija časa (leva stran: začetni del simuliranja, desna stran: celotno simuliranje) za stranski izliv taline (primer 1)*

Fig. 7. *Pressure at selected locations as a function of time (left-hand side: initial part of simulation, right-hand side: full simulation) for side-melt pour (Case 1)*

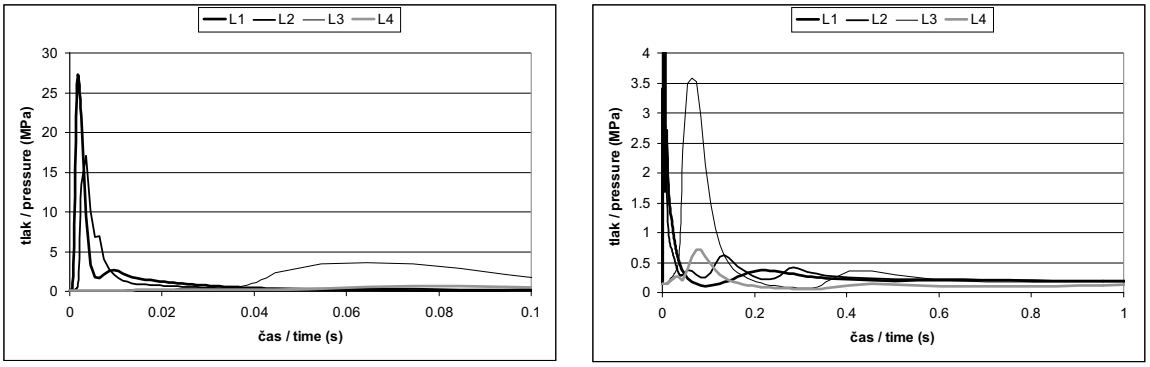

Sl. 8. *Tlak v izbranih krajih kot funkcija časa (leva stran: začetni del simuliranja, desna stran: celotno simuliranje) za osrednji izliv taline (primer 2)*

Fig. 8. *Pressure at selected locations as a function of time (left-hand side: initial part of simulation, right-hand side: full simulation) for central melt pour (Case 2)*

kateri smo upoštevali časovne poteke tlaka, ki smo jih dobili s simuliranjem RDT. Podrobnosti so predstavljene v [9].

Na sliki 9 je prikazana navpična komponenta tlačne sile na reaktorsko posodo. Navpično komponento tlačne sile smo izračunali z integriranjem relativnega tlaka po površini reaktorske posode v navpični smeri. Sila, ki je potrebna za dvig reaktorske posode tipičnega dvozančnega tlačnovodnega jedrskega reaktorja, znaša približno 120 MN, kar smo konservativno izračunali iz mase reaktorske posode ob predpostavki, da se je vsa sredica že izlila iz reaktorske posode, in sile, potrebne za pretrganje hladnih in toplih vej. Na sliki 9 vidimo, da je največja tlačna sila v navpični smeri pri obeh obravnavanih primerih (primer 1: 50 MN, primer 2: 14 MN) bistveno manjša od konservativno ocenjene sile, potrebne za dvig reaktorske posode, tako da lahko sklepamo, da se pri obravnavanih eksplozijah pare reaktorska posoda ne bi dvignila. Ker bi bilo dno reaktorske posode pri resni nezgodi, ki bi pripeljala do izlitja taline iz reaktorske posode, zaradi visokih temperatur in porušitve oslabljeno, bi se dno reaktorske posode pri visokih tlakih verjetno deformiralo in tako bi bila največja tlačna sila na reaktorsko posodo v navpični smeri še manjša, kar je prikazano na sliki 9.

3 SKLEPI

S splošnim programom za RDT smo opravili obsežno, smiselno konservativno parametrično analizo hipotetične eksplozije pare v poplavljeni reaktorski votlini tipičnega tlačnovodnega jedrskega reaktorja [9]. V tem prispevku smo predstavili le dva tipična primera

simulations, where the calculated pressure histories from the CFD simulations were applied. Further details are available in [9].

In Figure 9 the upward pressure force on the reactor vessel is presented. The upward pressure force was calculated as the integral of the relative pressure over the reactor vessel surface in the upward direction. For a typical two-loop PWR the reactor vessel's total restraining force is about 120 MN, calculated conservatively from the reactor-vessel mass (assuming that all the core has left the vessel) and the force needed to shear the cold and hot legs. In Figure 9 it can be seen that in both considered steam-explosion cases the maximum upward pressure force on the reactor vessel is much lower (Case 1: 50 MN, Case 2: 14 MN) than the conservatively estimated reactor vessel's total restraining force, so the reactor vessel would not be lifted in any of these steam explosions. Since during a severe accident resulting in an ex-vessel melt pour the reactor vessel's lower head would be weakened due to its heat up and failure, the reactor vessel's lower head would probably deform during high-pressure loads, and so the maximum upward pressure forces on the reactor vessel are expected to be even lower than presented in Figure 9.

3 CONCLUSIONS

A comprehensive analysis of a hypothetical ex-vessel steam explosion in a typical PWR reactor cavity was performed using a general purpose CFD code [9]. In this paper only two typical ex-vessel steam-explosion cases, differing in the location of

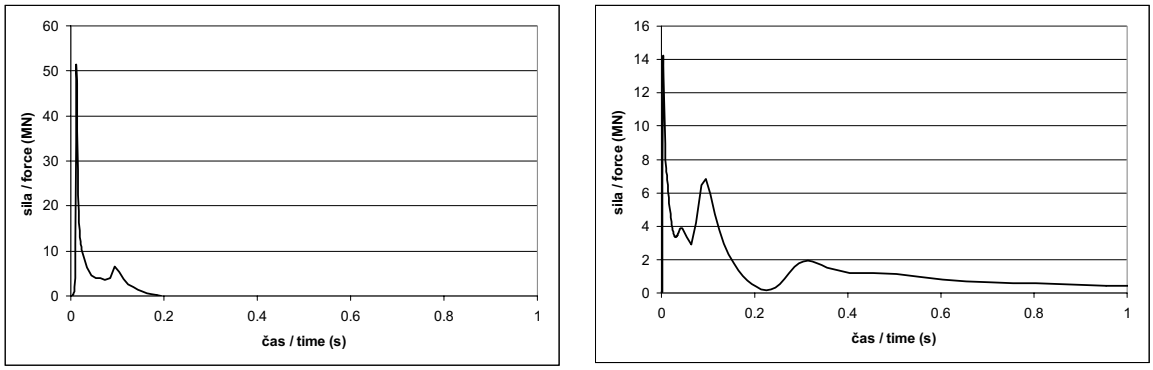

Sl. 9. *Tlačna sila na reaktorsko posodo v navpični smeri kot funkcija časa za primer 1 (leva stran) in primer 2 (desna stran)*

Fig. 9. *Upward pressure force on reactor vessel as a function of time for Case 1 (left-hand side) and Case 2 (right-hand side)*

eksplozije pare v reaktorski votlini, ki se razlikujeta po kraju izliva taline (stranski izliv in osrednji izliv).

Da smo lahko obravnavali eksplozijo pare s splošnim programom za RDT, smo najprej razvili ustrezen namenski model eksplozije pare. Izbrali smo smiselno konservativen potek izliva taline iz reaktorske posode, ki privede do nastanka obsežnega območja mešanice razpršene taline, vode in pare v reaktorski votlini. Predpostavili smo, da je energijski izkoristek eksplozije pare 1 % in izračunali pripadajoč začetni tlak mešanice 400 barov. Pri obeh obravnavanih primerih (stranski in osrednji izliv taline) smo večfazni tok med četrto fazo eksplozije pare, tj. fazo raztezanja, simulirali s programom CFX-5.7.1. Izračunane tlačne obremenitve sten reaktorske votline smo vzeli kot vhodni podatek za ABAQUS simulacijo napetosti v stenah reaktorske votline. Tlačne obremenitve sten reaktorske votline in reaktorske posode smo primerjali s kriteriji poškodb.

Rezultati opravljene analize RDT in analize mehanike trdnin so pokazali, da pri obeh obravnavanih primerih eksplozije pare kriteriji za poškodbe niso preseženi. To pomeni, da se pri eksploziji pare z energijskim izkoristkom 1 %, ki bi sledila predpostavljenemu konservativnemu poteku izliva taline iz reaktorske posode v poplavljeno reaktorsko votlino ob tlačno razbremenjenem primarnem sistemu, stene reaktorske votline v valjastem in instrumentacijskem delu reaktorske votline ne bi poškodovale in da se reaktorska posoda ne bi dvignila.

Celotna analiza eksplozije pare v poplavljeni reaktorski votlini, kjer so obravnavane tudi eksplozije pare z energijskim izkoristkom 10 %, je predstavljena v [9]. Nekaj rezultatov analiz potekev eksplozije pare z energijskim izkoristkom 10 % je predstavljenih tudi v [11].

Zahvala

Avtorji se zahvaljujejo Ministrstvu za visoko šolstvo, znanost in tehnologijo, ki je finančno podprlo raziskavo v okviru raziskovalnega programa P2-0026 in raziskovalnega projekta J2-6565. Institut Jožef Stefan je član mreže odličnosti 6.OP EU SARNET za trajnostno povezovanje evropskih raziskav na področju resnih nezgod.

the melt pour (side pour and central pour), are presented in some detail.

To be able to perform the analysis with a general purpose CFD code a fit-for-purpose parametric steam-explosion model was developed. A reasonably conservative ex-vessel melt-pour scenario producing a large pre-mixture region was selected. It was assumed that the steam-explosion energy conversion ratio is 1%, resulting in a pre-mixture pressure of 400 bar. The multiphase flow during the steam-explosion expansion phase was simulated by the CFX-5.7.1 code for both considered cases, i.e., the side-melt pour and the central-melt pour. The calculated pressure loads on the cavity walls were taken as the input for the ABAQUS simulation of the stresses in the cavity walls. The pressure loads on the cavity walls and on the reactor vessel were compared with the established damage criteria.

The results of the performed CFD and structural analyses show that the damage criteria are not exceeded during either of the presented two steam-explosion cases. That means that during an ex-vessel steam explosion with an energy conversion ratio of 1%, following a reasonably conservative assumed ex-vessel melt pour at a depressurised primary system, the reactor cavity walls in the cylindrical and in-core instrumentation part of the reactor cavity would not be damaged and the reactor vessel would remain in place.

The complete ex-vessel steam-explosion analysis, where steam explosions with an energy conversion ratio of 10% are also treated, is presented in [9]. Some results of the analysis of the steam-explosion scenarios with an energy conversion ratio of 10% are given in [11].

Acknowledgment

The authors acknowledge the support of the Ministry of Higher Education, Science and Technology of the Republic of Slovenia within the program P2-0026 and the research project J2-6565. The Jož ef Stefan Institute is a member of the Severe Accident Research Network of Excellence (SARNET) within the 6th EU Framework Programme.

5 LITERATURA
5 REFERENCES

[1] Berthoud, G. (2000) Vapour explosions. *Annu. Rev. Fluid Mech.* 32(2000), pp. 573-611.

[2] Turland, B.D., G.P. Dobson (1996) Molten fuel coolant interactions: A state-of-the-art report, *EUR 16874 EN*.

[3] Corradini, M.L., B.J. Kim, M.D. Oh (1988) Vapor explosions in light water reactors: A review of theory and modeling. *Prog. Nucl. Energy* 22(1988), pp. 1-117.

[4] Almstroem, H., T. Sundel, W. Frid, A. Engelbrektson (1999) Significance of fluid-structure interaction phenomena for containment response to ex-vessel steam explosions. *Nuclear Engineering and Design* 189(1999), pp. 405-422.

[5] Leskovar, M., J. Marn, B. Mavko (2000) The influence of the accuracy of the numerical methods on steam-explosion premixing phase simulation results. *Journal of Mechanical Engineering* 46(2000), pp. 607-621.

[6] Leskovar, M., B. Mavko (2002) An original combined multiphase model of the steam-explosion premixing phase. *Journal of Mechanical Engineering* 48(2000), pp. 438-448.

[7] Leskovar, M., B. Mavko (2002) Simulation of the isothermal QUEOS steam-explosion premixing experiment Q08. *Journal of Mechanical Engineering* 48(2000), pp. 449-458.

[8] Yuen, W.W., T.G. Theofanous (1995) The prediction of 2D thermal detonations and resulting damage potential. *Nuclear Engineering and Design* 155(1995), pp. 289-309.

[9] Leskovar, M., L. Cizelj, B. Končar, I. Parzer, B. Mavko (2005) Analysis of influence of steam explosion in flooded reactor cavity on cavity structures. *Jožef Stefan Institute*, Ljubljana, Report IJS-DP-9103.

[10] Ferziger, J.H., M. Perič (1996) Computational methods for fluid dynamics. *Springer-Verlag*, Berlin, Heidelberg.

[11] Cizelj, L., B. Končar, M. Leskovar (2005) Vulnerability of a partially flooded PWR reactor cavity to a steam explosio*n. ICONE 13, M*ay 16-20, 2005, Beijing, China, p. 8.

[12] ANSYS-CFX Development team (2004) CFX-5.7.1 documentation, ANSYS Inc., www.ansys.com .

[13] ABAQUS Inc. (2004) ABAQUS/EXPLICIT 6.4-1, www.abaqus.com .

Naslov avtorjev: dr. Matjaž Leskovar
dr. Boštjan Končar
prof. dr. Leon Cizelj
Institut "Jožef Stefan"
Odsek za reaktorsko tehniko
Jamova 39
1000 Ljubljana
matjaz.leskovar@ijs.si
bostjan.koncar@ijs.si
leon.cizelj@ijs.si

Authors' Address: Dr. Matjaž Leskovar
Dr. Boštjan Končar
Prof. Dr. Leon Cizelj
"Jožef Stefan" Institute
Reactor Engineering Division
Jamova 39
1000 Ljubljana, Slovenia
matjaz.leskovar@ijs.si
bostjan.koncar@ijs.si
leon.cizelj@ijs.si

Prejeto: 13.10.2005
Received:

Sprejeto: 23.2.2006
Accepted:

Odprto za diskusijo: 1 leto
Open for discussion: 1 year

Strojniški vestnik - Journal of Mechanical Engineering 52(2006)5, 309-316
UDK - UDC 534.2:004.41
Kratki znanstveni prispevek - Short scientific paper (1.03)

Simbolno-številčno analiziranje nihanj sistemov z velikim številom stopenj prostosti

A Symbolic-Numeric Vibrations Analysis of Systems with Many Degrees of Freedom

Regina Kulvietiene - Genadijus Kulvietis - Inga Tumasoniene
(Vilnius Gediminas Technical University, Vilnius)

Za analizo nihanja sistemov z velikim številom prostostnih stopenj smo uporabili metode računalniške algebre. Z vidika računalniške algebre smo primerjali dve metodi reševanja in izbrali metodo harmonskega ravnovesja. Sistem smo razdelili v linearni in nelinearni del. Linearni del lahko popišemo na običajen način. Za rešitev nelinearnega dela v zaključeni obliki pa smo uporabili simbolični izračun. Izbrani simbolno-številčni pristop ima veliko prednosti, še posebej pri sistemih z velikim številom stopenj prostosti: vodi v poenostavitev teoretičnih oblik modelov, opazno zmanjšanje obsežnosti dobljenih enačb in zato tudi skrajšanje časa računanja ter povečanje možnosti uporabe modelov z več objekti v drugih posebnih okoljih.
© 2006 Strojniški vestnik. Vse pravice pridržane.
(Ključne besede: analize nihanj, metode računalniške algebre, računanje simbolično, stanja ustaljena)

Computer algebra techniques were applied to analyze the vibrations of systems with many degrees of freedom. For this purpose, two solution methods were compared from the computer algebra point of view, and the harmonic balance method was chosen. The system is divided into linear and nonlinear parts. The linear part of the system can be formalized as usual, and symbolic computations were applied to perform a closed-form solution of the nonlinear part. The symbolic-numeric approach chosen, specially dedicated to systems with many degrees of freedom, affords various advantages: it leads to a simplification of the theoretical formulation of the models, a considerable reduction in the size of the generated equations, and hence in the resulting computing time, and also enhanced portability of the multibody models to other specific environments.
© 2006 Journal of Mechanical Engineering. All rights reserved.
(Keywords: vibration analysis, computer algebra, symbolic-numeric computations, steady state)

0 INTRODUCTION

It is difficult to find a branch of modern engineering or science in which vibration problems can be neglected. The theory of oscillations even creates the foundation for many fields in technical sciences, for example, acoustics, radio engineering, automatic control, vibro-isolation. The development and design of new machines belongs to many domains of modern engineering, where the investigation of the level of vibrations is one of the main goals of basic and applied research [14].

The well-elaborated mathematical theory of linear differential equations allows us to solve, with sufficient accuracy, almost all the problems resulting from the fast development of various types of machines, mechanisms, machine tools, robots, traffic means, etc. The increased requirements on the speed, power, long life and reliability of mechanical systems change the situation and prove that the linear models of mechanical systems are only a first approximation of the real process. Using the linear theory, we cannot explain all the phenomena arising during operation. This unexpected behavior is often connected with catastrophic accidents [15].

In view of the accelerating trends of innovation in machine design, in new technologies, new electronic systems and in other branches of science, more complex approaches and more exact solutions are required. This cannot be done without consideration of the very detailed mathematical models respecting the nonlinear characteristics of

real physical systems. For this reason it was necessary to use nonlinear models in the form of ordinary differential equations, differential equations with time-varying parameters, with random properties, with delayed arguments, [13] etc.

The nonlinear oscillations (or more precisely, the oscillations of nonlinear systems) have been intensively studied for half a century ([7] and [15]). A lot of new methods for solutions were elaborated and much new knowledge about the properties, behavior and applications were presented ([13] and [14]). These include the properties of free and forced vibrations, sub- and ultra-harmonic resonances, self-excited vibrations, the interaction of self-excitation and external excitation, transients, bifurcation and jump phenomena, stability problems, identification procedures, etc.

The natural vibration of nonlinear systems is of primary concern in studying resonance phenomena because the backbone curves (the amplitude-frequency relations) and the modes of vibrations, i.e., dynamic characteristics of systems, are determined. Analytical expressions for the backbone curves are very complex and numerical methods are not a convenient way to analyze nonlinear oscillations.

In some cases, such as the one in the range where the internal resonance exists, the corresponding backbone curves have a very complex shape owing to the presence of sharp peaks, looping characteristics and rapidly changing slopes. It is difficult to determine these types of backbone curves using the developed numerical methods ([1] and [2]). Simulations by means of numerical methods are powerful tools for the investigation in mechanics; however, they have serious drawbacks, e.g., finite precision, difficulties in determining transient states and steady states, and the investigation of stability is error-prone and complex.

The analytical steady-state solution by hand requires a lot of routine work, is error-prone and available only for very simple systems ([3] and [11]). Here, the computerized symbolic manipulation systems – so-called computer algebra – are indispensable tools. Symbolic manipulations provided by computer algebra systems in combination with the high-power number-crunching abilities of traditional hardware and software really opens a new way to the large-scale computations needed in steady-state solutions and stability analyses ([3], [5] and [9]).

Subsequently, Gilsinn [12] demonstrated that with the help of a symbolic manipulator package approximations to the invariant tori can be developed by using Galerkin's variational method. However, the amount of computation is so excessively large that it soon becomes impracticable with the increasing strength of the non-linearity.

The aim of this paper is to describe the theoretical background of systematic computer algebra methods for analyzing the free and steady-state periodic vibrations of nonlinear structures. Many analytical steady-state solution methods are developed, but each of them has different capabilities, e.g., small parameter methods give a solution in closed form, and the harmonic balance method only converts nonlinear differential equations to algebraic. On the other hand, it is very important to assess the efficiency of analytical methods in terms of the view of a computer algebra system. For this reason, the VIBRAN computer algebra system [4] was used. The VIBRAN system has been developed by authors and used for engineering problems since 1979. The VIBRAN computer algebra system is a FORTRAN pre-processor for analytical computation with polynomials, rational functions, and trigonometric series. The main distinction between VIBRAN and other computer algebra systems is the representation form of the analytical expressions. The analytical expressions are stored in matrix form and the analytical perturbations are replaced by matrix operations.

Analytical operations can be performed by calling VIBRAN procedures directly from FORTRAN code.

Figure 1 illustrates the VIBRAN procedure fragment for performing a Fourier transformation. A special VIBRAN procedure can generate an optimized FORTRAN code from the obtained analytical expressions, which can be directly used in the programs for numerical analysis.

In this paper the efficiency of two analytical methods is assessed from the point of view of a VIBRAN computer algebra system and a symbolic-numeric approach for vibrations analysis of the multibody systems is presented.

1 REALIZATION OF THE SMALL-PARAMETER METHOD

The small-parameter method (Poincaré's method) [7] was developed to solve systems of nonlinear differential equations. Consider the

```
POLINOM C,D
RATIONAL F
READ 1, N
PRINT 17, N
DO 101 I=1,NN …
BINT(C,D,F,IAR,I) …
END

PROCEDURE BINT(A,B,C,IAR,K)
POLINOM A,B,C …
FKCI(A,B,0)
SCA1(A,2.) …
MXN(A,PI,1)…
END
```

Fig. 1. *A fragment of the VIBRAN procedures*

algorithm of the small-parameter method realized by the VIBRAN computer algebra system for systems of nonlinear differential equations. For the sake of clarity, an algorithm of the small-parameter method is presented for one equation below:

$$\ddot{x} + k^2 x + f(t) = \mu F(t, x, \dot{x}, \mu) \qquad (1),$$

where

$x, \dot{x}, \ddot{x}$ - displacement, velocity and acceleration;
μ - small parameter;
$f(t)$ - continuous periodical time function with a period 2π;
k - constant, not integer in the non-resonant case and integer in the resonant case;
$F(t, x, \dot{x}, \mu)$ - integer polynomial function and periodic with respect to t.

The solution of Equation (1) according to the small-parameter method [7] can be found in the form:

$$x = x_0 + \mu x_1 + \mu^2 x_2 + \mu^3 x_3 + ... \qquad (2),$$

where x_0 is the solution of Equation (1) without nonlinearities, x_i, i = 1,2,3... are unknown functions of t with a period of 2π.

To find these functions, the series (2) is substituted into Equation (1) and the coefficients with the corresponding μ power are equalized. With respect to the μ power, the linear differential equations are obtained:

$$\ddot{x}_i + k^2 x_i = F_i, i = 1, 2, 3, .. \qquad (3),$$

where F_i are the integer rational functions of $x_0, x_1, ..., x_{i-1}; \dot{x}_0, \dot{x}_1, ..., \dot{x}_{i-1}$ and a continuous periodical function with respect to t. The solution of Equations (3) can be found in the form:

$$x_i = \frac{a_{i0}}{2k^2} + \sum_{j=1}^{\infty} \frac{a_{ij}\cos(jt) + b_{ij}\sin(jt)}{k^2 - j^2} \qquad (4),$$

where a_{ij} and b_{ij} are Fourier series coefficients of the function F_i.

In the resonant case, where k is an integer and nearly equal or equal to n, this means:

$$n^2 - k^2 = \varepsilon\mu$$

where ε has a finite value, the zero power solution must be expressed in the form:

$$x_0 = \varphi_0(t) + M_0\cos(nt) + N_0\sin(nt)$$
$$x_1 = \varphi_1(t) + M_1\cos(nt) + N_1\sin(nt)$$

and the i-th power solution can be expressed in the same manner.

In the general case, M_0 and N_0 can be found from the equations:

$$\int_0^{2\pi} F(t, \varphi_0 + M_0\cos(nt) + N_0\sin(nt),$$
$$\dot{\varphi}_0 - M_0 n\sin(nt) + N_0 n\cos(nt), 0)\sin(nt)dt = 0$$
$$\int_0^{2\pi} F(t, \varphi_0 + M_0\cos(nt) + N_0\sin(nt),$$
$$\dot{\varphi}_0 - M_0 n\sin(nt) + N_0 n\cos(nt), 0)\cos(nt)dt = 0$$

where φ_0 is the zero power solution of Equation (1) in the non-resonant case, excluding resonant harmonics. The other coefficients M_i and N_i can be found from the system of linear algebraic equations:

$$M_{i-1}\int_0^{2\pi}\left\{\left(\frac{\partial F}{\partial x}\right)\cos(nt) - n\left(\frac{\partial F}{\partial \dot{x}}\right)\sin(nt)\right\}\cos(nt)dt +$$
$$N_{i-1}\int_0^{2\pi}\left\{\left(\frac{\partial F}{\partial x}\right)\sin(nt) + n\left(\frac{\partial F}{\partial \dot{x}}\right)\cos(nt)\right\}\cos(nt)dt +$$

$$\int_0^{2\pi} F_i^* \cos(nt)dt = 0$$

$$M_{i-1}\int_0^{2\pi}\left\{\left(\frac{\partial F}{\partial x}\right)\cos(nt) - n\left(\frac{\partial F}{\partial \dot{x}}\right)\sin(nt)\right\}\sin(nt)dt +$$

$$N_{i-1}\int_0^{2\pi}\left\{\left(\frac{\partial F}{\partial x}\right)\sin(nt) + n\left(\frac{\partial F}{\partial \dot{x}}\right)\cos(nt)\right\}\sin(nt)dt +$$

$$\int_0^{2\pi} F_i^* \sin(nt)dt = 0$$

where:

$$F_i^* = F_i + \left(\frac{\partial F}{\partial x}\right)\varphi_{i-1} + \left(\frac{\partial F}{\partial \dot{x}}\right)\dot{\varphi}_{i-1}$$

are known periodic functions.

The small-parameter method was realized in VIBRAN for both resonant and non-resonant cases in systems of nonlinear differential equations [6].

2 REALIZATION OF THE HARMONIC BALANCE METHOD

The harmonic balance method is probably the oldest analytical method in the theory of nonlinear vibration ([6] and [15]). Consider the following nonlinear differential equation:

$$\ddot{x} + f(x,\dot{x}) = F(t) \quad (5),$$

where $x, \dot{x}, \ddot{x}$ denote displacement, velocity and acceleration; $f(x,\dot{x})$ is a nonlinear function, expandable in a Fourier series; $F(t)$ is assumed to be a periodic function:

$$F(t) = A_0 + \sum_{i=1}^{\infty}\left(A_i\cos(i\omega t) + B_i\sin(i\omega t)\right)$$

The solution of the above-mentioned Equation (5) can be expressed in a Fourier series in time:

$$x(t) = a_0 + \sum_{i=1}^{\infty}\left(a_i\cos(i\omega t) + b_i\sin(i\omega t)\right) \quad (6).$$

A nonlinear function is also expanded in the Fourier series in time:

$$f(x,\dot{x}) = \alpha_0 + \sum_{i=1}^{\infty}\left(\alpha_i\cos(i\omega t) + \beta_i\sin(i\omega t)\right) \quad (7),$$

where the Fourier-series coefficients are calculated using the following formulae:

$$\alpha_0 = \frac{\omega}{2\pi}\int_0^{2\pi/\omega} f(x,\dot{x})dt$$

$$\alpha_i = \frac{\omega}{\pi}\int_0^{2\pi/\omega} f(x,\dot{x})\cos(i\omega t)dt$$

$$\beta_i = \frac{\omega}{\pi}\int_0^{2\pi/\omega} f(x,\dot{x})\sin(i\omega t)dt$$

A substitution of the formule (6) and (7) into Equation (5) gives an infinite number of algebraic equations to determine the unknown coefficients of Solution (6) :

$$\begin{aligned} \alpha_0 &= A_0 \\ i^2\omega^2 a_i &= \alpha_i - A_i \\ i^2\omega^2 b_i &= \beta_i - B_i, i = 1,2,3... \end{aligned} \quad (8)$$

or

$$\begin{aligned} \alpha_0 &= \alpha_0(a_0, a_1, b_1, ...) \\ \alpha_i &= \alpha_i(a_0, a_1, b_1, ...) \\ \beta_i &= \beta_i(a_0, a_1, b_1, ...) \end{aligned}$$

The above-mentioned version of the harmonic balance method was realized in VIBRAN for the system of nonlinear equations [5].

3 EFFICIENCY MEASUREMENTS FOR BOTH METHODS

Two VIBRANs programs that realize the above-mentioned methods were tested for the following equation:

$$\ddot{x} + c_1\dot{x} + c_2 x + c_3 x^2 + c_4 x^3 = d_0 + d_1\sin(t) + d_2\cos(t)$$

This equation describes the dynamics of an aerodynamically supported magnetic head in a recording device ([8] and [10]). We present below the result of the solution for the first harmonics: the first index for the solution coefficients *A* and *B* is the equation number and the second one is the harmonics number. The first result corresponds the first equation in Formula (8) and afterwards we present the result for the cosine and sine coefficients of the first term of the Fourier series.

The result for the first equation of Formula (8) is:

```
0=A10*C2-.5*B11**2*C3-.5*A11**2*C3-
C3*A10**2+.75*C4*B11**2*A12-
1.5*C4*B11**2*A10-1.5*C4*B11*B12*A11-
1.5*C4*B12**2*A10-.75*C4*A11**2*A12-
1.5*C4*A11**2*A10-1.5*C4*A12**2*A10-
C4*A10**3-D0
```

The result for the cosine coefficient of the first term of the Fourier series is:

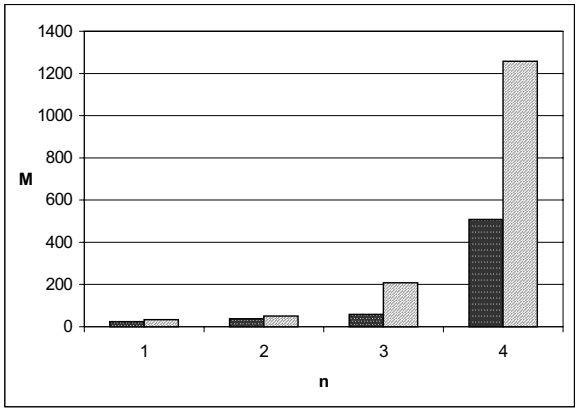

Fig. 2. *Number of terms in the solution's expression*

0=-A11-B11*C1+A11*C3-B11*B12*C3-
2*A11*A10*C3-A11*A12*C3-
.75*C4*B11**2*A11-3*C4*B11*B12*A10-
1.5*C4*B12**2*A11-.75*C4*A11**3-
1.5*C4*A11*A12**2-3*C4*A11*A10**2-
3*C4*A11*A12*A10-D2

The result for the sine coefficient of the first term of the Fourier series is as follows:

0=-B11-A11*C1+B11*C3-B11*A12*C3-
2*B11*A10*C3-A11*B12*C3-
.75*C4*B11**3+3*C4*B11*A12*A10-
1.5*C4*B12**2*B11-.75*C4*A11**2*B11-
1.5*C4*B11*A12**2-3*C4*B11*A10**2-
3*C4*A11*B12*A10-D1

In Figure 2 the number of terms in the solution expression (M) for the small-parameter (upper column) and for the harmonic balance method (lower column) with respect to the number of harmonics (n) in the solution (number of power in the case of small parameter method) is presented.

In Figure 3 the presented graphic illustrates the convergence of the above-mentioned analytical methods for the four coefficients.

The upper curve corresponds to the harmonic balance method and the lower one corresponds to the small-parameter method.

In this case, the magnetic head construction parameters were:

$$c_1 = 0.1, c_2 = 0.228*10^6, c_3 = 0.167*10^4,$$

$$c_4 = -0.587*10^3, d_0 = 0, d_1 = 0.12, d_2 = 0.12$$

The comparison of the above-mentioned analytical methods illustrates the similarities and differences of their application. The similarities illustrate the tolerance curves that are of the same shape.

There are 12045 terms in the solution's expression for the small-parameter method (5 harmonics), whereas only 1524 terms are observed for the harmonic balance method. This means that the harmonic balance method is much more convenient for computer algebra realization, especially for the multibody system, but needs a special stability analysis procedure for the steady-state solution.

5 SYMBOLIC-NUMERIC REALIZATION OF THE HARMONIC BALANCE METHOD

Computerized symbolic manipulation is a very attractive means to reliably perform analytical

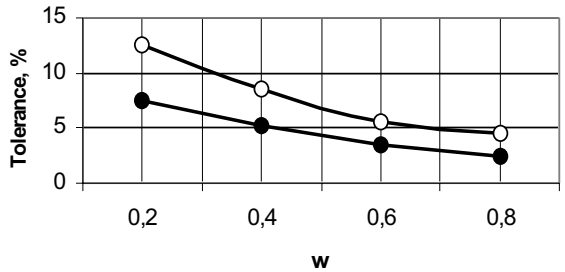

Fig. 3. *Tolerance for harmonic balance and small-parameter analytical methods*

calculations, even with complex formulae and expressions. But often, a semi-analytical approach, combining the features of analytical and numerical computations, is the most desirable synthesis. This allows the analytical work to be pushed further, before the numerical computations start.

For symbolic-numeric computation of the nonlinear oscillation multibody systems the VIBRAN computer algebra system was used. VIBRAN's special procedure can generate optimized FORTRAN code from obtained analytical expressions, which can be directly used in programs for numerical analysis. Figure 4 illustrates the scheme of the proposed approach.

Let us discuss the multibody system with *s* degrees of freedom. After good known perturbations the equations of motion can be rewritten in the matrix form:

$$[A]\{\ddot{x}\}+[B]\{\dot{x}\}+[C]\{x\}= \{H(x,\dot{x},t)\}+\{f(t)\} \quad (9),$$

where:

$$\{f(t)\}=\{f_0\}+\{f_1\}\sin(\omega t)+\{f_2\}\cos(\omega t)+...$$

$\{f(t)\}$ - continuous periodical time function or expandable into a Fourier series, and vector $H(x,\dot{x},t)$ is the result from block 1.

The solution of the above-mentioned system can be expressed using the harmonic balance method in the form:

$$\{x\}=\{D_0\}+\{D_1\}\sin(\omega t)+\{D_2\}\cos(\omega t)+...$$

where $\{D_i\}$ are the unknown vectors that can be found from the nonlinear algebraic equations.

Following the harmonic balance method ([6] and [15]) these equations for the first three vectors' coefficients are:

$$[U]\{D\}+\{f(D)\}=\{Q\} \quad (10),$$

where f_i are the coefficients of the function $f(t)$ Fourier expansion. Analogously, the equations for other harmonics can be found using VIBRAN's program, shown in block 4. The expressions of H_i and their required derivatives are expressed in closed form using computer algebra techniques with a FORTRAN code generation procedure. The programs' structure is shown in Figure 4.

Obviously, the matrix of coefficients [U] consists of independent sub-matrix blocks located at the main diagonal. Therefore, the linear part of the matrix equation decomposes into m separate systems (*m* is the number of harmonics in the solution vector) of size *2s* and one system (corresponding to the zero harmonic) of size *s*. The obtained solution of these systems serves as an initial approximation for further computation.

The Newton's iteration formula claims:

$$\{\mathrm{E}(D^i)\}+[E'(D^i)]\{D^{i+1}-D^i\}=\{0\} \quad (11),$$

where $\{E(D)\}$ is the system of equations and $[E'(D)]$ is the Jacobi matrix of the whole system (including the linear part as well). Substituting these two formulae the Newton iteration becomes

$$([U]+[f'(D^i)])\{D^{i+1}\}=[f'(D^i)]\{D^i\}- \{f(D^i)\}+\{Q\} \quad (12).$$

The iterations start with:

$$[U]\{A^0\}=\{f\} \quad (13).$$

This linear matrix equation must be solved for every iteration step. This equation can be rewritten in the simple form

$$([U]+[f'])\{D\}=\{F\} \quad (14).$$

It is not expedient to sum up the matrices $[U]$ and $[f']$ in advance, because they have quite different structures. Matrix $[U]$, as was already mentioned, is block-banded, i.e., consists of separate sub-matrix blocks located at the main diagonal. The structure of matrix $[f']$ depends on the type and location of nonlinear terms in the initial differential equation system, but it is always sparse and can possess nonzero elements far from the main diagonal. Thus, matrix $[D]$ is not stored in the computer memory at all, and its every element is computed by a reference to the special subroutine. Matrix $[f']$ is stored in the main memory as a sparse matrix. Of course, such storage demands corresponding modifications to the solution algorithm itself.

In many applications the solution of the differential equation system must be obtained in a specified domain of some varied parameters (frequency, stiffness, mass, etc.). Therefore, the program is designed in such a way that any parameter of the initial system can be varied with a regular or logarithmic step. Note that the analytical computation is performed only once, while the numerical calculations are repeated every time when the value of any parameter of the system is being changed.

The proposed symbolic-numeric method was tested for the dynamics of a double-head recording device with aerodynamic support [8]. The following equations describe the system behavior:

$$\ddot{x}_1 + k_1\dot{x}_1 + k_2\dot{x}_2 + k_3x_1 + u_0 + u_1x_1 + u_2x_1^2 + u_3x_1^3 = f_1(\tau)$$
$$\ddot{x}_2 + k_6\dot{x}_1 + k_7\dot{x}_2 + k_8x_1 + k_9x_2 = f_2(\tau)$$

where:

$$f_1(\tau) = k_4 \sin\tau + k_5 \cos\tau,$$
$$f_2(\tau) = k_{10} \sin\tau + k_{11} \cos\tau$$

Analytical expressions obtained according to the VIBRAN program conclude the part of the analytical calculations. The analytical result for H_i in Equation (5) is:

```
H0=k3*a10+u1*a10+.5*u2*a11**2+.5*u2*b
11**2+u2*a10**2+1.5*u3*a10*a11**2+1.5
*u3*a10*b11**2+u3*a10**3+u0
H1=a20*k9+k8*a10+u1*a10+.5*u2*a11**2
+.5*u2*b11**2+u2*a10**2+1.5*u3*a10*a1
1**2+1.5*u3*a10*b11**2+u3*a10**3+u0
H2=b21*w*k2+w*b11*k1+k3*a11+a11*u1+
2*u2*a11*a10+.75*u3*a11**3+.75*u3*a11*
b11**2+3*u3*a11*a10**2
H3=-a21*w*k2-
w*a11*k1+k3*b11+b11*u1+2*u2*b11*a10+
.75*u3*a11**2*b11+.75*u3*b11**3+3*u3*
b11*a10**2
H4=b21*w*k7+a21*k9+w*b11*k6+k8*a11+
a11*u1+2*u2*a11*a10+.75*u3*a11**3+.75
*u3*a11*b11**2+3*u3*a11*a10**2
H5=-a21*w*k7+b21*k9-
w*a11*k6+k8*b11+b11*u1+2*u2*b11*a10+
.75*u3*a11**2*b11+.75*u3*b11**3+3*u3*
b11*a10**2
```

The corresponding derivatives are very simple and there are only 25 nonzero terms:

```
H23 = k1*w+1.5*u3*b11*a11
H26 = k2*w
H31 = 2*u2*b11+6*u3*a10*b11
H32 = -k1*w+1.5*u3*b11*a11
H41 = 2*u2*a11+6*u3*a10*a11
H43 = k6*w+1.5*u3*b11*a11
H45 = k9
H46 = k7*w
H51 = 2*u2*b11+6*u3*a10*b11
H52 = -k6*w+1.5*u3*b11*a11
H55 = -k7*w
H56 = k9
```

Figure 4 illustrates the generated program code that could be directly used for numerical investigations.

This code is very simple and contains only 89 floating-point product operations.

```
SUBROUTINE ISRA01(A,O)
    IMPLICIT REAL(A-Z)
    DIMENSION A(20),O(60)
    u0  =A(    1)
    u3  =A(    2)
    u2  =A(    3)
    k3  =A(    4)
      …
   O(17)=a11*a10*u3
    O(19)=b11*a10*u3
    O(20)=O(31)*b21
    O(21)=O(29)*b1
      …
     END
SUBROUTINE ISRA(A,B,O)
    DIMENSION A(20),B(42),O(60)
    Y1=+.5*O(3)
    Y2=+.5*O(4)
    Y3=+1.5*O(6)
  …
    Y26=+.75*O(13)
    Y27=+2.25*O(1)

B(1)=+O(1)+O(2)+O(5)+O(8)+O(9)+Y1+Y2+Y3+Y4

    B(2)=+O(10)+O(11)+Y5
    …
      END
```

Fig. 4. *A fragment of the code generated by VIBRAN*

5 CONCLUSION

On the basis of non-linear differential equations solved by a harmonic balance method and the synthesis of the VIBRAN analytical calculation system an investigation method for non-linear systems was created. This method combines the advantages of analytical calculation methods and computer algebra. They are compared on the principle of a symbolic–numerical calculation, where the analytical rearrangements are applied only to the non-linear part of the system, and at the same time the linear part of the system could be easily solved in a numerical way. The proposed method provides smaller expressions for the analytical computation and allows the analysis of systems with greater order.

The problem considered in this paper clearly demonstrates the power of the symbolic-numeric perturbation method. An important feature of this approach is that it provides both quantitative and qualitative results regarding the dynamic behavior of multibody systems.

6 REFERENCES

[1] R. Lewandowski (1997) Computational formulation for periodic vibration of geometrically nonlinear structures, Part 1: Theoretical background, *Int. J. Solids Structures*, 34 (15) (1997) 1925-1947.

[2] E.Riks (1984) Some computational aspects of the stability analysis of nonlinear structures, *Computational Methods in Applied Mechanical Engineering*, 47 (1984) 219-259.

[3] D.M. Klymov, V.M. Rudenko (1989) Metody kompjuternoj algebry v zadačah mehaniki, Nauka, Moscow.

[4] R. Kulvietiene, G. Kulvietis (1989) Analytical computation using microcomputers, *LUSTI*, Vilnius.

[5] R. Kulvietiene, G. Kulvietis, J. Galkauskaite (1997) Computer algebra application to large nonlinear oscillation systems. *Mechanine technologija*, XXV, Kaunas, 126-130.

[6] R. Kulvietiene, G. Kulvietis (1996) Symbolic solution of nonlinear oscillation system using harmonic balance method, *Proc. of the 2nd European Nonlinear Oscillations Conference*, Vol. 2, 1996, 109-112.

[7] I.G. Malkin (1956) Some problems of the theory of nonlinear oscillations, *Gostehizdat*, Moscow.

[8] R. Kulvietiene (1982) Dynamics of aerodynamically supported magnetic head in the recording device, Ph.D. Thesis, *KTU*, Kaunas.

[9] F. San-Juan, A.Abad (2001) Algebraic and symbolic manipulation of poisson series. *Journal of Symbolic Computation,* 32 (5), (2001) 565-572.

[10] A. Cepulkauskas, R. Kulvietiene, G. Kulvietis (2003) Computer algebra for analyzing the vibrations of nonlinear structures, *Proc. CASA'2003, Lecture Notes in Computer Science, Vol. 2657, Springer-Verlag,* Berlin Heidelberg New York, 747-753.

[11] J.-C. Samin, P. Fisette (2003) Symbolic modeling of multibody systems, *Kluwer Academic Publishers*.

[12] Gilsinn, David E. (1995) Constructing Galerkin's approximations of invariant tori using MACSYMA. *Nonlinear Dynamics* 8 (2) (1995) 269-305.

[13] N.N. Bogolyubov, J.A. Mitropolskij (1995) Asymptotical methods in the theory of nonlinear oscillations. *TTL*, Moskva.

[14] L. Pust, F. Peterka, G. Stepan, G.R. Tomlinson, A. Tondl (1999) Nonlinear oscillations in machines and mechanisms theory. *Mechanism and Machine Theory* 34 (1999) 1237-1253.

[15] C. Hayashi (1964) Nonlinear oscillations in physical systems. *McGraw Hill*, New York.

Authors' Address: Doc. Dr. Regina Kulvietiene
Prof. Hab. Dr. Genadijus Kulvietis
Inga Tumasoniene
Vilnius Gediminas Technical University
Department of Information Technologies
rku@fm.vtu.lt
gk@fm.vtu.lt
tinga@gama.vtu.lt
Sauletekio 11
Vilnius 2040, Lithuania

Prejeto: 7.11.2005
Received:

Sprejeto: 23.2.2006
Accepted:

Odprto za diskusijo: 1 leto
Open for discussion: 1 year

Strojniški vestnik - Journal of Mechanical Engineering 52(2006)5, 317-322
UDK - UDC 534.2:681.892
Kratki znanstveni prispevek - Short scientific paper (1.03)

Popravni količniki za izračun Youngovega modula iz resonančnega upogibnega nihanja

Correction Coefficients for Calculating the Young's Modulus from the Resonant Flexural Vibration

Igor Štubňa - Anton Trník
(Constantine the Philosopher University, Nitra)

Enostavna enačba, dobljena iz poenostavljene diferencialne enačbe upogibnega nihanja za primer z enakomernim prerezom, nam ne da točne vrednosti Youngovega modula oz. hitrosti zvoka, če je razmerje dolžine in premera (oz. dolžine in debeline) vzorca manjše od 20. Napako lahko odpravimo z množenjem izmerjene resonančne frekvence ali izračunanega Youngovega modula s popravnim količnikom. V prispevku predstavljamo nekaj enačb za popravne količnike in novo enačbo ter jih primerjamo z enačbami Ameriškega združenja za preizkušanje in materiale (American Society for Testing and Materials - ASTM).
© 2006 Strojniški vestnik. Vse pravice pridržane.
(Ključne besede: nihanja upogibna, frekvence resonančne, moduli Youngovi, izračuni)

A simple formula derived from the simplified differential equation of flexural vibration of a sample with a uniform cross-section does not give exact values for the Young's modulus or the velocity of sound if the ratio of the length to the diameter (or the length to the thickness) of the sample is less than 20. The error can be eliminated by multiplying the measured resonant frequency or the calculated Young's modulus by a correction coefficient. Some formulae for the correction coefficients as well as a new formula are presented and compared with the ASTM formulae.
© 2006 Journal of Mechanical Engineering. All rights reserved.
(Keywords: flexural vibrations, resonant frequencies, Young's modulus, calculations)

0 INTRODUCTION

One of the best methods for determining the velocity of sound or the Young's modulus of solids is based on the resonant flexural vibrating of a sample of a cylindrical or a prismatic shape. It is easy to excite this vibration, and its magnitude is sufficiently high. Its resonant frequency is less than the resonant frequency of a longitudinal vibration of a sample with the same length. These properties of the flexural vibration make it preferable for measuring the Young's modulus or the velocity of sound.

For measuring purposes the most suitable vibration is the vibration of a free-free sample because of the relative ease of fulfilling the boundary condition of the theoretical solution. A widely used method, which is also suitable for high temperatures, is based on Föster's idea [1], later improved by Spinner and Tefft [2].

The solution for the three-dimensional form of the partial differential equation of flexural vibration is complex, but the mathematical approach can be simplified, and a reasonably exact solution can be obtained. For long samples the simplified partial differential equation of the flexural vibration can be used. This equation has the form [3]:

$$\frac{\partial^2 y}{\partial t^2} + c_0^2 i^2 \frac{\partial^4 y}{\partial x^4} = 0 \qquad (1),$$

where x and y are the coordinates of the mass element of the sample, t is time, c_0 is the velocity of sound (i.e., the velocity of longitudinal wave propagation in the sample), i is the radius of inertion of the cross-section. For a sample with a circular cross-section, the radius of inertion is $i = d/4$ and for a sample with a rectangular cross-section it is $i = d/\sqrt{12}$, where d is the diameter of a cylindrical sample or the thickness of a prismatic sample in the direction of

the vibration. The frequency equation derived from Eq. (1) for the free-free sample is:

$$\cos(al)\ \mathrm{ch}(al) = 1 \qquad (2),$$

where l is length of the sample, $a = \sqrt{\omega/(ic_0)}$, ω is a resonant angular frequency. The formulae for the velocity of sound c_0 and the Young's modulus E derived from Eq. (2) have the form:

$$c_0 = K\frac{l^2 f}{d}\ ,\ E = \left(K\frac{l^2 f}{d}\right)^2 \rho \qquad (3),$$

where f is the resonant frequency, ρ is the material density and the values of the constant K are:

K = 1.12336 for a cylindrical sample and the fundamental resonant frequency,

K = 0.97286 for a prismatic sample and the fundamental resonant frequency,

K = 0.40752 for a cylindrical sample and the 1st overtone,

K = 0.35292 for a prismatic sample and the 1st overtone.

If a relatively short sample is used (with the ratio $l/d < 20$) it is necessary to take into account the influence of the shear forces and the rotary inertia. There are two possible ways to do this: 1) solving the complicated frequency equation derived from the partial differential equation accounting for these influences, 2) using the simple formula (3) and multiplying the calculated Young's modulus (or measured resonant frequency) by a correction coefficient.

Formulae for calculating the correction coefficients for the fundamental mode as well as for the first overtone of the flexural vibration of a cylindrical or a prismatic sample and comparisons of these coefficients are given in this paper.

1 CORRECTION COEFFICIENTS DERIVED FROM AN ALTERNATIVE EQUATION

If the ratio of $l/d > 20$, the measured resonant frequency is in a good agreement with that calculated from Eq. (3). If the ratio of $l/d < 20$, the measured resonant frequency is less than the frequency calculated from Eq. (3) for the same sound velocity: the shorter the sample, the bigger the discrepancy between the theoretical and the measured frequencies. To avoid this disagreement, the effect of the shear forces and the rotary inertia has to be taken into account. This leads to Timoshenko's equation [1] or to the alternative equation [4]:

$$\frac{\partial^2 y}{\partial t^2} + c_0^2 i^2 \frac{\partial^4 y}{\partial x^4} - pi^2 \frac{\partial^4 y}{\partial t^2 \partial x^2} = 0 \qquad (4).$$

Here $p = 2(1+\mu)/\kappa$, where μ is Poisson's ratio, and $\kappa = 0.710$. The frequency equation for the "free-free sample" derived from Eq. (4) is:

$$\begin{aligned} &2R_a R_b P_a P_b[\mathrm{ch}(al)\cos(bl) - 1] - \\ &-[R_b^2 P_a^2 - R_a^2 P_b^2]\mathrm{sh}(al)\sin(bl) = 0 \end{aligned} \qquad (5),$$

where:

$$R_a = R + a^2,\ R_b = R - b^2,\ P_a = Pa + a^3,\ P_b = Pb - b^3,$$
$$R = p(\omega/c_0)^2\ ,\ P = (1+p)(\omega/c_0)^2,$$
$$a = (\omega/c_0)\sqrt{-p/2 + \sqrt{p^2/4 + (c_0/i\omega)^2}}\ ,$$
$$b = (\omega/c_0)\sqrt{+p/2 + \sqrt{p^2/4 + (c_0/i\omega)^2}}\ .$$

The frequency equation (5) is complex and can be solved only by a numerical method. This is the reason why correction coefficients are used.

If the measured resonant frequency f is multiplied by the correction coefficient Q then the correct value of the velocity of sound (or the Young's modulus) can be obtained from Eq. (3). Then Eq. (3) becomes:

$$c_0 = K\frac{l^2 (Qf)}{d}\ ,\ E = \left(K\frac{l^2 (Qf)}{d}\right)^2 \rho \qquad (6),$$

where the coefficients K are the same as above. The correction coefficient Q was obtained from the resonant frequencies $f_{(2)}$ and $f_{(5)}$ computed using the numerical bisection method from the frequency equations (2) and (5) respectively. Then the correction coefficient is:

$$Q = \frac{f_{(2)}}{f_{(5)}} \qquad (7).$$

The correction coefficients Q are dependent on the ratio of l/d as well as on Poisson's ratio μ, but the dependence between Q and μ is weak. The values of Q could be considered constant for $l/d > 6$ and $0.15 < \mu < 0.4$ (see Fig. 1 and 2). The values of Q were computed for the fundamental mode and $l/d > 2.5$, and for $l/d > 5$ for the 1st overtone. The tabulated coefficients Q for the fundamental mode of flexural vibration and the cylindrical and prismatic samples are shown in [5] and [6] and for the 1st overtone of the flexural vibration and cylindrical and prismatic samples in [7].

It is often more convenient to have correction coefficients in the form of a formula than a table. Therefore, the formula for calculating the correction coefficients was suggested [8]:

$$Q = 1 + \frac{1}{l/d}\left\{\frac{A}{\mu} + \frac{1}{l/d}\left[B + \frac{1}{l/d}\left(C + \frac{D}{l/d}\right)\right]\right\} \quad (8).$$

Parameters *A, B, C, D* were obtained from a regression analysis of the correction coefficients listed in [5] to [7]. The values of the parameters *A, B, C, D* are in Tab. 1 and Tab. 2.

2 CORRECTION COEFFICIENTS DERIVED FROM TIMOSHENKO'S EQUATION

Timoshenko's equation describes the flexural vibration of samples with a uniform cross-section with a sufficient precision [3]. Resonant frequencies predicted by the frequency equation derived from Timoshenko's equation are in agreement with experimentally measured values. But this frequency equation is complex (even more than Eq. (5)) so correction coefficients together with the simple formula (3) are commonly used. The values of these coefficients calculated by Pickett are in table form in [9]. Pickett's values served as the basis for the formulae of correction coefficients for the fundamental mode of flexural vibration ([9] to [13]). The application of Pickett's coefficient *T* consists of its multiplication by the Young's modulus calculated from the simple formula (3). For the fundamental mode and a cylindrical sample:

$$T_{0c} = 1.000 + 4.939(d/l)^2, \quad \text{if} \quad l/d \geq 20$$

$$T_{0c} = 1 + 4.939(1 + 0.0752\mu + 0.8109\mu^2)(d/l)^2 - 0.4883(d/l)^4 - \left[\frac{4.691(1 + 0.2023\mu + 2.173\mu^2)(d/l)^4}{1.000 + 4.754(1 + 0.1408\mu + 1.536\mu^2)(d/l)^2}\right], \quad \text{if} \quad l/d < 20 \quad (9).$$

For the fundamental mode and the prismatic sample:

$$T_{0p} = 1.000 + 6.585(d/l)^2, \quad \text{if} \quad l/d \geq 20$$

$$T_{0p} = 1 + 6.585(1 + 0.0752\mu + 0.8109\mu^2)(d/l)^2 - 0.868(d/l)^4 - \left[\frac{8.340(1 + 0.2023\mu + 2.173\mu^2)(d/l)^4}{1.000 + 6.338(1 + 0.1408\mu + 1.536\mu^2)(d/l)^2}\right], \quad \text{if} \quad l/d < 20 \quad (10).$$

Then the correct value of the Young's modulus is $E = T_{0c}E_{(3)}$ or $E = T_{0p}E_{(3)}$, where $E_{(3)}$ is calculated by Eq. (3). Another, complicated formula was proposed by Martinček [14].

The relationship $T(\mu)$ or $Q(\mu)$ is weak, and for $l/d > 10$ the correction coefficients can be considered independent of the Poisson's ratio (see Fig. 1, Fig. 2). Therefore, a simpler formula for the correction coefficient can be used in such a case. For example, Acegorian and Chočian used:

$$T = 1 + 83(i/l)^2 - \frac{1370(i/l)^4}{1 + 83.4(i/l)^2} - 125(i/l)^4 \quad (11),$$

where *i* is a radius of inertia of the cross-section and *l* is the length of the sample [15].

3 CORRECTION COEFFICIENTS FOR SAMPLE WITH CHAMFERED EDGES

If the prismatic sample is not ideal but has chamfered or rounded edges an additional correction should be made. Correction factors *F* are in the range of 1.0031 to 1.0287 for the chamfer size of 0.08 to 0.25 mm. If the density of the sample is determined from its weight and dimensions then the density correction is made by multiplying Young's modulus by the factor $P \in (1.0011,\ 1.0105)$ for the same chamfer size. The

Table 1. *Parameters A, B, C, D for the fundamental mode*

	cross-section	
Parameter	circular	square
A	0.00002	-0.00002
B	2.5719	3.44347
C	-0.14069	-0.44952
D	-2.43588	-3.34228

Table 2. *Parameters A, B, C, D for the 1st overtone*

	cross-section	
Parameter	circular	square
A	-0.00131	-0.00249
B	7.44851	10.0605
C	-3.56057	-7.076
D	-4.50048	-2.02022

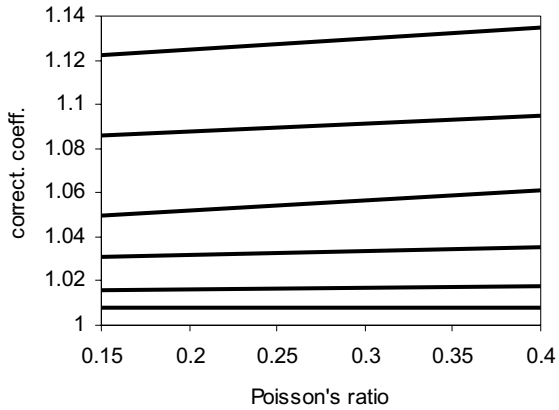

Fig. 1. *Correction coefficients Q_{0p} for the fundamental mode and prismatic sample. Graphs are (from the top) for: l/d = 5, 6, 7, 10, 15, 20*

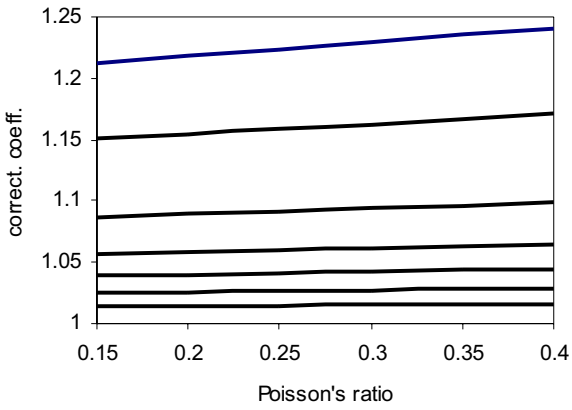

Fig. 2. *Correction coefficients Q_{1c} for 1st overtone and cylindrical sample. Graphs are (from the top) for: l/d = 5, 6, 8, 10, 12, 15, 20*

true Young's modulus $E = FPE_0$, where E_0 is the Young's modulus calculated for the ideal prismatic sample. The correction factors F and P as a function of the chamfer size were calculated by G. Quinn [16].

4 COMPARISON OF THE CORRECTION COEFFICIENTS

The correction coefficients calculated from Eq. (10) and Eq. (8) for the fundamental mode and a prismatic sample are shown in a graph in Fig. 3. The comparison of the coefficients Q_{1p} could not be made because there is not a formula for the correction coefficient for the 1st overtone and a prismatic sample in the ASTM standards ([10] to [13]), and correction coefficients for this case are not in [9]. An indirect verification of the correctness of the coefficients Q_{1p} calculated from the formula (8) is in good agreement between resonant frequencies calculated from commonly accepted Timoshenko's equation and Eq. (4), [4]. The graph of the correction coefficients Q_{1p} calculated from Eq. (8) is in Fig. 6.

The correction coefficients calculated from Eq. (9) and Eq. (8) for the fundamental mode and the cylindrical sample are in Fig. 4, and the correction coefficients for the 1st overtone and a cylindrical sample are plotted in Fig. 5. The coefficients T_{1c} tabulated in [9] served as a basis for the comparison.

As we can see in Fig. 3, 4 and 5, the correction coefficients calculated from Formula (8) show good agreement with those calculated with the help of Eq. (9) and Eq. (10), and with the coefficients presented in [9].

Acknowledgement

This work was supported by grant VEGA 1/0279/03.

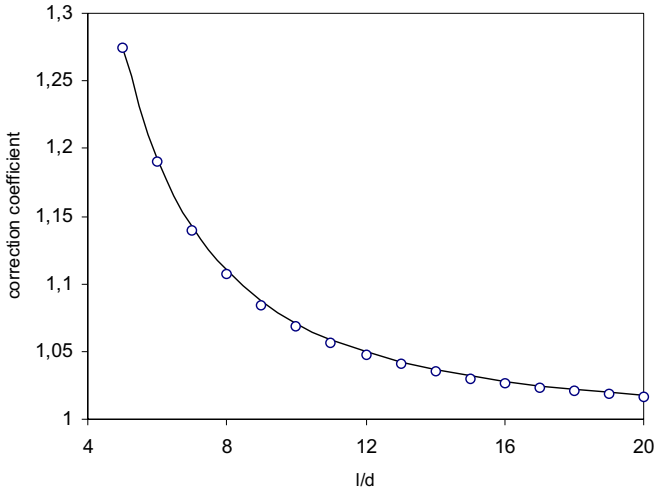

Fig. 3. *Correction coefficients for prismatic sample and fundamental mode: line - T_{0p} after ASTM, points - $(Q_{0p})^2$ calculated from Eq. (8), $\mu = 0.3$*

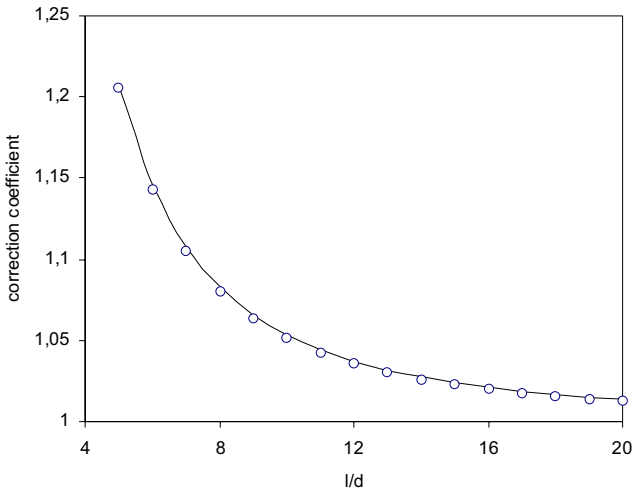

Fig. 4. *Correction coefficients for cylindrical sample and fundamental mode: line - T_{0c} after ASTM, points - $(Q_{0c})^2$ calculated from Eq. (8), $\mu = 0.3$*

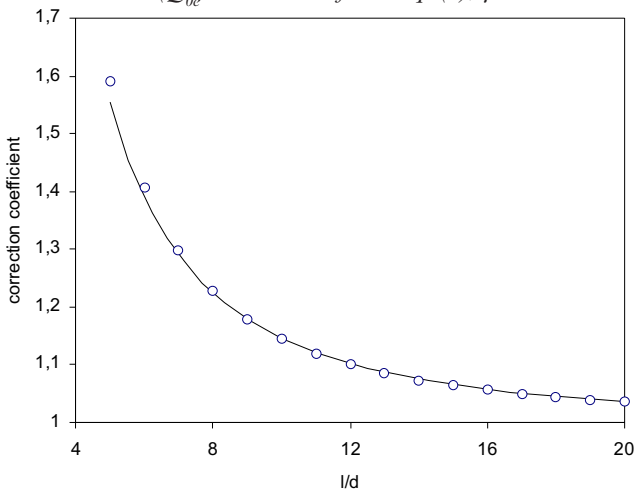

Fig. 5. *Correction coefficients for cylindrical sample and the1st overtone: line - T_{1c} after ASTM, points - $(Q_{1c})^2$ calculated from Eq. (8), $\mu = 0.3$*

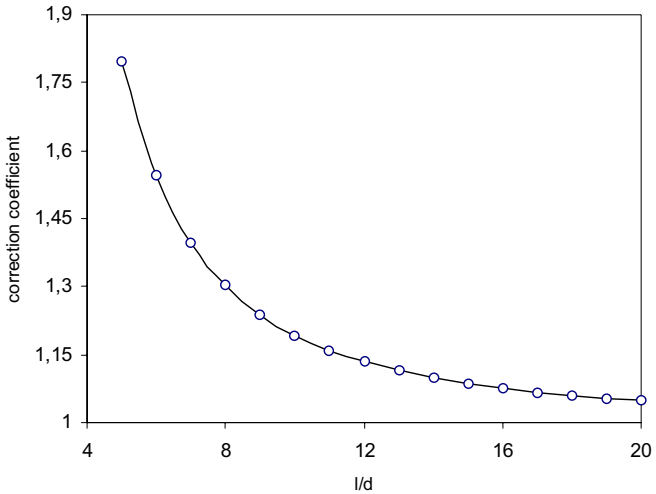

Fig. 6. *Correction coefficients for prismatic sample and the 1st overtone: $(Q_{1p})^2$ calculated from Eq. (8), $\mu = 0.3$*

5 REFERENCES

[1] Förster, F. (1937) Ein neues Messverfahren zur Bestimmung des Elastizitätsmodulus und der Dämpfung. *Zeitschrift für Metallkunde*, 29, 1937, N2, pp. 109-113.

[2] Spinner, S., Tefft, W.E. (1961) Method for determining mechanical resonance frequencies and for calculating elastic moduli from these frequencies. *Am. Soc. Test. Mater. Proc.*, 61, 1961, pp. 1221-1230.

[3] Timoshenko, S. P. (1955) Vibration problems in engineering. *D. Van Nostrand Inc.*, New York.

[4] Štubňa, I., Majerník, V. (1998) An alternative equation of the flexural vibration. *Acustica - Acta Acustica*, 84, 1998, N6, 999-1001.

[5] Štubňa, I., Liška, M. (1999) Correction coefficients for calculation of Young's modulus from resonant frequencies, I: Cylindrical sample. In: *Proc. 4-th Inter. Conf. Theoretical and Experimental Problems of Material Engineering*, Púchov.

[6] Štubňa, I., Liška, M. (1999) Correction coefficients for calculation of Young's modulus from resonant frequencies, II: Prismatic sample. In: *Proc. Conf. DIDMATTECH 1999*, Nitra, pp. 140-143.

[7] Štubňa, I., Liška, M., Malinarič, S. (2001) Correction coefficients for calculation of sound velocity from resonant frequencies, III: 1st Overtone In: *Proc. Conf. DIDMATTECH 2000*, Prešovská univerzita, Prešov, pp. 419-422.

[8] Štubňa, I., Liška, M. (2001) Formula for correction coefficients for calculating Young's modulus from resonant frequencies. *Acustica - Acta Acustica*, 87, 2001, N1, pp. 149-150.

[9] Schreiber, E., Anderson, O.L., Soga, N. (1973) Elastic constants and their measurement. *McGraw-Hill Book Co.*, New York.

[10] ASTM C 1198-01 (2001) Standard test method for dynamic Young's modulus, shear modulus and Poisson's ratio for advanced ceramics by sonic resonance. (published in *Standard Documents*, Philadelphia USA).

[11] ASTM C 848-88 (1999) Standard test method for dynamic Young's modulus, shear modulus and Poisson's ratio for ceramic whiteware by sonic resonance. (published in *Standard Documents*, Philadelphia USA).

[12] ASTM C 1548-02 (2003) Standard test method for dynamic Young's modulus, shear modulus and Poisson's ratio of refractory materials by impulse excitation of vibration. (published in *Standard Documents*, Philadelphia USA).

[13] ASTM C 1259-01 (2001) Standard test method for dynamic Young's modulus, shear modulus and Poisson's ratio for advanced ceramics by impulse excitation of vibration. (published in *Standard Documents*, Philadelphia USA).

[14] Martinček, G. (1975) Teória a metodika dynamického nedeštruktívneho skúšania plošných prvkov. *SAV*, Bratislava.

[15] Acegorian, Z.A., Chočian, M.G. (1960) An investigation of strength of the stone materials. *Zavodskaya Laboratoriya*, 26, 1960, N11, pp. 98-100.

[16] Quinn, G.D. (2000) Elastic modulus by resonance of rectangular prisms: Corrections for edge treatments. *J. Amer. Ceram. Soc.*, 83, 2000, N2, pp. 317-320.

Authors' Address: Doc.Dr. Igor Štubňa
Dr. Anton Trník
Constantine the Philosopher University
Department of Physics
A. Hlinku 1
949 01 Nitra, Slovakia
istubna@ukf.sk

Prejeto: Received: 24.5.2005

Sprejeto: Accepted: 23.2.2006

Odprto za diskusijo: 1 leto
Open for discussion: 1 year

Strojniški vestnik - Journal of Mechanical Engineering 52(2006)5, 323-334
UDK - UDC 699.86:62-404.8
Strokovni članek - Speciality paper (1.04)

Teoretične in eksperimentalne osnove za izdelavo mehanskih izolacijskih pen

Theoretical and Experimental Foundations for the Manufacturing of Mechanical Insulation Foams

Darko Drev - Jože Panjan
(Fakulteta za gradbeništvo in geodezijo, Ljubljana)

V tem prispevku obravnavamo teoretične pogoje, ki so potrebni za izdelavo stabilne mehanske izolacijske pene. Poleg tega navajamo tudi stvarne predloge za izvedbo izdelave mehanske pene in nanosa na gradbene površine. Mehanska pena se oblikuje razmeroma preprosto, zagotovljeni morajo biti samo ustrezni pogoji. Izolacijske lastnosti dajo drobno porazdeljeni zračni mehurčki v izolacijski plasti. Podobne lastnosti imajo tudi različni izdelki iz penjenega betona in penjenega polistirena, ki pa se ne izdelujejo neposredno na gradbišču, temveč v proizvodnih obratih. Glavna zamisel pri tem je nastanek porozne mehanske pene na gradbišču in nanašanje le te na gradbene površine. Pena mora biti dovolj stabilna, da se lahko nanaša na gradbene površine in se tam tudi utrdi.
© 2006 Strojniški vestnik. Vse pravice pridržane.
(Ključne besede: pene izolacijske, pene mehanske, stabilnost, lastnosti reološke)

This paper deals with the theoretical conditions necessary for the formation of stable mechanical insulation foam. In addition to this it gives concrete proposals for the formation of mechanical foam and its application to surfaces in the field of civil engineering. Mechanical foam is formed relatively easily, provided suitable conditions are present. The insulating character is provided by finely distributed air bubbles in the insulation layer. Similar characteristics can be found in various products made of foamed concrete as well as foamed polystyrene, which are not manufactured on site but in manufacturing plants. The main objective is the formation of a porous mechanical foam on the construction site and its application onto construction elements. The foam must be stable enough to be applied to the construction surface and then solidify.
© 2006 Journal of Mechanical Engineering. All rights reserved.
(Keywords: insulating foams, mechanical foams, stability, rheological characteristics)

0 UVOD

Na tržišču je veliko število različnih izolacijskih gradbenih gradiv, ki se v glavnem izdelujejo v proizvodnih obratih v obliki plošč ali zidakov. S pripravljenimi izolacijskimi gradivi se oblagajo gradbene površine, v nekaterih primerih pa se lahko uporabljajo tovrstna gradiva namesto zidakov. V tem prispevku obravnavamo mehanizem nastajanja mehanske izolacijske pene ter postopek nanašanja na gradbene površine. Izhajamo z vidika, da ima gradivo z velikim številom majhnih zračnih mehurčkov zelo dobre izolacijske lastnosti. Podobne lastnosti imajo tudi različni izdelki iz penjenega betona, ki pa se ne izdelujejo neposredno na gradbišču, temveč v proizvodnih obratih, kjer se

0 INTRODUCTION

A large number of insulating construction materials exist on the market. These materials are mostly manufactured in production plants in the form of plates and bricks/blocks. Confectional insulating materials are used for the cladding of construction surfaces and in some cases as a substitute for brick. This paper deals with the mechanism of forming mechanical insulating foam and the procedure of its application onto construction elements. We start from the basis that a material with a large number of small air bubbles has very good insulating characteristics. Various products made of foamed concrete posses similar characteristics. These are not manufactured on site but in production plants

pripravijo v obliki različnih zidakov in izolacijskih plošč. Tako kakor izdelki iz penjenega betona, se proizvajajo v industrijskih obratih tudi izolacijski materiali iz steklenih vlaken, penjenega polistirena, penjenega poliuretana itn. Ta izolacijska gradiva se vgradijo v obliki različnih pripravljenih kosov na fasade, stropove, tla in druge gradbene površine, kjer želimo povečati toplotno in zvočno izolacijo. Na takšne in podobne izolacijske materiale je treba nato nanesti ali pritrditi še pročelna gradiva za lepši videz in ustrezno mehansko trdnost (omet, pročelne obloge itn.).

1 MATERIALI IN METODE

V kašasto snov, ki je sestavljena iz veziva, polnil, vode in drugih dodatkov, želimo vmešati čim večjo količino zraka. Mehanska pena je lahko stabilna le takrat, ko so mehurčki čim manjši, saj je pri tem vzgon najmanjši. Velikost mehurčka je odvisna od gostote razpršnine, površinske napetosti, specifične teže razpršnine, njene homogenosti (vrste gradiv) ter parametrov, ki so odvisni od nastavitve strojne opreme (tlak, vrtenje mešalne glave itn.). Zunanji tlak razpršnine na stene mehurčka in notranji tlak v mehurču morata biti v stabilnem ravnovesju:

$$P_R = P_\infty - \frac{2\gamma.P_\infty.M}{R\,\rho_d.\mathrm{Re}.T} \quad (1),$$

pri tem morata biti vzgon in površinska napetost v ravnovesju:

$$v.g.\rho = 2\pi.\gamma.r \quad (2)$$

$$\rho = \rho_d - \rho_z \quad (3).$$

Na sliki 1 je prikazan nastanek mehurčka v razpršnini in sile, ki delujejo nanj pri stabilnih pogojih.

Pri stabilni mehanski peni je specifična teža razpršnine enaka:

$$\frac{P_\infty M}{\mathrm{Re}.T} = \rho_d \quad (4),$$

prostornina mehurčka je pri tem:

$$V = \frac{4}{3}\Pi r^3 \quad (5),$$

tlak v mehurčku mora biti v ravnovesju z vsoto atmosferskega tlaka in kritičnih tlakov na notranji in

where they are confectionalized in the form of bricks and insulation plates. Likewise, insulation materials made of glass fibres, foamed polystyrene, foamed polyurethane, etc. are produced in production plants. These insulating materials are fitted in the form of standardised pieces on facades, ceilings, floors and other surfaces where we wish to increase the heat and sound insulation. After the application of these and similar insulating materials it is only necessary to apply or fasten the facade material for an improved appearance and adequate mechanical strength (mortar, facade cladding etc).

1 MATERIALS AND METHODS

Our objective is to mix in an as much air as possible into a pasty material composed of binder, filler, water and other admixtures. The mechanical foam is stable only when the bubbles are as small as possible, since the corresponding buoyancy is then minimized. The size of the bubble depends on the density of the dispersion, its homogeneity and other parameters that vary with the settings of the mechanical equipment (pressure, rotation of the mixer etc.) The outer pressure of the dispersion on the wall of the bubble and the inner pressure in the bubble itself must be in stable equilibrium:

the buoyancy and surface tension must be in equilibrium:

Figure 1 presents the formation of a bubble in the dispersion and the forces that act on it under stable conditions.

In a stable mechanical foam the specific weight of the dispersion equals:

the volume of the bubble is:

the pressure inside the bubble must be in equilibrium with the sum of the atmospheric pressure and critical

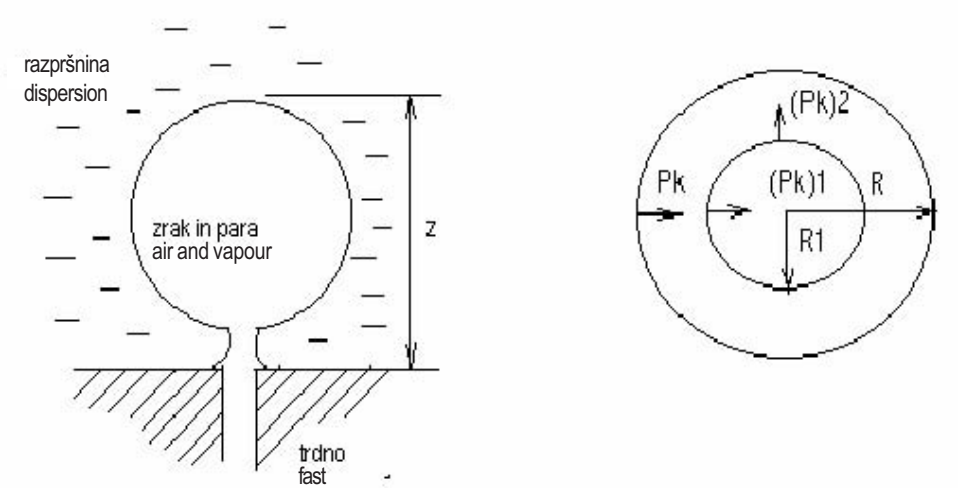

Sl. 1. *Shematski prikaz oblikovanja mehurčka mehanske pene*
Fig. 1. *A schematic representation of the formation of a bubble of mechanical foam*

zunanji steni mehurčka:

pressures on the inner and outer sides of the bubble wall:

$$P_i = P_A + P_K + \left(P_K\right)_1 \tag{6},$$

kritični tlak na notranji steni mehurčka je odvisen od površinske napetosti in velikosti mehurčka:

the critical pressure on the inner wall of the bubble depends on the surface tension and the bubble size:

$$\left(P_k\right)_2 = -\frac{2\gamma}{r} \tag{7},$$

tlak v mehurčku je v ravnovesju z vsoto atmosferskega tlaka in pritiskov na zunanji in notranji steni:

the pressure inside the bubble is in equilibrium with the sum of the atmospheric pressure and the pressures on the outer and inner walls:

$$P_i = P_A + \frac{2.\gamma}{r} + \frac{2.\gamma}{r_1} = P_A + 2.\gamma.\left[\frac{1}{r} + \frac{1}{r_1}\right] \tag{8},$$

za zelo tanke stene mehurčkov velja:

for very thin walls:

$$r \approx r_1 \tag{9},$$

pri čemer je:

where:

$$P_i = P_A + \frac{4.\gamma}{r} \tag{10}$$

in velikost mehurčka je odvisna od površinske napetosti in razlike notranjega in atmosferskega tlaka:

and the size of the bubble depends on the surface tension and the difference in the internal and atmospheric pressures:

$$r = \frac{4.\gamma}{P_i - P_A} \tag{11}.$$

Na sliki 2 so prikazani kritični pogoji, ki veljajo za stabilno mehansko peno. V razpršnino je mogoče pri danih pogojih vmešati samo določeno količino

Figure 2 presents the critical conditions that apply for a stable mechanical foam. Under given circumstances only a specific amount of air can be

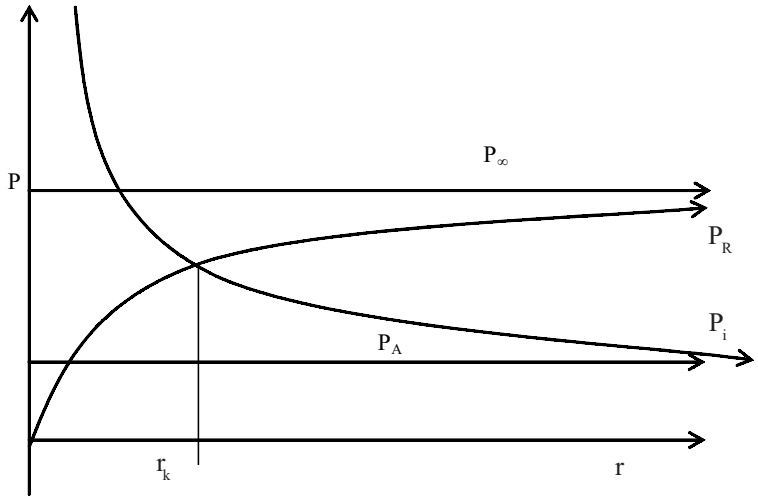

Sl. 2. *Kritični pogoji pri oblikovanju polimerne mehanske pene*
Fig. 2. *Critical conditions in the formation of polymer mechanical foam*

zraka. Če dovedemo na stroj za oblikovanje mehanske pene večjo količino zraka od teoretično dovoljene, dobimo neenakomerno strukturo z velikimi mehurčki. Premajhna količina zraka pa povzroči nastanek debelih sten, večjo gostoto in slabše izolacijske značilnosti nanosa.

applied to a dispersion. In the event that a larger quantity of air, with regards to the theoretically permitted limit, is applied to the mechanical foam-forming machine, we get a non-homogenous structure with large bubbles. On the other hand, an insufficient quantity of air causes the formation of thick walls, a larger density and poorer insulation characteristics of the coating.

Kritični pogoji: $R = R_\infty$

Critical conditions $R = R_\infty$

$$\left(P_i\right)_k = \left(P_R\right)_k \tag{12}$$

$$\ln\frac{P_\infty}{\left(P_R\right)_k} = \frac{M.\left(\left(P_R\right)_k - P_A\right)}{\mathrm{Re}.T.\rho_d} = \frac{M}{\mathrm{Re}.T.\rho_d}.\frac{2.\gamma}{P_k} \tag{13}.$$

Pri dviganju mehurčka mora biti vzgon večji od sil, ki držijo mehurček v razpršitvi:

In the event of the rising of the bubble the buoyancy must be greater than the forces that hold the bubble in the suspension:

$$v = \frac{2.g.r^2}{9.\eta_d}.\left(\rho_d - \rho_z\right)\frac{3.\eta_z + 3.\eta_d}{3.\eta_z + 2.\eta_d} \tag{14},$$

pri tem sta gostota in površinska napetost razpršnine mnogo večji kakor pri zraku:

where the density and surface tension of the dispersion are greater than with the air:

$$\rho_d >> \rho_z \qquad \text{in / and} \qquad \eta_d >> \eta_z$$

pri takšnih pogojih je hitrost dviganja mehurčka:

under these conditions the velocity of the rising bubbles is:

$$v = \frac{2.g.r^2.\rho_d}{9.\eta_d} \tag{15},$$

kjer pomenijo:
Indeksi:
1 = zrak + para
2 = tekočina (razpršnina)

where the indexes and symbols mean:
Indexes:
1 = air + steam
2 = fluid (dispersion)

3 = trdno
r = na krivulji
Simboli:
ρ_d = gostota polimerne razpršnine
ρ_z = gostota zraka u mehurčku
V = prostornina
r_1, r_2 = polmer mehurčka
$P\infty$ = tlak pare pri ravni površini ($r\infty$)
P_l = notranji tlak
P_R = tlak na konkavno ali konveksno površino
P_A = atmosferski tlak
ρ_D = gostota pare
Re = Reynoldsovo število
v = hitrost dviganja mehurčka
η_d = viskoznost polimerne razpršnine
η_z = viskoznost zraka v mehurčku
γ = površinska napetost
g = težnostni pospešek (9,81 m/s^2)
m = masa polimerne razpršnine

2 PREIZKUSNI DEL

Mehansko izolacijsko peno bi lahko izdelovali neposredno na gradbišču z ustrezno strojno opremo. Za izdelavo mehanske pene bi lahko v načelu uporabili strojno opremo, ki se uporablja za oplemenitenje tekstila, ali pa posebej za to izdelane stroje. Ker gre za novost, še ni izdelane namenske strojne opreme za oblikovanje mehanske izolacijske pene v gradbeništvu. Pri praktičnih preizkusih se je zato uporabljala laboratorijska strojna oprema za oplemenitenje tekstila ter kuhinjski mešalnik za smetano. Strojno opremo razdelimo na dva dela:

- strojno opremo za oblikovanje mehanske pene,
- strojno opremo za nanos na gradbene površine.

Nekaj mogočih sestav mehanske pene:

- cement, voda, anorganski prah, stabilizator mehanske pene, pigmenti, drugi dodatki,
- mavec, voda, stabilizator mehanske pene, pigmenti, drugi dodatki,
- gašeno apno, voda, anorganski prah, stabilizator mehanske pene, pigmenti, drugi dodatki,
- polimerno vezivo, voda, anorganski prah, stabilizator mehanske pene, pigmenti, drugi dodatki,
- polimerno vezivo, voda, organski prah, stabilizator mehanske pene, pigmenti, drugi dodatki,
- polimerno vezivo, voda, lesni prah, stabilizator mehanske pene, pigmenti, drugi dodatki, itn.

3 = solids
r = on graph
Symbols:
ρ_d = density of the polymer dispersion
ρ_z = density of the air in the bubble
V = volume
r_1, r_2 = radius of the bubble
$P\infty$ = steam pressure in the event of a flat surface ($r\infty$)
P_l = internal pressure
P_R = pressure on a concave or convex surface
P_A = atmospheric pressure
ρ_D = steam density
Re = Reynolds number
v = velocity of rising bubble
η_d = viscosity of the polymer dispersion
η_z = viscosity of the air inside the bubble
γ = surface tension
g = ground acceleration (9.81 m/s^2)
m = mass of the polymer dispersion

2 EXPERIMENTAL SECTION

The mechanical foam could be produced on site with the appropriate mechanical equipment. In principle we could use the equipment employed in the upgrading of textiles or specially developed machinery. However, because this is an innovation, special, purposely constructed machines for the formation of mechanical foam in civil engineering do not exist. Therefore, in practise, mechanical laboratory equipment, such as that for the upgrading of textiles and kitchen food-mixers, is used. The mechanical equipment can be divided into two parts:

- mechanical equipment for the formation of mechanical foam,
- mechanical equipment for its placement on construction surfaces.

Some of the possible compositions of the mechanical foam are as follows:

- cement, water, inorganic dust, mechanical foam stabilisers, pigments, other additives,
- gypsum, water, mechanical foam stabilisers, pigments, other additives,
- lime, water, inorganic dust, mechanical foam stabilisers, pigments, other additives,
- polymer binders, water, inorganic dust, mechanical foam stabilisers, pigments, other additives,
- polymer binders, water, organic dust, mechanical foam stabilisers, pigments, other additives,
- polymer binders, saw dust, mechanical foam stabilisers, pigments, other additives.

Preglednica 1. Nekaj podatkov o snoveh, ki se uporabljajo v gradbeništvu (Pravilnik o toplotni zaščiti in učinkoviti rabi energije v stavbah (Ur.l. RS, št. 42/02))
Table 1. A few characteristics of the materials frequently used in civil engineering (Regulation regarding the efficient use of energy in buildings (Ur.l. RS, št. 42/02))

gradivo material	ρ kg/m^3	C J/kgK	λ W/mK	μ	α_i 10^{-6} K^{-1}
apnena malta lime mortar	1600	1050	0,81	10	0,8
cementna malta cement mortar	2100	1050	1,4	30	1,1 do/to 1,2
cementna malta + lateks cement mortar + latex	1900	1050	0,7	30	1,2
porolit porolit – clay blocks	1200	920	0,52	4	0,5
steklena pena glass foam	145	840	0,056	100000	0,8
PS plošče (v kladah) PS plates (in blocks)	15	1260	0,041	25	6
penjeno steklo foamed glass	140	1100	0,06	?	
klada iz celičnega betona, porobetona blocks of cell concrete, porous concrete	450 500	860 860	0,14 0,15	3,5 4	

Pravilnik o toplotni zaščiti in učinkoviti rabi energije v stavbah (Ur.l. RS, št. 42/02) ima v prilogi navedene snovne podatke o velikem število izolacijskih materialov, med katere bi lahko uvrstili tudi mehanske izolacijske pene, ki bi bile narejene po našem postopku. V preglednici 1 zato navajamo neaj skupin materialov, kamor bi lahko uvrstili izolacijske mehanske pene.

2.1 Mogoče tehnične rešitve oblikovanja in nanašanja mehanske pene na gradbene površine

Tehnološki postopek lahko razdelimo na naslednje faze:
- priprava razpršitve,
- oblikovanje mehanske pene,
- nanašanje mehanske pene na gradbeno površino.

Priprava razpršitve

Pri opisu se bomo omejili le na vodne razpršnine, čeprav so mogoče tudi druge razpršitve. Priprava razpršnine poteka:

V vodo doziramo med mešanjem ustrezne deleže posameznih komponent (vezivo, polnilo, pigment, stabilizator mehanske pene, drugi dodatki).

The regulations regarding the efficient use of energy in buildings (Ur.l. RS, št. 42/02) specify the material characteristics for a large quantity of insulation materials, among which we could include mechanical insulation foams produced according to our procedure. Table 1 lists a few groups of materials where we could list insulation mechanical foams.

2.1 Possible technical solutions for the formation and application of mechanical foam onto surfaces in civil engineering

The technological procedure can be broken down into the following phases:
- the preparation of the dispersion,
- the formation of the mechanical foam,
- the application of mechanical foam onto surfaces in civil engineering.

The preparation of the dispersion

Although other dispersions are possible we will limit the description of the procedure to water dispersions. The preparation of the dispersion includes:

While stirring we mix in the required quantities of individual components (binder, filler, pigment, mechanical foam stabiliser, other admixtures).

Priprava razpršnine lahko poteka prekinjano ali zvezno. Pomembno je, da je zagotovljena ustrezna sestava razpršnine (deleži ustreznih komponent, homogenizacija).

Če je v razpršitvi takšno vezivo, ki se zelo hitro utrdi (mavec, cement itn.), je treba zagotoviti takojšnjo obdelavo na stroju za nastanek mehanske pene in uporabo produkta na gradbeni površini, ki jo želimo izolirati ali dekorativno obdelati. Stabilizatorji mehanske pene in drugi dodatki za izboljšanje reoloških lastnosti se dodajajo glede na stvarne potrebe (nastanek pene, barva, utrjevanje itn.).

Nastanek mehanske pene

Iz pripravljene razpršnine, ki mora vsebovati predpisano sestavo in biti ustrezno homogenizirana, se lahko izdela mehanska pena. Za to pa morajo biti izpolnjeni pogoji, ki so navedeni v teoretičnem delu. Na sliki 3 je prikazana shema strojne opreme, ki se uporablja za nastanek mehanske polimerne pene za oplemenitenje tekstila. Ta shema vsebuje vse značilne sestavine, ki bi jih moral imeti namenski stroj za nastanek mehanske pene v gradbeništvu. Na dotoku v mešalno glavo priteka razpršnina, v katero želimo vmešati čim večjo količino zraka. Vmešavanje zraka poteka na mešalni glavi, kjer se mešata razpršnina in zrak. Količino razpršnine in zraka se lahko uravnava. Pri zraku je treba poleg količine uravnavati tudi tlak. Na iztoku iz stroja izstopa stabilna mehanska pena, ki se mora čimprej nanesti na ustrezno gradbeno površino.

The preparation of the dispersion can be continuous or discontinuous. It is important that an adequate composition of the dispersion is guaranteed (parts of the individual components, homogeneity).

If the dispersion contains fast-setting binders (gypsum, cement etc.) it is necessary to ensure immediate treatment in the machine for the formation of mechanical foam and use of the product on the surface we wish to insulate or decorate. Stabilisers of the mechanical foam and other additives for the improvement of its rheological characteristics are added according to specific needs. (formation of the foam, colour, hardening etc.).

The formation of the mechanical foam

Mechanical foam can be made from a prepared dispersion composed of the required ingredients, adequately homogenised. In this case all the conditions listed in the theoretical part must be fulfilled. Figure 3 presents a scheme of the mechanical equipment needed for the preparation of mechanical polymer foam used for the upgrading of textiles. This scheme includes all the characteristic components necessary for a purpose-built machine for the production of mechanical foam in the field of civil engineering. The dispersion into which we wish to mix a large as possible quantity of air flows into the mixing head. The admixing of the air takes place in the mixing head, where the dispersion and air are mixed. The quantity of dispersion and air can be regulated. When regulating the quantity of air its pressure is also regulated. On its outflow from the machine we obtain a stable mechanical foam, which has to be applied to the construction surface.

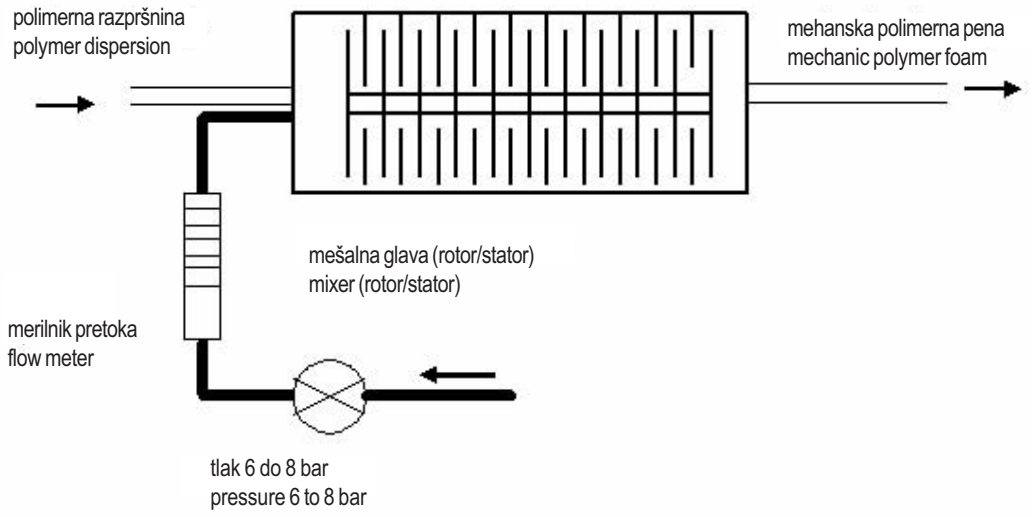

Sl. 3. *Shematski prikaz stroja za oblikovanje mehanske pene*

Fig. 3. *A schematic drawing of the machine for the production of mechanical foam*

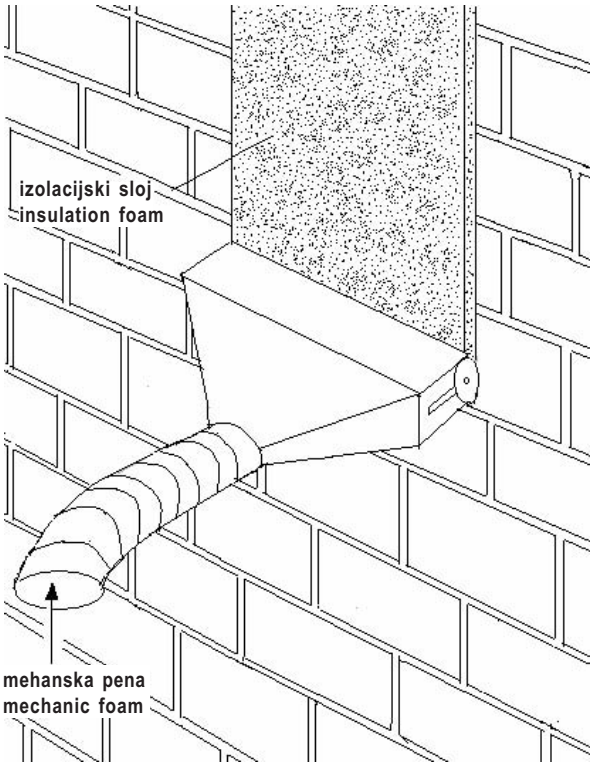

Sl. 4. *Prikaz nanosa mehanske izolacijske pene na ravno steno*
Fig. 4. *The application of mechanical insulation foam on a flat wall*

Nanašanje mehanske pene na gradbeno podlago

Nastala mehanska pena se mora obnašati kot tekočina pri prenosu in nanašanju, nato pa kot trdna snov. Te značilne reološke lastnosti je treba upoštevati pri prenosnem sistemu (dovodni cevi) mehanske pene na mesto nanosa ter pri obliki nanašalne glave. Mogočih načinov nanašanja mehanske pene na gradbeno podlago je lahko več. Podajamo le eno izmed mogočih rešitev, ki je prikazana na sliki 4.

Pri nanašalni glavi mora biti ustrezen distančnik, ki določa debelino nanosa. V stvarnem primeru je prikazan ta distančnik v obliki koleščka ob robu nanašalne glave. Z nastavitvijo stranskih koleščkov se lahko uravnava želen odmik od stene. S tem je določena tudi debelina nanosa mehanske izolacijske pene.

2.2 Primer oblikovanja mehanske pene iz vodne razpršnine polimernega veziva (poliakrilat), anorganskega polnila in dodatkov

Pogoji oblikovanja mehanske pene pri preizkusu so:

The application of mechanical foam onto surfaces

The produced mechanical foam must behave as a fluid during both transport and placement, while its latter behaviour must be as a solid material. These typical rheological characteristics must be considered in the transport system (feeding hoses) of the mechanical foam to the placement surfaces as well as in the construction of the applicator. There are several ways of placing mechanical foam on surfaces in civil engineering. We present one of the possibilities in Figure 4.

An appropriate spacer must be located on the applicator. Its purpose is to control the thickness of the placed layer. In this case the spacer is in the form of a guide wheel located at the edge of the applicator. By adjusting the wheels the distance from the wall can be regulated. This procedure determines the thickness of the layer of the mechanical insulation foam.

2.2 An example of the formation of mechanical foam from a water dispersion of polymer binder (polyacrilat), inorganic filler and admixtures

The conditions of mechanical foam formation in the experiment are:

Polimerna razpršnina:
$\rho_d = 1200$ kg/m^3
$\eta_d = 300$ m Pa s

Nastavitve na stroju za oblikovanje mehanske pene za oplemenitenje tekstila Mondomix:
- zračni tlak: 4 bar
- dotok polimerne razpršnine: 500 do 600 ml/min
- dotok zraka: 0,5 l/min
- vrtilna frekvenca mešalne glave: 1200 vrt./min
- gostota mehanske pene: 180 do 220 g/l

Izračun teoretične hitrosti gibanja mehurčka za določen preizkus:

Polymer dispersion:
$\rho_d = 1200$ kg/m^3
$\eta_d = 300$ m Pa s

Settings on the machine for the production of mechanical foam for the upgrading of textiles Mondomix:
- air pressure: 4 bar
- intake of polymer dispersion: 500 to 600 ml/min
- intake of air: 0.5 l/min
- mixing head velocity: 1200 rpm
- density of mechanical foam: 180 to 220 g/l

Calculation of the velocity of the bubble for this concrete experiment:

$$\phi_{\text{pene/foam}} = \phi_{\text{disp.}} + \phi_{\text{zraka/air}} \quad \text{(pri/at 1 bar)}$$

$$\Phi_{zraka} = \frac{P}{P_0}\Phi = \frac{4\ \text{bar}}{1\ \text{bar}} \cdot \frac{0,5\ \text{l}}{\text{min}} = 2\,\frac{\text{l}}{\text{min}}$$

$$\varphi_{pene} = 0,5\ \frac{\text{l}}{\text{min}} + 2\,\frac{\text{l}}{\text{min}} = 2,5\,\frac{\text{l}}{\text{min}}$$

teoretična gostota pene:

the theoretical density of the foam:

$$\rho_{\text{pene/foam}} = \frac{m_{\text{zraka/air}} - m_{\text{disp.}}}{V_{\text{pene/foam}}} = \frac{500\ \text{g}}{2,5\ \text{l}} = 200\ \text{g/l}$$

Dobljena gostota pene pri preizkusu: 180 do 220 g/l.

The achieved density of foam during the experiment: 180 to 220 g/l.

Hitrost dviganja mehurčkov:

The velocity of the rising bubbles:

$$v = \frac{2gr^2}{9\eta_d}\left(\rho_d - \rho_z\right)\frac{3\eta_z + 3\eta_d}{3\eta_z + 2\eta_d} \qquad \text{m/s}$$

Izmerjena velikost por (z mikroskopom): r = pribl. 10^{-5} m

The measured size of the pores (using a microscope): r = approx. 10^{-5} m

$$\rho_2 >> \rho_1 \qquad \text{in / and} \qquad \eta_2 >> \eta_1$$

$$v = \frac{2gr^2}{9\eta_d}\cdot\rho_d = \frac{2\cdot 9,81\frac{\text{m}}{\text{s}^2}\cdot(1\cdot 10^{-5}\,\text{m})^2\cdot 1200\frac{\text{kg}}{\text{m}^3}}{9\cdot 300\ \text{m.Pa.s}} = 8,7\cdot 10^{-10}\ \text{m/s}$$

Izračunana hitrost je tako majhna, da se mehurčki praktično ne gibljejo. Mehanska pena je bila zato zelo stabilna. Takšno peno se lahko nanaša na podlago brez poškodbe njene strukture. Pri tem mora biti izbran ustrezen postopek nanašanja, pri katerem se ne poškoduje struktura pene. Na sliki 5 je prikazana fotografija toplotno utrjene obravnavane mehanske pene, posnete z elektronskim mikroskopom. S slike je razvidno, da se po utrditvi ni bistveno spremenila struktura mehanske pene.

Količina zraka v nastali mehanski peni:

The calculated velocity is so small that the bubbles are practically stationary. Therefore, the mechanical foam was very stable. Such a foam can be applied to a surface without damage to its structure. An appropriate application procedure must be chosen in order to prevent damage to the foam structure. Figure 5 presents a photograph of a hardened mechanical foam taken with an electron microscope. From the photograph it is evident that the hardening process did not have a significant influence on the mechanical foam's structure.

The quantity of air in the mechanical foam:

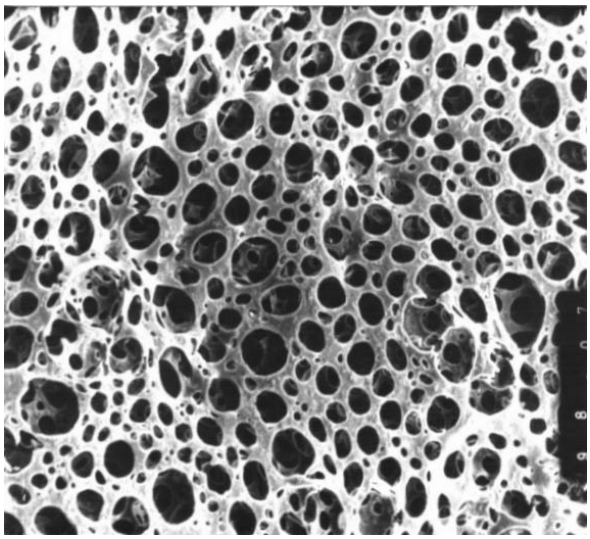

Sl. 5. *Fotografija mikroporozne mehanske pene na podlagi poliakrilatne razpršitve, povečava 190-krat*
Fig. 5. *A photograph of the micro-porous mechanical foam on the basis of polyacril dispersion, enlargement 190 times*

Delež polimerne razpršnine:

The percentage of the polymer dispersion:

$$(\%) = \frac{\rho_{pene} \cdot 100}{\rho_d} = \frac{0,22 \frac{\text{kg}}{\text{l}} \cdot 100}{1,2 \frac{\text{kg}}{\text{l}}} = 18\%$$

Delež zraka v mehanski peni:

The percentage of air in the mechanical foam:

$$(\%) = 100\% - 18\% = 82\%$$

3 REZULTATI IN RAZPRAVA

Izolacijske mehanske pene so lahko ena izmed mogočih tehnoloških rešitev za dodatno toplotno zaščito stavb in okrasni zgornji sloj. Nastanek mehanske izolacijske pene je teoretično razmeroma preprost. Tudi nanos na gradbeno površino ne bi smel pomeniti prevelikega problema. Večje težave lahko nastanejo v primeru, kadar je čas utrjevanja bistveno počasnejši od časa stabilnosti mehanske pene. Če bi oblikovali mehansko peno iz gašenega apna, bi verjetno nastale težave s pravočasno utrditvijo strukture. Apno se namreč utrdi z vezavo CO_2 iz zraka. Morda bi lahko oblikovali mehansko peno z dodatkom CO_2. V tem primeru bi prišlo do hitrejše utrditve. Pri uporabi različnih cementov ali cementnih malt je mogoče laže uravnavati čas utrditve strukture mehanske izolacijske pene. To je glede na omejeno stabilnost mehanske pene zelo pomembno. Tudi mavec se zelo hitro utrdi. Problem pa lahko nastane pri oblikovanju stabilne mehanske pene.

3 RESULTS AND DISCUSSION

Insulation mechanical foams can be one possible technological solution for the additional thermal protection of buildings as well as for decorative coatings. Theoretically, the formation of mechanical insulation foam is relatively simple. Its application onto surfaces in civil engineering should not pose any major problems. Larger problems could occur in the event that the hardening time is greater than the time the mechanical foam is stable. If we were to form mechanical foam from hydrated lime we would most likely have problems with timely hardening of its structure. Lime hardens by binding with CO_2 from the air. Perhaps we could form a mechanical foam with the addition of CO_2. In this case we could achieve a faster binding. With the use of various cements or cement mortars it is easier to regulate the hardening time of the mechanical insulation foam structure. Even gypsum hardens quickly. Problems can occur in the formation of a stable mechanical foam. The simplest way is the formation of mechanical foam

Najpreprostejše je oblikovanje mehanske pene pri vodni razpršnini na podlagi polimernih veziv, kar smo prikazali s praktičnim preizkusom.

Preizkusi uporabe različnih anorganskih veziv so šele v začetni fazi, zato še nimamo ustreznih rezultatov. Ne glede na to, ali je vezivo anorganskega ali organskega porekla, velja enak mehanizem oblikovanja mehanske izolacijske pene. Tudi nanos na gradbeno površino se ne more bistveno razlikovati. Mehanska pena ima v vsakem primeru približno enake reološke lastnosti, ki jih je potrebno upoštevati. Penasto gradivo nastane tudi v zmesi vodnega stekla in alkohola. Po utrditvi pa je nastalo penasto gradivo zelo trdno. V primeru, da bi bila mehanska pena hidrofobna, bi imela tudi hidroizolacijske lastnosti. Hidrofobnost bi lahko zagotovili predvsem pri mehanskih penah na podlagi polimernih veziv. Če bi bilo vezivo na podlagi polisikolsanov ali fluorogljikov, bi dosegli zelo veliko hidrofobnost, polimerni material pa bi se razmeroma hitro utrdil na zraku.

Poleg izbire ustreznih materialov je pomembna tudi strojna izvedba oblikovanja mehanske pene in sistem za nanašanje na gradbeno podlago. V tem prispevku podajamo le idejne rešitve, ki jih je treba v praksi preizkusiti in dograditi. Po nanosu na gradbeno podlago je treba utrjene materiale še testirati glede toplotno-izolacijskih zmožnosti in drugih fizikalnih in kemijskih lastnosti.

S tem prispevkom želimo odpreti novo področje na področju izolacijskih in dekorativnih materialov v gradbeništvu, ki ga je treba šele razviti in preizkusiti v praksi.

with a water dispersion made on the basis of polymer binders, as we showed in our practical test.

Usage tests of various inorganic binders are still in the developing stage, so we do not have any results available. Regardless of the binder, be it of organic or inorganic origin, the mechanism of the mechanical insulation foam remains the same. Not even its application to construction surfaces can differ significantly. In all cases the mechanical foam has approximately the same rheological characteristics, which need to be considered. Foamy material also forms in mixtures of water glass and alcohol. After it hardens the formed foamy material is very hard. In the event that the mechanical foam would be hydrophobic it would also have hydro-insulation characteristics. Hydrophobic characteristics could be obtained mainly with mechanical foams on the basis of polymer binders. If the binder was based on polysicolsan or fluorine-carbons we could achieve good hydrophobic characteristics and the polymer material would harden relatively quickly in air.

Apart from the choice of appropriate materials, the execution of the formation of mechanical foam as well as its application to surfaces in civil engineering are of great significance. This paper presents only the idea for the solution, which must be tested in practise and upgraded. After the application of the materials it is necessary to test the hardened materials with regards to their insulating capacities and other physical and chemical characteristics.

The intention of this article is to open a new segment in the field of insulation and decorative materials in civil engineering. This segment must be developed and proven in practise.

4 LITERATURA
4 REFERENCES

[1] A. J. Wilson (1989) Foams, physics, chemistry and structure.
[2] J.J. Bikerman (1973) Foams.
[3] J.F. Danielli, K.G.A. Pankhurst, A.C. Riddiford (1973) Recent progress in surfance science.
[4] W. Bumbullis, Schäumfäigkeit.
[5] Prospekti in navodila firm: Hansa, Mondomix, Stork, Pfersee, Bayer, Hoechst, itn.
[6] D. Drev (2005) Izdelava mehanskih pen za izolacijo in njihova uporaba v gradbeništvu, *Urad za intelektualno lastnino*, patent št. 21557.
[7] D. Drev (1997) Filtri za otprašivanje s mikroporoznim polimernim slojevima = Dust filtering with microporous polymer layers. *Polimeri*, 1997, 18, 5-6, str.: 228-232, Zagreb.
[8] N. Thomas, S. Tait, T. Koyaguchi (1993) Mixing of stratified liquids by the motion of gas bublles with application to magma mixing, *Earth Planet. Sc. Lett.*, 115, 161-175, 1993.
[9] W.Müller (2002) Mechanische Grundoperationen, *Fachhochschule Düsseldorf*.
[10] K.G.Kornev, A.V.Neimark, A.N.Rozhkov (1999) Foam in porous: thermodynamic and hydrodynamic peculiartis, *Advences in Colloid and Interface Science*, 82, 1999.

Naslov avtorjev: dr. Darko Drev
doc.dr. Jože Panjan
Univerza v Ljubljani
Fakulteta za gradbeništvo in geodezijo
1000 Ljubljana
darko.drev@izvrs.si
joze.panja@fgg.uni-lj.si

Authors' Address: Dr. Darko Drev
Doc.Dr. Jože Panjan
University of Ljubljana
Faculty of Civil Eng. and Gheodesy
1000 Ljubljana, Slovenia
darko.drev@izvrs.si
joze.panja@fgg.uni-lj.si

Prejeto: 20.9.2005
Received:

Sprejeto: 23.2.2006
Accepted:

Odprto za diskusijo: 1 leto
Open for discussion: 1 year

Osebne vesti - Personal Events

Doktorati, magisteriji in diplome - Doctor's, Master's and Diploma Degrees

DOKTORATI

Na Fakulteti za strojništvo Univerze v Ljubljani sta z uspehom zagovarjala svoji doktorski disertaciji:

dne *5. aprila 2006*: **mag. Damjan Klobčar**, z naslovom: "Matematično modeliranje procesov pri reparaturnem varjenju orodij";

dne *5. aprila 2006*: **mag. Andrej Lešnjak**, z naslovom: "Študij procesov navarjanja trdih plasti in njihovih lastnosti z elektroiskrnim postopkom".

Na Fakulteti za strojništvo Univerze v Mariboru so z uspehom zagovarjali svoje doktorske disertacije:

dne *12. aprila 2006*: **mag. Primož Pogorevc**, z naslovom: "Vpliv biodizelskega goriva na karakteristike vbrizganega curka";

dne *21. aprila 2006*: **mag. Jure Ravnik**, z naslovom: "Metoda robnih elementov za hitrostno vrtinčno formulacijo simulacije velikih vrtincev" in **mag. Zoran Žunič**, z naslovom: "Mešana metoda robnih in končnih elementov za reševanje hitrostno vrtinčne formulacije Navier-Stokesovih enačb".

S tem so navedeni kandidati dosegli akademsko stopnjo doktorja znanosti.

MAGISTERIJI

Na Fakulteti za strojništvo Univerze v Ljubljani je z uspehom zagovarjal svoje magistrsko delo:

dne *25. aprila 2006*: **Denis Giacomelli**, z naslovom: "Inženirski informacijski sistem za podporo dinamičnih grozdnih struktur".

Na Fakulteti za strojništvo Univerze v Mariboru je z uspehom zagovarjal svoje magistrsko delo:

dne *7. aprila 2006*: **Uroš Očko**, z naslovom: "Metode za zagotavljanje celovitosti ležajnega obroča".

S tem sta navedena kandidata dosegla akademsko stopnjo magistra znanosti.

DIPLOMIRALI SO

Na Fakulteti za strojništvo Univerze v Ljubljani sta pridobila naziv univerzitetni diplomirani inženir strojništva:

dne *25. aprila 2006*: Miha ERJAVEC, Radoica GAVRANOVIĆ.

*

Na Fakulteti za strojništvo Univerze v Ljubljani so pridobili naziv diplomirani inženir strojništva:

dne *13. aprila 2006*: Luka ČIBEJ, Jernej DEMŠAR, Darko KRAJNC, Borut PUC;

dne *14. aprila 2006*: Emin DURAKOVIĆ, Boris KRAŠEVEC, Janez OGRINC, Matej ERŽEN, Gregor ROMIH, Danjel ZOBEC.

Na Fakulteti za strojništvo Univerze v Mariboru so pridobili naziv diplomirani inženir strojništva:

dne *20. aprila 2006*: Aleš BRENCE, Albin FERLEŽ, Uroš TRATNJEK.

Bled, Slovenia, September 11th - 14th 2007

ICIT&MPT 2007

6th International Conference on Industrial Tools and Material Processing Technologies

6. mednarodna konferenca o industrijskih orodjih in tehnologijah predelave materialov

Cilji

Industrijska orodja se lahko opišejo kot ena najpomembnejših vlečnih sil sodobnih proizvodnih tehnologij. Proizvodnja in gospodarstvo se danes opisujeta kot turbulentna, polna sprememb, konkurence, priložnosti in tveganj. Povsem enako velja tudi za področje orodjarstva in proizvodnje.

Nove tehnologije predelave materialov in izdelave orodij, navidezna proizvodnja, inteligentni sistemi, hitra proizvodnja orodij, orodja za prilagodljivo in proizvodnjo majhnih serij, upravljanje orodjarskih tehnologij, novi materiali in njihova obdelava, sočasni postopki in metode načrtovanja izdelkov,... na vseh teh področjih bodo potekale razprave med strokovnjaki, inženirji, raziskovalci in znanstveniki iz industrije, raziskovalnih ustanov ali univerz.

Eden predpogojev za uspešno konferenco je gotovo kraj, zato vas vabimo na Bled, slovenski biser s čisto vodo in zrakom, obkrožen s temnimi gozdovi in visokimi belimi gorami.

Za več informacij obiščite uradno spletno stran konference.

Objectives

Industrial tools can be described as one of the most important driving forces of modern manufacturing technologies. As nowadays the production and economy can be described as turbulent, full of changes, competition, opportunities and risks, the same is valid also for tool development and production.

New material processing and tool manufacturing technologies, virtual manufacturing, intelligence systems, rapid tooling, tools for flexible and small quantity production, management of tool making, new materials and their treatments, concurrent processes and part (re)design methods,...all these topics will be discussed during the gathering of respected specialists, engineers, researchers and scientists coming from the industry, research institutions or academia.

One of preconditions for having a successful conference is also the meeting place, therefore we invite you to Bled - a Slovene pearl with pure air and water, surrounded by dark forests and high white mountains.

For more information please visit official website of the conference.

Organizatorja

TECOS - SLOVENIAN TOOL AND DIE DEVELOPMENT CENTRE

Organizers

Splošne informacije / General information: **Tanja Ferleš**, T: +386 3 490 09 20, F: +386 3 426 46 11, E: icit@tecos.si, I: http://www.tecos.si/icit

Strojniški vestnik - Journal of Mechanical Engineering 52(2006)5, 337-338
Navodila avtorjem - Instructions for Authors

Navodila avtorjem - Instructions for Authors

Članki morajo vsebovati:
- naslov, povzetek, besedilo članka in podnaslove slik v slovenskem in angleškem jeziku,
- dvojezične preglednice in slike (diagrami, risbe ali fotografije),
- seznam literature in
- podatke o avtorjih.

Strojniški vestnik izhaja od leta 1992 v dveh jezikih, tj. v slovenščini in angleščini, zato je obvezen prevod v angleščino. Obe besedili morata biti strokovno in jezikovno med seboj usklajeni. Članki naj bodo kratki in naj obsegajo približno 8 strani. Izjemoma so strokovni članki, na željo avtorja, lahko tudi samo v slovenščini, vsebovati pa morajo angleški povzetek.

Za članke iz tujine (v primeru, da so vsi avtorji tujci) morajo prevod v slovenščino priskrbeti avtorji. Prevajanje lahko proti plačilu organizira uredništvo. Če je članek ocenjen kot znanstveni, je lahko objavljen tudi samo v angleščini s slovenskim povzetkom, ki ga pripravi uredništvo.

VSEBINA ČLANKA

Članek naj bo napisan v naslednji obliki:
- Naslov, ki primerno opisuje vsebino članka.
- Povzetek, ki naj bo skrajšana oblika članka in naj ne presega 250 besed. Povzetek mora vsebovati osnove, jedro in cilje raziskave, uporabljeno metodologijo dela,povzetek rezulatov in osnovne sklepe.
- Uvod, v katerem naj bo pregled novejšega stanja in zadostne informacije za razumevanje ter pregled rezultatov dela, predstavljenih v članku.
- Teorija.
- Eksperimentalni del, ki naj vsebuje podatke o postavitvi preskusa in metode, uporabljene pri pridobitvi rezultatov.
- Rezultati, ki naj bodo jasno prikazani, po potrebi v obliki slik in preglednic.
- Razprava, v kateri naj bodo prikazane povezave in posplošitve, uporabljene za pridobitev rezultatov. Prikazana naj bo tudi pomembnost rezultatov in primerjava s poprej objavljenimi deli. (Zaradi narave posameznih raziskav so lahko rezultati in razprava, za jasnost in preprostejše bralčevo razumevanje, združeni v eno poglavje.)
- Sklepi, v katerih naj bo prikazan en ali več sklepov, ki izhajajo iz rezultatov in razprave.
- Literatura, ki mora biti v besedilu oštevilčena zaporedno in označena z oglatimi oklepaji [1] ter na koncu članka zbrana v seznamu literature. Vse opombe naj bodo označene z uporabo dvignjene številke[1].

OBLIKA ČLANKA

Besedilo članka naj bo pripravljeno v urejevalnilku Microsoft Word. Članek nam dostavite v elektronski obliki.

Ne uporabljajte urejevalnika LaTeX, saj program, s katerim pripravljamo Strojniški vestnik, ne uporablja njegovega formata.

Enačbe naj bodo v besedilu postavljene v ločene vrstice in na desnem robu označene s tekočo številko v okroglih oklepajih

Papers submitted for publication should comprise:
- Title, Abstract, Main Body of Text and Figure Captions in Slovene and English,
- Bilingual Tables and Figures (graphs, drawings or photographs),
- List of references and
- Information about the authors.

Since 1992, the Journal of Mechanical Engineering has been published bilingually, in Slovenian and English. The two texts must be compatible both in terms of technical content and language. Papers should be as short as possible and should on average comprise 8 pages. In exceptional cases, at the request of the authors, speciality papers may be written only in Slovene, but must include an English abstract.

For papers from abroad (in case that none of authors is Slovene) authors should provide Slovenian translation. Translation could be organised by editorial, but the authors have to pay for it. If the paper is reviewed as scientific, it can be published only in English language with Slovenian abstract, that is prepared by the editorial board.

THE FORMAT OF THE PAPER

The paper should be written in the following format:
- A Title, which adequately describes the content of the paper.
- An Abstract, which should be viewed as a mini version of the paper and should not exceed 250 words. The Abstract should state the principal objectives and the scope of the investigation, the methodology employed, summarize the results and state the principal conclusions.
- An Introduction, which should provide a review of recent literature and sufficient background information to allow the results of the paper to be understood and evaluated.
- A Theory
- An Experimental section, which should provide details of the experimental set-up and the methods used for obtaining the results.
- A Results section, which should clearly and concisely present the data using figures and tables where appropriate.
- A Discussion section, which should describe the relationships and generalisations shown by the results and discuss the significance of the results making comparisons with previously published work. (Because of the nature of some studies it may be appropriate to combine the Results and Discussion sections into a single section to improve the clarity and make it easier for the reader.)
- Conclusions, which should present one or more conclusions that have been drawn from the results and subsequent discussion.
- References, which must be numbered consecutively in the text using square brackets [1] and collected together in a reference list at the end of the paper. Any footnotes should be indicated by the use of a superscript[1].

THE LAYOUT OF THE TEXT

Texts should be written in Microsoft Word format. Paper must be submitted in electronic version.

Do not use a LaTeX text editor, since this is not compatible with the publishing procedure of the Journal of Mechanical Engineering.

Equations should be on a separate line in the main body of the text and marked on the right-hand side of the page with numbers in round brackets.

Enote in okrajšave

V besedilu, preglednicah in slikah uporabljajte le standardne označbe in okrajšave SI. Simbole fizikalnih veličin v besedilu pišite poševno (kurzivno), (npr. *v, T, n* itn.). Simbole enot, ki sestojijo iz črk, pa pokončno (npr. ms^{-1}, K, min, mm itn.).

Vse okrajšave naj bodo, ko se prvič pojavijo, napisane v celoti v **slovenskem jeziku**, npr. časovno spremenljiva geometrija (ČSG).

Slike

Slike morajo biti zaporedno oštevilčene in označene, v besedilu in podnaslovu, kot sl. 1, sl. 2 itn. Posnete naj bodo v ločljivosti, primerni za tisk, v kateremkoli od razširjenih formatov, npr. BMP, JPG, GIF. Diagrami in risbe morajo biti pripravljeni v vektorskem formatu.

Pri označevanju osi v diagramih, kadar je le mogoče, uporabite označbe veličin (npr. *t, v, m* itn.), da ni potrebno dvojezično označevanje. V diagramih z več krivuljami, mora biti vsaka krivulja označena. Pomen oznake mora biti pojasnjen v podnapisu slike.

Vse označbe na slikah morajo biti dvojezične.

Preglednice

Preglednice morajo biti zaporedno oštevilčene in označene, v besedilu in podnaslovu, kot preglednica 1, preglednica 2 itn. V preglednicah ne uporabljajte izpisanih imen veličin, ampak samo ustrezne simbole, da se izognemo dvojezični podvojitvi imen. K fizikalnim veličinam, npr. *t* (pisano poševno), pripišite enote (pisano pokončno) v novo vrsto brez oklepajev.

Vsi podnaslovi preglednic morajo biti dvojezični.

Seznam literature

Vsa literatura mora biti navedena v seznamu na koncu članka v prikazani obliki po vrsti za revije, zbornike in knjige:

[1] A. Wagner, I. Bajsić, M. Fajdiga (2004) Measurement of the surface-temperature field in a fog lamp using resistance-based temperature detectors, *Stroj. vestn.* 2(2004), pp. 72-79.

[2] Vesenjak, M., Ren Z. (2003) Dinamična simulacija deformiranja cestne varnostne ograje pri naletu vozila. *Kuhljevi dnevi '03*, Zreče, 25.-26. september 2003.

[3] Muhs, D. et al. (2003) Roloff/Matek Maschinenelemente – Tabellen, 16. Auflage. *Vieweg Verlag*, Wiesbaden.

Podatki o avtorjih

Članku priložite tudi podatke o avtorjih: imena, nazive, popolne poštne naslove in naslove elektronske pošte.

SPREJEM ČLANKOV IN AVTORSKE PRAVICE

Uredništvo Strojniškega vestnika si pridržuje pravico do odločanja o sprejemu članka za objavo, strokovno oceno recenzentov in morebitnem predlogu za krajšanje ali izpopolnitev ter terminološke in jezikovne korekture.

Avtor mora predložiti pisno izjavo, da je besedilo njegovo izvirno delo in ni bilo v dani obliki še nikjer objavljeno. Z objavo preidejo avtorske pravice na Strojniški vestnik. Pri morebitnih kasnejših objavah mora biti SV naveden kot vir.

Units and abbreviations

Only standard SI symbols and abbreviations should be used in the text, tables and figures. Symbols for physical quantities in the text should be written in italics (e.g. *v, T, n,* etc.). Symbols for units that consist of letters should be in plain text (e.g. ms^{-1}, K, min, mm, etc.).

All abbreviations should be spelt out in full on first appearance, e.g., variable time geometry (VTG).

Figures

Figures must be cited in consecutive numerical order in the text and referred to in both the text and the caption as Fig. 1, Fig. 2, etc. Pictures may be saved in resolution good enough for printing in any common format, e.g. BMP, GIF, JPG. However, graphs and line drawings sholud be prepared as vector images.

When labelling axes, physical quantities, e.g. *t, v, m,* etc. should be used whenever possible to minimise the need to label the axes in two languages. Multi-curve graphs should have individual curves marked with a symbol, the meaning of the symbol should be explained in the figure caption.

All figure captions must be bilingual.

Tables

Tables must be cited in consecutive numerical order in the text and referred to in both the text and the caption as Table 1, Table 2, etc. The use of names for quantities in tables should be avoided if possible: corresponding symbols are preferred to minimise the need to use both Slovenian and English names. In addition to the physical quantity, e.g. *t* (in italics), units (normal text), should be added in new line without brackets.

All table captions must be bilingual.

The list of references

References should be collected at the end of the paper in the following styles for journals, proceedings and books, respectively:

[1] A. Wagner, I. Bajsić, M. Fajdiga (2004) Measurement of the surface-temperature field in a fog lamp using resistance-based temperature detectors, *Stroj. vestn.* 2(2004), pp. 72-79.

[2] Vesenjak, M., Ren Z. (2003) Dinamična simulacija deformiranja cestne varnostne ograje pri naletu vozila. *Kuhljevi dnevi '03*, Zreče, 25.-26. september 2003.

[3] Muhs, D. et al. (2003) Roloff/Matek Maschinenelemente – Tabellen, 16. Auflage. *Vieweg Verlag*, Wiesbaden.

Author information

The information about the authors should be enclosed with the paper: names, complete postal and e-mail addresses.

ACCEPTANCE OF PAPERS AND COPYRIGHT

The Editorial Committee of the Journal of Mechanical Engineering reserves the right to decide whether a paper is acceptable for publication, obtain professional reviews for submitted papers, and if necessary, require changes to the content, length or language.

Authors must also enclose a written statement that the paper is original unpublished work, and not under consideration for publication elsewhere. On publication, copyright for the paper shall pass to the Journal of Mechanical Engineering. The JME must be stated as a source in all later publications.